

Rubber Soul –  
The Investigation of Rubber by Vibrational Spectroscopy

Master of Science Program in Polymer Science of the  
Freie Universität Berlin, Humboldt Universität zu Berlin,  
Technische Universität Berlin and Universität Potsdam

Submitted by  
**Katharina Sophia Haider**

Born in Munich/ Germany, on 28<sup>th</sup> November 1980

Based on the research done at the  
Technische Universität Berlin,  
Max-Volmer-Laboratory for Biophysical Chemistry

**1st Revisor:** Prof. Dr. Peter Hildebrandt (TU Berlin)  
**2nd Revisor:** Prof. Dr. Regine von Klitzing (TU Berlin)

5<sup>th</sup> March 2012



# Abstract

Since natural rubber is found in museums as part of cultural assets and artworks, the material characterisation and degradation of rubber is an important issue for both conservators and scientists. In the present work, IR and Raman spectroscopy in different setups were employed to study more than 40 samples of various naturally or artificially light-induced degraded natural rubbers (cis-polyisoprene) and gutta percha (trans-polyisoprene), as well as new natural and synthetic reference materials. IR spectra of the specimen surfaces could be successfully measured in the attenuated total reflection (ATR) mode, employing either a germanium tip embedded in a microscope objective or a diamond crystal. Complementary polyisoprene FT-Raman spectra of high quality were recorded with 1064-nm excitation using a microscope setup. Both IR and Raman spectroscopy allow distinguishing between 1,4-cis and 1,4-trans conformational isomers in synthetic reference samples. Two fresh samples of raw and purified balata were identified to exist in the  $\alpha$ - and  $\beta$ -crystalline form of 1,4-trans polyisoprene, respectively. On the basis of the characteristic vinyl stretching modes, Raman spectroscopy enables a sound analysis of degraded samples. The spectroscopic comparison of naturally degraded samples with artificially aged latex specimens reveals far-reaching similarities in terms of degradation products and thus degradation mechanisms. In the Raman spectra of the raw latex samples, a spectral marker for ammonia pre-vulcaniser has been identified. On the basis of the spectroscopic analyses of the synthetic and natural materials, the vibrational spectroscopic investigations were exemplarily extended to a museum's object, the original (degraded) and the new seating of the chaise longue "Mies" of the Vitra Design Museum. It was found that both the original and its replacement seating included a high content of degradation products, underpinning the sensitivity of natural rubber to degradation. Alternatively, it may be that the new seating has been produced and stored for a longer period of time prior to the assembly to the chaise longue. On the other hand, no traces of vulcaniser could be detected in the "Mies"-samples

which may be due to the lack of sensitivity of the present IR and Raman spectroscopic methods. Nevertheless, it has been shown that vibrational spectroscopy provides a variety of information on rubber-type materials and their (time-dependent) modifications, ie, their “history”, implying that these techniques have a high potential for *in situ* analyses.

# Zusammenfassung

Die Materialbestimmung und das Alterungsverhalten von Naturgummi sind Themen, die für Wissenschaftler und Restauratoren gleichermaßen von Interesse sind, denn als Bestandteil von Gebrauchsgegenständen und Kunstwerken ist Naturgummi in musealen Sammlungen zahlreich vertreten. In vorliegender Arbeit wurden über 40 verschiedene natürlich und künstlich lichtgealterte Proben aus Naturgummi (cis-Polyisopren) und Gutta Percha (trans-Polyisopren), sowie natürliche und synthetische Referenzen mit unterschiedlichen IR- und Raman-spektroskopischen Methoden untersucht.

IR Spektren der Probenoberflächen konnten erfolgreich im abgeschwächten Totalreflexionsmodus (ATR) aufgezeichnet werden, über eine Germanium-Messspitze an einem IR-Mikroskop einerseits, andererseits auf einer Diamant-Messzelle. Ergänzend wurden FT-Raman Spektren von hoher Qualität bei einer Anregungsfrequenz von 1064 nm durch ein Raman-Mikroskop gemessen. Sowohl die IR als auch die Raman Spektroskopie ermöglicht eine Unterscheidung der beiden Konformationsisomere 1,4-cis und 1,4-trans in synthetischen Referenzen.

Zwei Proben aus frischem rohen bzw. gereinigten Balata wurden als  $\alpha$ - bzw.  $\beta$ -kristalline Form von 1,4-trans Polyisopren identifiziert. Anhand von charakteristischen Streckschwingungen der Vinylgruppen ist eine eindeutige Materialanalyse auch gealterter Proben durch Raman Spektroskopie möglich. Der spektroskopische Vergleich von natürlich gealtertem Gummi und künstlich gealterten Latexproben zeigt eine breite Übereinstimmung hinsichtlich der Alterungsprodukte und -mechanismen. In den Raman Spektren des Naturlatex wurden spektrale Marker eines Ammoniak-Vorvulkanisierungsmittels gefunden.

Durch die spektroskopische Analyse von synthetischen und natürlichen Materialien gewonnene Erkenntnisse wurden exemplarisch auf die Untersuchung eines Museumsobjekts angewandt (die gealterte originale Sitzbespannung und die neue Ersatzbespannung der Chaise Longue "Mies" aus der Sammlung des Vitra Design Museums). In beiden Proben wurde ein

hoher Gehalt an Degradationsprodukten gefunden, was die Unbeständigkeit von Polyisopren gegenüber Alterungseinflüssen untermauert, wobei jedoch auch denkbar ist, dass die neue Sitzbespannung nach ihrer Herstellung längere Zeit gelagert wurde, bevor sie an der Chaise Longue montiert wurde. Hinweise auf die Verwendung eines Vulkanisierungsmittels wurden an den beiden "Mies"-Proben nicht gefunden, was an der Empfindlichkeit der gewählten IR- und Raman spektroskopischen Methoden liegen kann. Es wurde gezeigt, dass die Schwingungsspektroskopie eine Vielzahl an Informationen über Gummi-Materialien und ihre (zeitlichen) Veränderungen, d. h. ihre "Geschichte" liefert, und somit ein hohes Potential für *in situ* Untersuchungen besitzt.

# Contents

<b>Contents</b>	<b>7</b>
<b>1 Incentive</b>	<b>9</b>
<b>2 Characteristics and Extraction of Natural Rubber</b>	<b>11</b>
<b>3 Vibrational Spectroscopic Investigations of Rubber</b>	<b>15</b>
<b>4 Theory: IR and Raman Spectroscopy</b>	<b>21</b>
4.1 Infrared Spectroscopy . . . . .	21
4.2 Attenuated Total Reflection Spectroscopy . . . . .	22
4.3 Raman Spectroscopy . . . . .	24
4.4 NIR-FT Raman Microscopy . . . . .	25
<b>5 Experimental</b>	<b>27</b>
5.1 Samples . . . . .	27
5.2 Artificial Light-Ageing . . . . .	28
5.3 ATR-Microscopy . . . . .	31
5.4 Diamond-ATR . . . . .	31
5.5 Raman Spectroscopy . . . . .	33
<b>6 Results and Discussion</b>	<b>35</b>
6.1 Polyisoprene Standards: cis and trans . . . . .	35
6.2 Spectra of Natural Rubber Samples . . . . .	43
6.3 Artificially versus Naturally Degraded Rubber Samples . . . . .	44
6.4 Brown and White Balata . . . . .	50

6.5 Analysing an Art Object . . . . .	57
<b>7 Conclusions</b>	<b>65</b>
<b>Bibliography</b>	<b>69</b>
<b>List of Figures</b>	<b>75</b>
<b>Appendix</b>	<b>79</b>
<b>A IR and Raman Spectra</b>	<b>79</b>
<b>B Images of Rubber Samples</b>	<b>93</b>
<b>C Light Ageing Apparatus</b>	<b>99</b>
<b>D Suppliers List</b>	<b>101</b>
<b>E Acknowledgements</b>	<b>103</b>

# Chapter 1

## Incentive

*“Plastics and rubbers have become so ubiquitous in our daily lives that they are often taken for granted. It is no surprise that they are represented in most collections. Plastics are found not only in art, historic and technological collections, they are among the ethnographic materials of the twentieth century. Even some materials used in storing and conserving collections are plastic, technically synthetic polymers. Once plastics reach collectors and museums, they become the problem of conservators. Plastics will not be with us for ever; in fact, they are already posing preservation problems.”*[1]

For more than 170 years, natural rubber has been used in Europe and America for manufacturing articles of daily use. Starting out in the late 19<sup>th</sup> century elastomers have become increasingly important for technical developments and in everyday life. As part of cultural assets and in fine arts, rubber also found its way into museums and has become increasingly significant part of our cultural heritage. Examples are found in seating furniture (see Fig. 1.1) and in the oeuvre of artists such as Tadeusz KANTOR, Eva HESSE or Keith SONNIER [2, 3, 4, 5, 6].

Polyisoprene is very sensitive to oxidation induced by light, heat, ozone, stress, chemicals, pollutants and metal catalysts. Chemical changes that occur during degradation are chain-truncation, oxidation and cross-linking at the olefinic C=C bond, resulting first in softening and stickiness of polymer, followed by subsequent embrittlement. Therefore, it is of particular interest for conservators to identify the material, elucidate the degradation process (which specific to each polymer) and be aware of the actual condition of the rubber artefacts.



(a) Chaise longue "Mies" by ARCHIZOOM.



(b) "S-Chair" by Tom DIXON before and



(c) after restauration.

Figure 1.1: Images of design lassics made of rubber and found in museum's collections. Image "Mies": © <http://www.decoratum.com>; images "S-Chair": © Die Neue Sammlung. The International Design Museum Munich.

## Chapter 2

# Characteristics and Extraction of Natural Rubber

### Polyisoprene Rubber

Natural rubber is composed of isoprene polymers. The sum formula of one repeat unit is  $C_5H_8$ , but it can occur in four different conformers: 1,4-cis, 1,4-trans, 1,2-vinyl and 3,4-vinyl (Fig. 2.1). In addition, a twisted structure of the polymer is assumed [7]. 1,4-cis polyisoprene usually remains in the amorphous state at room temperature, although, upon long term storage (months or even years), the rubber hardens due to crystal formation. At lower temperatures the rate of crystallisation increases. The maximum rate is reached at  $-25^\circ\text{C}$ , where half of the crystallisation occurs in a few hours. Also stretch induced crystallisation has been reported [7, 8]. In contrary, 1,4-trans polyisoprene is either found in the  $\alpha$ - or in the  $\beta$ -crystalline modification at room temperature [7]. Suggested structures of the two crystalline modifications of 1,4-trans polyisoprene are shown in Fig. 2.2. While the  $\alpha$ -modification is in good agreement with X-ray studies, the  $\beta$ -modification could be brought to agreement with the X-ray studies by rotating the carbons at the 1-2 and 3-4 position in opposite directions.[9].

### Rubber Extraction

Several plant families with more than 2500 rubber producing species furnish a milky sap, the rubber latex [10]. Polyisoprene can also be chemically synthesised, which has greatly reduced the demand for many natural latexes. However, the elasticity, flexibility and

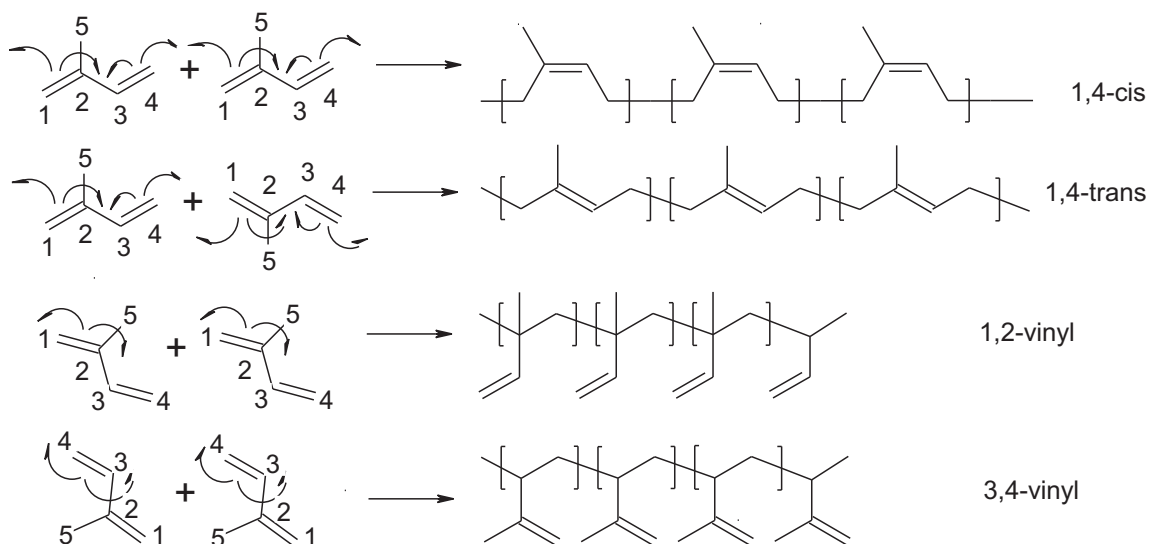


Figure 2.1: Scheme of different polyisoprene constitutional isomers. The formation of the polymeric chain is assumed to start with homolytic cleavage of the monomer units.

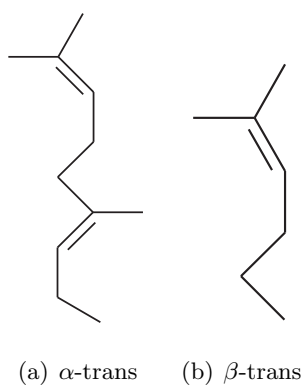


Figure 2.2: Proposed structure of  $\alpha$ - and  $\beta$ -1,4-trans polyisoprene [9].

resilience of the natural product are still superior [11].

The raw rubber or natural caoutchouc is obtained by drying the latex sap or by acid induced coagulation. At elevated temperatures, the material is sticky and highly self-adhering while it becomes hard and brittle at low temperatures. Due to the C=C functional groups of the thermoplastic polymer, raw rubber can be cross-linked with sulfur and heat, forming disulphur bonds. By this so called vulcanization treatment, the material is transformed into an elastomer, becomes less sensitive to temperatures and has improved shape-retaining properties. Depending on the degree of cross-linking, soft or hard rubber is obtained.

A special treatment of raw rubber is the so called mastication, ie, the mechanical disruption of the macromolecules of high viscous raw rubber. In air, radicals formed at the disrupted chain ends react with oxygen, thereby preventing the polymer chain from recombination. By this oxidation process the chain length and in this way also the viscosity of the polymer is reduced in order to facilitate further processability, eg, mixing with additives and fillers before vulcanisation. Formerly, one of these additives was antimon-penta-sulphide, which reduces the vulcanisation temperature. While the sulphur is built into the vulcanisate, the remaining antimon-tri-sulphide causes a red colour, as is often found in old rubber tubes and gaskets [8]. Nowadays, this red rubber is simply dyed with red pigments to achieve a familiar look.

## Natural Polyisoprenes

The rubber furnishing plants are divided into two main groups: the *hevea brasiliensis* produces the most common cis-polyisoprene, while the trans-polymer is produced by different trees such *aspalaquium gutta*, *mimusops balata* and *chicle*. Mixtures of cis- and trans-isomers have never been found in nature.<sup>1</sup>

Ninety percent of all natural rubber comes from the latex sap of the Brazilian rubber tree *hevea brasiliensis* (euphorbiaceae) which provides para rubber that is composed of up to 6000 isoprene subunits [13]. The plant combines excellent quality, high rubber concentration and production capabilities [10]. The composition of the latex sap of *hevea brasiliensis* varies from tree to tree, but generally it consists of 36% solid components (of which 33% are dry latex), 60% water, 1-1.5% proteinaceous components, 1-2.5% resinous components, 1% sugars and <1% ember[8] Recently, a new cis-furnishing species, the Brazilian *hancornia speciosa* has been explored. Due to its very low protein content, it is investigated for

---

<sup>1</sup>HENDRICKS et al. 1945, Archives of Biochemistry (7), p. 427, cited after [7], p. 958.

nonallergic applications [10].

Gutta percha is the overall term for the solidified juice produced by various trees belonging to the *sapodilla* family (sapotaceae), along with balata and chicle. The main source of gutta percha is, however, the gutta percha tree which is mainly cultivated in Malaysia, Indonesia and Sumatra. The balata tree in contrary is native to the Caribbean (Barbados, Venezuela and Guyana), chicle is native to Mexico. It should be noted that the nomenclature for gutta percha, balata and chicle is generally inconsistent.

The coagulated latex sap of the gutta percha tree contains 11% (in individual cases up to 40%) of resins, which is a much higher percentage than in *hevea* latex. Other components are 70% hydrocarbons, 14% water and 3% impurities. The balata latex has in average an even higher resin content than the gutta percha latex. Its coagulated sap consists only of approx. 50% polyisoprene and mainly resins.

Gutta percha resembles caoutchouc in many of its properties but it is less reactive than the rubber from *hevea brasiliensis*. A smaller number of branched polyterpene chains in the latex causes a reduced elasticity compared to *hevea* rubber. However, due to the difference in the molecular configuration, gutta percha is more stable [13]. Chicle is more plastic than natural rubber and more elastic than gutta percha [14]. Although the latex is also a polyterpene, it does not vulcanise into durable rubber [13].

As mentioned above, the cis-polyisoprene is in the amorphous state at room temperature and exhibits a glass-transition temperature between -68 and -65°C. Depending on the crystalline form, polyisoprene in the trans-state presents a melting temperature varying from 52 to 69°C. The  $\alpha$ -modification shows melting temperatures close to 70°C, while the  $\beta$ -form has its fusion point below 60°C [15]. Although gutta percha, balata and chicle were common replacement materials for natural rubber in the first half of the 20<sup>th</sup> century, nowadays their use is limited to special applications. For example, chicle is still partially used for chewing gum production [13], high quality golf balls often have a core of balata [8] and cones for filling dental root canals consist of gutta percha or balata [16].

In addition, WAENTIG [8] gives a very detailed description of the history, development and application of rubber. MALMONGE et al. [10] have investigated the technological properties of natural cis-polyisoprenes. Detailed technical information on the work-up of natural latex and on different commercial grades of natural rubber is available online [17]. A clear explanation of the terms ‘caoutchouc’, ‘latex’ and ‘rubber’ and the vulcanisation process was published by LANGER [5].

## Chapter 3

# Vibrational Spectroscopic Investigations of Rubber

There are numerous publications on the degradation processes of both vulcanised and unvulcanised natural rubber. Degradation products of polyisoprene that have been identified are hydroperoxides, alcohols, ketones, aldehydes, epoxides, carboxylic acid and esters. Depending on the ambient conditions (in air or *in vacuo*), the type of isomer (cis, trans, vinyl) and the type of irradiation source (monochromatic UV light, radiation  $>310$  nm) during degradation, the prevailing processes differ significantly [7, 18, 19, 20, 21, 15]. SAUNDERS and SMITH [7] were the first who identified *hevea* rubber and gutta percha as cis- and trans-polyisoprene, respectively, including  $\alpha$ - and  $\beta$ -1,4-trans variations. Moreover, they provided the first vibrational assignment for cis- and trans-polyisoprene, which was based upon polarised IR-measurements of crystallised samples. The different bond orientation in the cis- and trans-conformer (see Fig. 2.1) was used for the spectra interpretation. A neat explanation of IR spectroscopy using polarised irradiation is given in [22].

ADAM, LACOSTE and LEMAIRE [21] investigated the degradation mechanism of cis-, trans- and vinyl-type polyisoprene during photo- and low temperature thermo-oxidation. The conditions for photo-degradation were similar to those of a museum environment. The degradation mechanism was monitored by IR analysis, while the reaction products were also identified by wet chemistry. A scheme of the degradation mechanism is presented in Fig. 3.1. The authors pointed out that polyisoprene does not absorb light at wavelengths above 300 nm and revealed, that defects or impurities act initially as extrinsic chromophores. These chromophors can form light-induced radicals that can either ab-

stract an allylic hydrogen or add to a double bond.

MORAND [18] investigated the rate of light-induced chain scission of different vulcanised polyisoprenes by relaxation measurements as a function of the irradiation wavelength at 30°C. She observed a local minimum at 340 nm and a local maximum at 355 nm before the chain scission stopped using excitation wavelengths in the visible spectral region. She explained the high value of chain scission near 330 nm by photolysis of the main chain C-C bonds next to the double bond, resulting in random breaks of the polymer chain. The high rate of chain scission at 355 nm presumably results from the photochemical dissociation of the  $\alpha$ -methylene C-H bonds. Radicals formed in such away initiate an auto-oxidation process. YANO [23] found that degradation occurred in general below 430 nm, cross-linking reactions in particular below 340 nm. Scission of C-C and C-S links takes place between 340 and about 400 nm. In contrary, scissions of polysulfide cross-links occur between 400 and 600 nm. MORAND'S investigation of the influence of extractable substances present in different vulcanisates showed, that non-rubber constituents exhibit a protective effect. On the other hand, mercaptobenzothiazole and sulfur slow down the degradation by solar UV light considerably, while zinc oxide protects only against radiation below 370 nm. However, zinc oxide displays a sensitising effect on the rubber in the near visible range of the electromagnetic spectrum. Interestingly, the most harmful irradiation for most of the pure rubber vulcanisates is found in the region above 400 nm, but not as low as at 200 nm (the start of the UV-C region of the sunlight).

The sensitivity regarding light-induced degradation (at 254, 300 and 350 nm) of natural rubber in comparison with synthetic *cis*- and *trans*-polyisoprene standards was investigated using IR spectroscopy by DOS SANTOS, SUAREZ and RUBIM [15]. The results suggest, that both natural conformers exhibit a shorter induction time than synthetic standards due to impurities. Since the C=C vibration at  $1666\text{ cm}^{-1}$  in degraded polyisoprene samples overlaps with the strong band of the carbonyl stretching vibration of the degraded product, the authors suggest that bands at  $837$  and  $800\text{ cm}^{-1}$ , originating from =C-H wag modes, are most suitable to monitor the oxidation of C=C double bonds in *cis*- and *trans*-polyisoprene, respectively. Also MANIGLIA-FERREIRA, SILVA, DE PAULA et al. [16], did not observe any induction time for gutta percha in their IR studies.

MOHAN, ARJUNAN and SUBJAMANIAN [24] provide detailed assignments for the vibrational modes of *trans*-1,4 polyisoprene. The calculated frequencies as well as Raman and IR intensities are in good agreement with the experimental data.

Commercial synthetic polyisoprenes in the *cis*-, ( $\alpha$ - and  $\beta$ -crystalline) *trans*-form and syn-

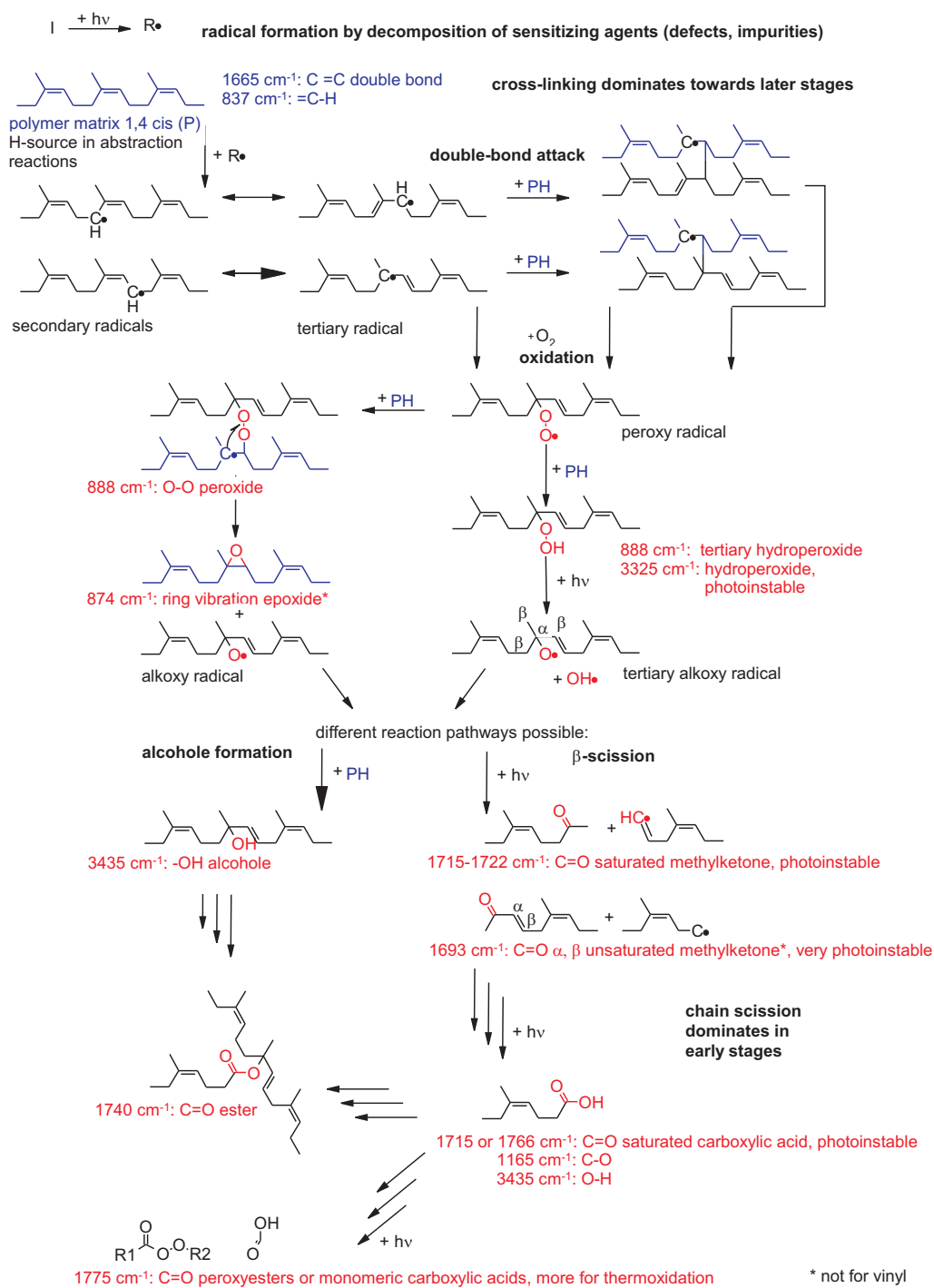


Figure 3.1: Scheme of photo-induced oxidation processes of 1,4-cis polyisoprene in air at wavelengths  $>300$  nm, according to the mechanism suggested by [21].

thesised mixtures of cis-, trans- and vinyl-form were investigated by BUNCE, EDWARDS, JOHNSON et al. [9] using FT-Raman spectroscopy. The authors expected limitations for the use of Raman spectroscopy for mixtures of conformers. However, characteristic bands have already been found for pure polyisoprene conformers and can therefore be used for the investigation of natural polyisoprenes.

JACKSON, LOADMAN, JONES et al. [25] and HENDRA and JACKSON [26] employed FT-Raman spectroscopy to investigate different synthetic types of elastomers including polyisoprene. Both publications pointed out the difficulty in obtaining spectra from samples that contain carbon black or impurities due to fluorescence and / or absorbance, causing burn of the sample. JACKSON, LOADMAN, JONES et al. applied Raman spectroscopy to get insight into the ratios of the copolymer composition. HENDRA and JACKSON, however, focussed on the analysis of various polyisoprene vulcanisates and have chosen Raman spectroscopy to detect strain crystallisation during mechanical deformation.

The application of Raman spectroscopy in art and archaeology has become increasingly important as a means of material investigation in the recent years. In 2004, a whole issue of the Journal of Raman Spectroscopy was dedicated to this field. The articles, however, discuss mostly pigments and inorganic materials such as ceramics, oxidation products on metal. An exception is the investigation of paper, parchment, biomaterials and historical binding media [27]. A rare example for the application of Raman spectroscopy for the investigation of a contemporary artwork made of plastic was presented at a conference in 2007 by COLOMBINI and LÉAL [28]. A polyether urethane sculpture covered with natural latex was investigated using a Raman microscope with an excitation laser line of 785 nm. For the blackened and severely degraded natural rubber of the sculpture the C=C stretch vibrational mode at  $1665\text{ cm}^{-1}$  could no longer be observed. In contrary, no significant changes in the Raman spectra of degraded polyether polyurethane foam became visible in the Raman spectra. In order to overcome signal corruption due to fluorescence, photo-bleaching and a special sample preparation are proposed. By sandwiching a thin sample between aluminium foil and a cover glass, the heating by the laser beam is reduced, which in turn allows increasing the laser power. Thus a higher signal-to-noise ratio is obtained and the spectra quality is improved.

As mentioned before, IR and FT-Raman spectroscopy are common techniques for the material characterisation of polyisoprene. These techniques are used to determine the involved conformers, the degree of degradation and can also be employed to differentiate crystalline forms. All spectral investigations discussed above require specific sample preparations and

demand in such a way modifications for analysing museum objects. LANGER [5], however, published numerous ATR (attenuated total reflexion) IR spectra of natural latex and a single Raman spectrum that was recorded of a latex artwork by Eva HESSE.



## Chapter 4

# Theory: IR and Raman Spectroscopy

IR and Raman spectroscopy give complementary information on molecular structures at an atomic level by probing molecular vibrations. These vibrations can be excited by photon absorption (IR) or by inelastic scattering of the incident light (Raman). In the following, the underlying principles of both methods and the two mainly employed techniques used in this study are outlined in brief.

### 4.1 Infrared Spectroscopy

To record an IR spectrum, the sample is irradiated with polychromatic light. The amount of light that is attenuated in total reflection mode or absorbed by the sample in the transmission mode is detected relative to the incident light. IR spectroscopy is sensitive to the changes in the dipole moment of atomic bonds. Thus, preferentially polar bonds can be easily monitored due to strong variations of the dipole moment during the vibration. Therefore, functional groups such as C-O, C=O, O-H or C-H, which are present in the oxidation products of the polyisoprenes are in particular suitable for detection by IR spectroscopy.

## 4.2 Attenuated Total Reflection Spectroscopy

Internal reflection spectroscopy, better known as attenuated total reflection spectroscopy (ATR) is an infrared spectroscopic technique, that is extensively used. The centrepiece of an ATR-unit is a waveguide, the internal reflection element (IRE), in which the infrared radiation propagates in total reflection. Commonly IREs are crystals with a high refractive index  $n_D$  such as thallium bromide-iodide (KRS-5), germanium or diamonds. In a common ATR-measurement, the sample is in close contact with the IRE. The basic setup of an ATR-unit is given in Fig. 4.1.

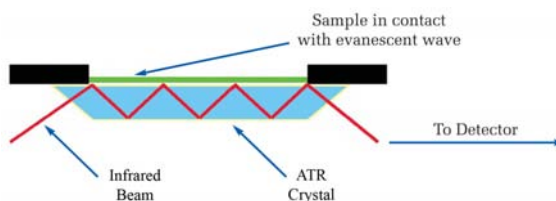


Figure 4.1: Scheme of the ATR setup [29].

Light from the infrared source is coupled into the IRE. At the optical interface the incident beam is partially reflected due to the difference of the refractive index at the optical interface. If the light enters from a medium with a high refractive index, such as the IRE, into a medium with a lower refractive index, total reflection can occur. Assuming that the angle of the incoming light exceeds the critical angle  $\theta_c$ :

$$\theta_c = \sin^{-1} \left( \frac{n_2}{n_1} \right) \quad (4.1)$$

where  $n_1$  is the optically denser medium and  $n_2$  the optically rarer medium. However, a small portion totally reflected light penetrates the rarer medium (sample material) in form of an evanescent wave, as shown in Fig. 4.2.

The evanescent wave emerges inside the optically thinner medium near the surface, perpendicularly to the interface and attenuates the totally reflected light. Multiple internal reflections increase the attenuation. While the incoming radiation is a transverse wave and oscillates perpendicularly to the direction of the propagation, the evanescent field is non-transversal and has components in all spatial directions. Thus, it can interact with the randomly oriented dipoles in the sample. Its intensity decreases exponentially:

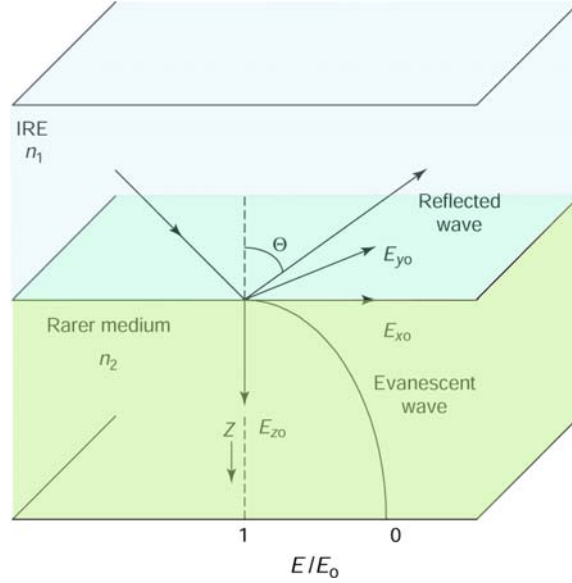


Figure 4.2: Attenuated total reflection (ATR) at an internal reflection element (IRE).  $n_2$  - refractive index of the sample,  $n_1$  - refractive index of the IRE,  $z$  - distance normal to the optical interface,  $E_{(i)0}$  - energy of the special components of the evanescent wave,  $\theta$  - angle of incidence [30].

$$E = E_0 \exp\left(-\frac{z}{d_p}\right) \quad (4.2)$$

where  $E_0$  is the energy at the optical interface,  $z$  the distance normal to the optical interface and  $d_p$  the of penetration depth of the evanescent field, which equals the probed sample thickness:

$$d_p = \frac{\lambda}{2\pi \sqrt{\sin^2\theta - (n_2/n_1)^2}} \quad (4.3)$$

where  $\lambda$  is the wavelength in the optically denser medium,  $n_2$  - refractive index of the sample,  $n_1$  - refractive index of the IRE and  $\theta$  - angle of incidence [30, 22, 31]. The penetration depth is an arbitrarily defined parameter. It describes the distance from the interface, at which the amplitude of the electrical field decreases to  $1/e$  (37%) of the amplitude at the interface. However, it has been experimentally determined, that the real

penetration depth is similar to three  $d_p$ . As a general approximation, a penetration depth of  $\lambda/4$  bis  $\lambda/10$  can be assumed [30].

### 4.3 Raman Spectroscopy

In contrast to the IR method, Raman spectroscopy probes selectively those vibrations in which the incident monochromatic light (nowadays a laser source) induces a dipole moment, for example in carbon-carbon double bonds in the polymeric backbone. Only a very small portion of the laser light is scattered inelastically and has a higher (“Anti-Stokes shift”) or lower (“Stokes shift”) energy than the incident radiation. In the present study, only the Stokes-spectrum is considered.

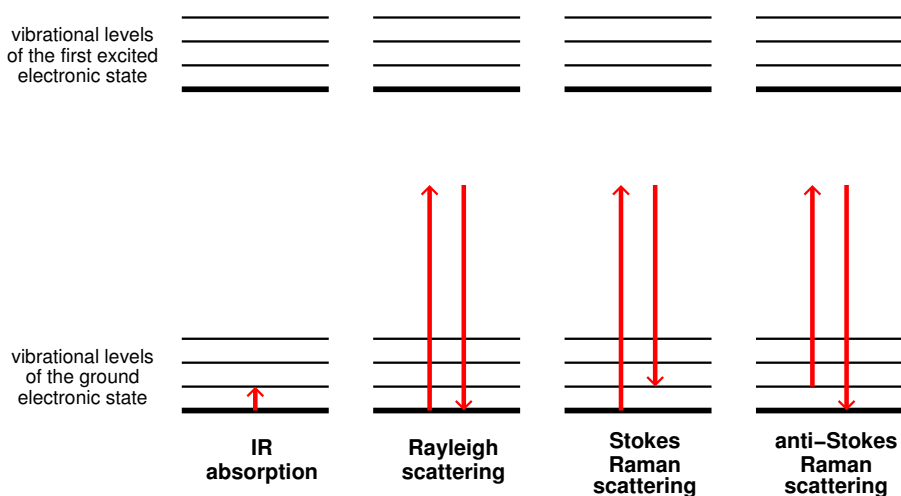


Figure 4.3: Possible consequences of a photon-molecule interaction [32].

This energy represents a vibrational transition of the molecular vibrational mode. The intensity of the Raman radiation is proportional to the fourth power of the absolute frequency of the Raman line. Since the Raman-effect is very weak, it can easily be swamped by fluorescence, which is several orders of magnitude larger than the Raman-effect. Traces of impurities in the range of ppm or ppb - which can be present even in chemicals of analytical purity grade, may already be enough to corrupt a spectrum[33]. Depending on the sample material, the excitation laser line can be adjusted to overcome fluorescence and to avoid laser induced sample degradation by heating and / or burning.

## 4.4 NIR-FT Raman Microscopy

By using laser light of a wavelength in the near infrared range, eg, 1064 nm, the probability of fluorescence of the sample or impurities such as oxidation products is considerably reduced. However, to achieve the same intensity of a Raman line the flux of the exciting radiation at 1064 nm has to be larger by a factor between 23 and 87 compared to excitation with the 488 nm line [34]. The intensity loss of the Raman-effect using an IR-laser due to the  $\nu^4$ -dependence can be largely compensated using Fourier-transform technique. This is related to the fact, that the interferometer used in FT-spectrometers has an optical conductance which is about two orders of magnitude higher than in dispersive spectrometers using a monochromator instead [34]. Additional advantages of interferometers are a reduced recording time as the sampling signal is recorded for all wavelengths at the same time and that the frequency scale is highly reproducible. A problem inherent of the FT-technique is, that fluctuations of light quanta in the laser source generate statistical intensity fluctuations throughout the interferogram. After the transformation into the spectrum, they may mask the weak Raman bands completely.

As many other techniques, also the Raman spectroscopy can be coupled with an optical microscope. The setup is given in Fig. 4.4.

The laser light is bundled by a system of lenses and focused onto the sample. The scattered Raman radiation is sent through an aperture (Jaquinot-aperture) into the interferometer. In the Raman-microscope, the FT-advantages are lost and noise is transmitted through the optics in the microscope, worsening the signal-to-noise ratio. In the microscopic setup, the probing area is much smaller, but the power density at the sample is much higher compared to a macroscopic setup.[35] The small laser spot increases the risk of local heating of the sample and spoils the signal-to-noise ratio further. Thus, Raman investigation of samples sensitive to thermal degradation are only possible at low laser powers.

In the microscope setup, optics and spectrometer are connected via a glass fibre that causes an additional signal loss. For the application in a museum, however, a portable Raman device with a flexible head is desirable. TENNENT et al. [36] have already described the successful application of a compact Raman spectrometer connected to a fibre optic probe. For the characterisation of polymers and pigments used in past conservation treatments of glass artefacts an excitation laser line of 785 nm and a spot diameter of  $100\mu\text{m}$  was applied.

An extended accumulation time due to losses in the microscopic setup needs to be ac-

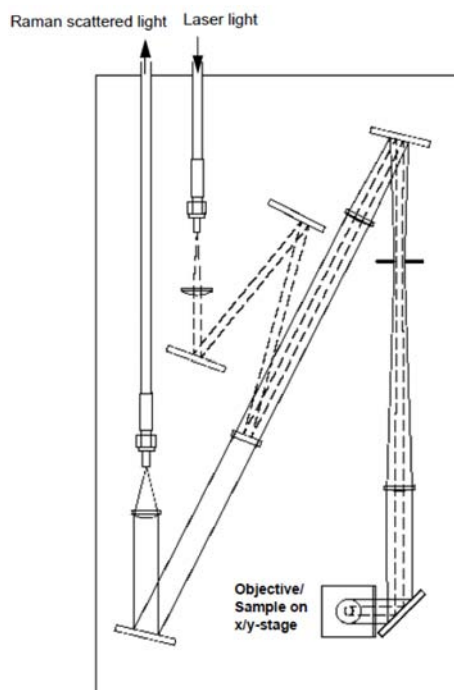


Figure 4.4: Setup of a Raman microscope.

cepted. Advantages of the microscope are, that the sample can be placed on a horizontal surface and does not require any fixation. Moreover, the small size of the laser spot makes it possible to scan heterogeneous samples at different positions and the probed spots can be monitored online and captured.

## Chapter 5

# Experimental

In the present study FT-IR and FT-Raman spectra were recorded from very pure, additive-free and uncompounded material. In contrast to the examples given in chapter 3, the investigated material required no special treatment or preparation. A spectroscopic library of fresh and degraded samples of natural as well as synthetic 1,4-cis- and 1,4-trans polyisoprene was created. This allowed the material identification and a determination of the degree of ageing. Artificial degradation by constant light exposure was applied to simulate and monitor the natural ageing process. A sample of a museum object was analysed in order to apply the two complementary techniques in a “real-life” situation.

### 5.1 Samples

Essence and motivation of the research was an approximately one hundred years old sample case with various naturally degraded pure rubber samples of the hevea and gutta percha type (Fig. 5.1). Labels of Continental Caoutchouc and Gutta=Percha Compagnie Hannover with trade name and origin were attached to the majority of the samples, originating from South America, Africa and Ceylon. The label saying ‘Dtsch. Ostafrika’ (German East Africa) allowed to date the collection to the 20<sup>th</sup> century colonial era. Additionally new reference samples were investigated, including natural and synthetic cis- and trans-polyisoprene ( $\alpha$ - and  $\beta$ -form) as well as naturally and artificially light-aged films prepared from a commercial latex milk (Fig. B.1).<sup>1</sup> A photographic documentation of the samples

---

<sup>1</sup>Spectra of the following samples were recorded: South American rubbers from Peru, Ecuador, Colombia and Brazil; different para rubbers, raw, washed and masticised, lumps and mats; plantation rubbers from

is included in the appendix.

Samples of the chaise longue “Mies” by ARCHIZOOM, which is part of the Vitra Design Museum’s collection were also investigated. The chaise longue consists of a rubber seating that is stretched onto a frame of chromed steel (76×74×130 cm). The original seating from 1969 has not only changed its colour from beige to dark brown, but it has lost its tension and is partly torn. Therefore, the original seating was replaced in autumn 2011 by a new rubber seating manufactured by Poltronova Srl., Agliana/Pistoia, Italy (Fig. 5.2). The analysis of the original and replacement seating should clarify, if both seating materials are made of the same material and if the description ‘rubber’ refers to polyisoprene rubber.

## 5.2 Artificial Light-Ageing

Films of raw latex milk (CREARTEC) were prepared and light-aged according to ISO 4892/1-2 [37, 38] and to ISO 11341 [39]. The latex milk consists of Malaysian natural caoutchouc concentrate, distilled water, soda and ammonia for pre-vulcanisation.<sup>2</sup> It was cast in three layers to an approximately 0.2 mm thick film. Test specimens (95×50 mm) were inserted into a sample holder made of acid-free cardboard covered with a self-adhering polytetrafluoroethylene (PTFE) film. Thus, only a square of 55×30 mm was exposed. The specimens were irradiated in a Suntest CPS (ATLAS) run on maximum power. The chamber had an inner surface of 280×200 mm. The light reflection of the xenon arc lamp (1.8 kW, new<sup>3</sup>) was performed mainly with a parabolic mirror. The inner walls of the chamber were covered with a reflecting material (regularly rough surface), which improved the overall sample irradiation. A sketch of the chamber is given in Fig. C.1 [41]. The light was passed through an IR-absorbing filter and through conventional window glass. At the level of the specimens the indirect irradiation power was 2.64 kW/m<sup>2</sup> at the centre and 1.76 kW/m<sup>2</sup> at the corner of the chamber (measured using a laser power meter with a power detector, TPM-300 and UP19K-15S-W5, GENTEC-EO). The contribution of 3.3% in the region be-

---

Ceylon and Africa; African rubber from Mozambique, Tansania, Cameroun; gutta percha (three types). Products: regenerated rubber; unvulcanised and vulcanised baby teat; patented tube unvulcanised (half-finished); billard bank (rosset); pump covers (rosset, brown, black and grey). New reference materials: synthetic trans (182168), natural cis (182141), natural cis (431257) and synthetic cis (431265) purchased from SIGMA-ALDRICH; purified white  $\alpha$ -trans and processed grey  $\beta$ -trans balata (Brazil, TANARIMAN Ltd.) and natural Malaysian latex milk (cis), pre-vulcanised with ammonia (CREARTEC).

<sup>2</sup>Pre-vulcanised latex milk usually contains 60% isoprene. LANGER [5], p. 298.

<sup>3</sup>Since the intensity of the shortest wavelengths decreases, xenon arc lamps should be burned for at least 100 hours before using them in an accelerated ageing experiment. FELLER [40], p. 104.



Figure 5.1: Sample case with naturally degraded, uncompounded and unvulcanised rubber materials (hevea and gutta type) from different continents as well as few vulcanised product samples.



Figure 5.2: Original and replacement seating of the chaise longue “Mies” by ARCHIZOOM in the conservation studio of the Vitra Design Museum in 2011. Left: dismounted darkened and torn original seat cover from 1969. Centre: chaise longue with new seat cover. Right: chaise longue with oxidised, darkened and stripped out seat cover.

tween 300-400 nm was measured using an EPP 200 USB spectrometer (STELLARNET Inc). Air temperature and relative humidity were monitored using a Tinytag Ultra TGU-4500 data logger (GEMINI). The black panel temperature was 61°C after 1h, the air temperature and relative humidity in the chamber were 50°C and 16% rh. The samples were irradiated for 1, 3, 4, 5, 25, 63 and 73 hours. Additionally, a sample was naturally aged for 4.5 months under indoor conditions (summer period, south facing window). According to FELLER, the maximum acceleration in xenon arc tools is 7-9 times higher than under outdoor conditions [40], while TWEEDIE, MITTON and STURGEON equal five hours of irradiation in a xenon arc device to the dose of a summer day [42]. According to the manufacturer the ratio of the irradiation in is 1:8 between a Suntest CPS device equipped with a 1800 W source and natural irradiation, irrespective of seasonal or geographic variations.<sup>4</sup> The real acceleration factor does not only depend on the light source and filtering, but also on the

<sup>4</sup>Personal communication of R. LEHN from ATLAS Material Testing Technology B.V., May 2011.

tested material, its moisture content and air temperature and relative humidity. Thus, a correlation between, eg, 1 hour of artificial ageing and the real time irradiation was not attempted.

### 5.3 ATR-Microscopy

An FT-IR microscope (HYPERION) equipped with an ATR objective with a Germanium tip (sampling spot size about 75  $\mu\text{m}$ ) which was located in a chamber flushed with dry air was initially used. The liquid nitrogen cooled mercury cadmium telluride (MCT) detector was suitable for MIR-studies in a wavenumber range between 4000-650  $\text{cm}^{-1}$ . All spectra were measured with a resolution of 4  $\text{cm}^{-1}$ . The accumulation time for a single spectrum was approx. 2 min, (100 individual scans). For each sample five single spectra were accumulated and averaged to improve the signal-to-noise ratio. Depending on the particular sample morphology, the measurements were performed either with or without the application of pressure from the tip. Due to the elasticity or viscosity of many samples, the signal intensity varied significantly within a single measurement. Additionally, drifts of the spectral baseline could be observed, eg, due to the sensitivity regarding changes in the atmosphere. In order to establish an equilibrium after mounting the sample on the specimen platform stabilising periods were required. Still, the reproducibility was not satisfactory and baseline correction and atmospheric compensation using the OPUS 5.5 software (BRUKER) were necessary to obtain comparable results. The difficult handling procedures prevailed over the advantage of exact sample positioning and the general advantage of obtaining spectra in an entirely non-invasive way. For this reason, a different ATR setup was tested.

### 5.4 Diamond-ATR

The GladiATR Vision<sup>™</sup> single reflection unit (PIKE Technologies, kindly provided by RESULTEC) with a diamond crystal (2.2 $\times$ 3 mm) was mounted on a Vector 22 spectrometer (BRUKER). The attenuated total reflected light was collected by a DTGS detector. The measurement window was restricted to a wavenumber range between 4000-400  $\text{cm}^{-1}$ . For each spectrum, 128 individual scans were accumulated (resolution of 4  $\text{cm}^{-1}$ ). The pressure applied for the contact between sample and the diamond crystal was always set to a maximum to ensure the highest energy throughput (this maximum was factory set to 40

pounds). Since the exerted pressure on the sample is a function of the area, the pressure ranged from 6,8 psi for large samples that covered the full window and higher values for smaller samples. For elastic samples a flat-tipped cone was used to ensure good contact between sample and diamond. For most of the naturally degraded hardened samples a swivel tip was chosen, taking into account their irregular shape (see Fig. 5.3) [43].

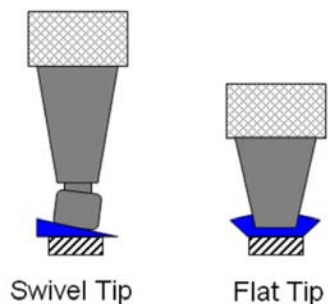


Figure 5.3: Tip attachments for the pressure clamp [43].

The duration of a complete measurement including accumulation of a background spectrum was approximately five minutes. The spectra had an excellent quality and reproducibility. Therefore no additional manipulation was necessary. Since the diamond has strong and broad phonon absorbance bands in the region of  $2300\text{-}1800\text{ cm}^{-1}$ , where also  $\text{CO}_2$  and water absorb, it can be disregarded in the spectra.

The penetration depth was calculated according to Eq. 4.2. The sampled spectral range covered  $4000\text{-}400\text{ cm}^{-1}$  and  $2500\text{-}25000\text{ nm}$ , respectively. The refractive indices were 2.4 for the diamond IRE and 1.5161 (at  $\lambda=2480\text{ nm}$ ) for polyolefines<sup>5</sup> and the angle of incidence was  $45^\circ$ . Using these parameters, a wavenumber dependent penetration depth between  $0.5$  and  $5\text{ }\mu\text{m}$  has been estimated. Since the samples had an uneven surface and especially the naturally degraded old rubber samples often were porous and brittle, the exact penetration depth cannot be determined.

---

<sup>5</sup>Since it was not possible to find exact literature values for the refraction index of polyisoprene at wavelengths between  $25000\text{-}2500\text{ nm}$ , a general refractive index of 1.5161 for polyolefines at  $2480\text{ nm}$  was used for the calculation. This assumption seems to be reasonable, since the CAUCHY-dispersion model holds for polyolefines, which is almost monotonous at higher wavelengths. Personal communication of Filmetrics Europe GmbH, 21.02.2012.

## 5.5 Raman Spectroscopy

FT-Raman measurements were performed with an RFS-Raman spectrometer (BRUKER) connected to a microscope (Ramanscope BRUKER, equipped with a long working distance objective of OLYMPUS BX 40, 20 $\times$ , NA 0.35). Sample excitation was achieved by an Nd:YAG continuous wave laser (Compass 1064-1500N, COHERENT). The scattered light was collected with a liquid nitrogen cooled Germanium detector. The respective laser power was kept at 30-40 mW, in order to avoid unwanted sample heating or burning. Very dark samples were additionally flushed with nitrogen to cool down the surface to room temperature during the measurement. All spectra were measured with a resolution of 4  $\text{cm}^{-1}$ . Accumulation time for one single spectrum was approx. 3.5 min (100 individual scans). For each sample 20 single spectra were accumulated and averaged. Laser damage or simple spectral drifts were checked by analysing the residual standard deviation of the sum spectrum. Background correction and data handling were performed using the OPUS 5.5 software.

Excitation with 1064 nm laser wavelength reveals a good spectral quality without sample degradation, additionally no or very little fluorescence is observed. This is a clear advantage over excitation with laser wavelengths in the VIS or UV range (eg, 413 nm) [44, 45]. Confocal measurements (Raman microscope HR-800, HORIBA Jobin Yvon) with a violet excitation laser light (413 nm, cw Kr<sup>+</sup> laser, Innova 300, COHERENT) confirmed that this wavelength is not suitable for probing polyisoprene due to the strong fluorescence [44]. Conventional FT-Raman spectroscopic measurements were performed using the frontal collector lens of the RFS-Raman spectrometer [46]. The measurement protocol was similar as for FT-Raman microscopic experiments. Since the mounting of large and very small samples was inconvenient and the laser spot was much larger than for the microscope, this technique was not used further.



## Chapter 6

# Results and Discussion

### 6.1 Polyisoprene Standards: cis and trans

In order to visualise the spectral differences between cis- and trans-polyisoprenes, the two types are juxtaposed in IR (Fig. 6.1) and Raman spectra (Fig. 6.2). The spectra were recorded using the diamond ATR-IR spectrometer and the Raman microscope, respectively. Additional IR and Raman spectra with marked peak positions for these samples are given in the appendix, Figs. A.1 and A.2 (IR) and Figs. A.8 and A.7 (Raman). DOS SANTOS et al. [15] have published IR spectra of cis- and trans-polyisoprene, while BUNCE et al. [9] and CORNELL and KOENIG [47] have studied the differences in Raman spectra of polyisoprene. In Tab. 6.1, the characteristic bands for cis- and trans-polyisoprene in IR and Raman spectra are summarised.

**IR spectra of cis and trans reference compounds** In the IR spectra of cis- and trans-polyisoprene (Fig. 6.1), differences throughout the whole spectral range are visible. They match very well the literature data in Tab. 6.1. In the high-energy spectral range of CH<sub>2</sub> and CH<sub>3</sub> stretching modes (3000-2800 cm<sup>-1</sup>), there are obvious differences in band intensity and peak positions. For cis-polyisoprene, the CH<sub>3</sub> mode at 2960 cm<sup>-1</sup> is the strongest band in this spectral range. Additionally, a characteristic band doublet at 2912 and 2926 cm<sup>-1</sup> due to the CH<sub>2</sub> stretching is observed. In contrast, the CH<sub>2</sub> stretching band at 2910 cm<sup>-1</sup> with a shoulder at 2938 cm<sup>-1</sup> dominates this region the trans-polymer. Moreover, the CH<sub>3</sub> stretching mode of 2960 cm<sup>-1</sup> is shifted to 2964 cm<sup>-1</sup> in the trans-form, which exhibits a second CH<sub>3</sub> stretching band at 2878 cm<sup>-1</sup>, that is not found in the

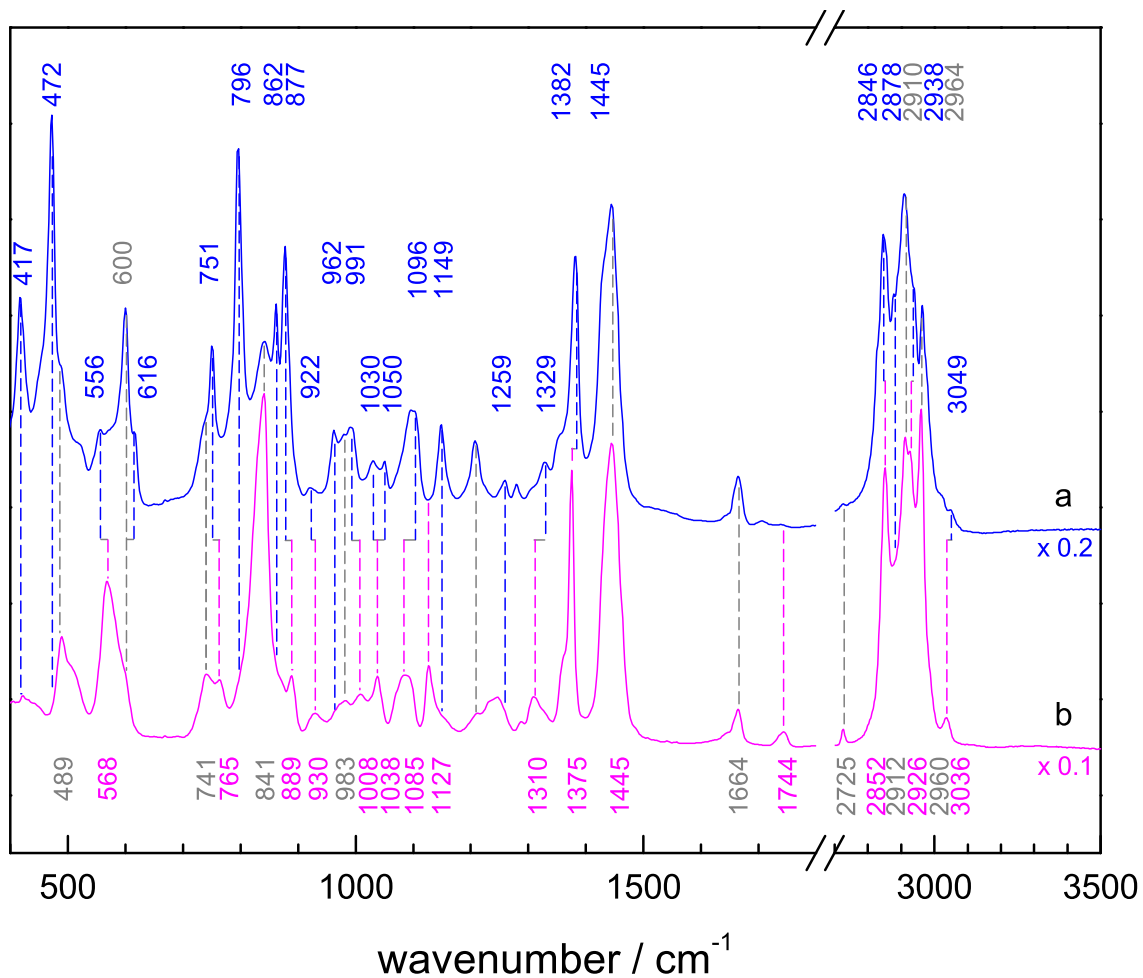


Figure 6.1: Comparison of IR spectra of (a) 1,4-trans (blue line) and of (b) 1,4-cis polyisoprene references (red line) from SIGMA-ALDRICH. Grey lines indicate vibrational modes occurring for both samples at a nearly identical position. Spectrum (a) is multiplied by a factor of 0.2, spectrum (b) is multiplied by a factor of 0.1.

IR cis	IR $\alpha$ -trans	Raman cis	Raman $\alpha$ -trans	Assignment
3036 w	3053 vw	3033	3052 w/sh	=C-H str
	3015 w		3019 m	=C-H str
	2975 vs		2972 m	CH <sub>3</sub> str <sub>asym</sub>
2962 vs	2965 sh	2957		CH <sub>3</sub> str <sub>asym</sub>
2928 vs	2936 sh	2929	2934 s/sh	CH <sub>2</sub> str <sub>asym</sub>
2915 sh	2915 vs	2910	2910 vs	CH <sub>2</sub> str <sub>sym</sub>
	2890 wsh			
	2880 wsh	2878	2881 vs	CH <sub>3</sub> str <sub>sym</sub>
2855 vs	2852 vs	2853	2857 s/sh	CH <sub>2</sub> str <sub>sym</sub>
	2830 sh		2828 m/sh	CH <sub>3</sub> str <sub>sym</sub>
		2724	2728 w/br	
1665 w	1668 m	1662	1670 s/1666 s/sh	C=C str
1645 w	1447 s	1445	1643 w/sh	C=C vinyl
1450 s			1452 m	CH <sub>2</sub> def <sub>asym</sub>
	1433 sh	1431	1432 ms	CH <sub>2</sub> def <sub>sym</sub>
	1382 s		1384 m	CH <sub>3</sub> def/C-C str
1377 s		1369	1371 mw	CH <sub>3</sub> def
1359 sh	1358 sh	1359	1361 vw	CH <sub>3</sub> /CH <sub>2</sub> def
	1330 vw		1329 m/1319 vw	CH <sub>2</sub> wag/twist
		1321		=C-H def (1,2)
1311 w		1308		CH <sub>2</sub> wag/=C-H def (3,4)
1286 vw		1286	1288 m	=C-H bend <sub>ip</sub>
	1280 vw		1279 m	CH <sub>2</sub> wag/twist
1242 w	1254 vw	1238	1252 mw	CH <sub>2</sub> wag/twist
	1207 m	1201		=C-H bend <sub>ip</sub>
1166 m	1150 m		1158 w/br	C-O str/CH <sub>3</sub> wag
1130 w		1130		CH <sub>2</sub>
1100 w	1096 m		1100 w/br	C-CH <sub>2</sub> str
1089 w	1089 w	1070		C-CH <sub>2</sub> str
	1051 w		1053 m	CH <sub>3</sub> rock
1038 w	1030 w	1038	1035 m/br	CH <sub>3</sub> rock
929 vw	990 w	996	1010 m/998 m	C-C str/C-CH <sub>3</sub> str
975* w				C-C str
889 mw		889		CH <sub>3</sub>
	883 m		881 mw	=C-H bend <sub>oop</sub> /
	862 m			CH <sub>3</sub> wag
837 m	844 w			=C-H wag
	800 m	816	802 m	=C-H wag
764 w	751 w		785 m/758 mw/br	CH <sub>2</sub> rock
740 w		728		CH <sub>2</sub> rock
			600 w/br	C-C-C def
565		565		C-C bend (cis)
496		493		C-C bend (cis)

Table 6.1: Literature values for bands in the following polyisoprene spectra: IR spectra of 1,4-cis and 1,4-trans [15], Raman spectra of 1,4-cis [47] and of  $\alpha$ -1,4-trans polyisoprene [9]. Asterisks indicate modes observed in degraded material.

cis-polyisoprene. The very strong  $\text{CH}_2$  stretching bands at  $2852\text{ cm}^{-1}$  (cis) and at  $2846\text{ cm}^{-1}$  (trans) are the only bands of equal intensity in this spectral region. As compared to literature, they are both shifted to lower frequencies ( $\Delta\tilde{\nu}=5\text{ cm}^{-1}$ ). Adjacent to the intense bands between  $3000$  and  $2800\text{ cm}^{-1}$ , there are two weak bands at  $3036$  and  $2725\text{ cm}^{-1}$ . While the former band is assigned to the  $=\text{C-H}$  stretching, no assignment was found for the latter.

In the range of  $\text{C=C}$  and  $\text{C=O}$  stretching ( $1800\text{-}1500\text{ cm}^{-1}$ ) there are two weak bands in the cis-spectrum (at  $1744\text{ cm}^{-1}$ , probably due to  $\text{C=O}$  stretching and  $1664\text{ cm}^{-1}$  caused by  $\text{C=C}$  stretching vibration of 1,4-unsaturation), but only the band at  $1664\text{ cm}^{-1}$  is visible in the trans-spectrum. For both samples, the band at  $1664\text{ cm}^{-1}$  has a shoulder at the low-frequency side of this peak, which might be due to the  $\text{C=C}$  stretching mode of the vinyl function at  $1645\text{ cm}^{-1}$ . The strong  $\text{CH}_2$  deformation band at  $1447\text{ cm}^{-1}$  with a shoulder at around  $1430\text{ cm}^{-1}$  in the fingerprint region of trans-polyisoprene is also in accordance with literature data. In the cis-spectrum this band is asymmetric, shifted to  $1445\text{ cm}^{-1}$  and does not show this shoulder. The observed peak shift of the prominent  $\text{CH}_3$  deformation mode from  $1375\text{ cm}^{-1}$  (cis) to  $1382\text{ cm}^{-1}$  (trans) has also been reported. The strongest band in the low-energy region of the cis-spectrum belongs to a  $\text{CH}_3$  wagging mode at  $862\text{ cm}^{-1}$ . In contrast, the strongest bands for trans-polyisoprene are located at  $796$ ,  $600$   $472\text{ cm}^{-1}$ , which can be related to  $=\text{C-H}$  wagging,  $\text{C-C-C}$  deformations and  $\text{CH}_3$  out-of-plane deformation modes in Raman spectra [9].

**Discussion of the IR spectra of cis and trans reference compounds** It is known, that the phenomenon of Fermi-resonance occurs for aldehydes, where the aliphatic  $\text{C-H}$  stretch vibration of the aldehyde group interacts with an overtone of a  $\text{H-C=O}$  rocking vibration at  $1410\text{-}1380\text{ cm}^{-1}$ . This leads to a characteristic pair of absorption bands at  $2900\text{-}2800\text{ cm}^{-1}$  and  $2775\text{-}2695\text{ cm}^{-1}$  in aldehydes [22], which are often located at  $2840\pm 30\text{ cm}^{-1}$  [ $\nu(\text{C-H})$ ] and at  $2720\pm 20\text{ cm}^{-1}$  [ $2\times\delta(\text{C-H})$ ]. Due to the fact that the  $2725\text{ cm}^{-1}$  band is also found in fresh samples DOS SANTOS et al. exclude an assignment to aldehydes, which are known to occur during polyisoprene degradation [21]. Thus, an assignment of the  $2725\text{ cm}^{-1}$  band to an overtone of the  $\text{CH}_3$  deformation vibration at  $1375\text{ cm}^{-1}$  seems to be most likely.

While the  $1375\text{ cm}^{-1}$  band is sharp and very intense in cis-polyisoprene, it is broadened, less intense and shift to  $1382\text{ cm}^{-1}$  in the trans-form. This would explain, why also the peak at  $2725\text{ cm}^{-1}$  is broader and weaker in the trans-polymer. Moreover, the band of

=C-H stretching at  $3036\text{ cm}^{-1}$  corresponds to the peak intensity of the  $2725\text{ cm}^{-1}$  mode in both spectra and both seem to be related to each other, but also to  $\text{CH}_2$  and  $\text{CH}_3$  deformations at  $1446$  and  $1375\text{ cm}^{-1}$ .

The band at  $1744\text{ cm}^{-1}$  in the cis-spectrum could be due to C=O stretching of esters or ketones (see Fig. 3.1). Since the containers of the reference samples were opened six months before the spectra were recorded, some oxidation may have occurred. While the cis-reference consisted of soft and sticky chunks, the trans-polyisoprene was provided as hard pellets. Because the cis-polyisoprene is in the amorphous state at room temperature, while the trans-form is semi-crystalline [7], the latter is most likely denser and less permeable for oxygen, which should also reduce its sensitivity to degradation. It is probably for this reason, that the spectrum of trans-polyisoprene does not show the peak at  $1744\text{ cm}^{-1}$ . Moreover, the bands in the lower energy range in the cis-spectrum are generally broader than in the trans-spectrum. This could either be due to small contributions of degradation products, or, more likely, to the difference in physical state. In liquids, a broadening of rotational bands is observed, whereas this rotation is frozen in solids, leading to decreasing half-widths of the band [22]. Since the highly viscous cis-sample is in the amorphous and the semi-crystalline trans-reference in the solid state, this explanation seems reasonable.

The weak modes of  $\text{CH}_2$  wagging at  $1310\text{ cm}^{-1}$  for cis- and at  $1329\text{ cm}^{-1}$  for trans-polyisoprene are both broadened and seem to contain small contributions of the respective modes. Moreover, the =C-H bending mode of trans-polyisoprene at  $1207\text{ cm}^{-1}$  is also present in the broad feature of the cis-spectrum, suggesting, that there are also some 1,4-trans unsaturations in the cis-polymer. According to the provider, both polymers are >98% pure cis- or trans-polyisoprene, respectively. Thus, it is questionable if a maximum of 2% other conformational isomers has become visible in the spectra. Moreover it remains unclear, if the small feature at  $1645\text{ cm}^{-1}$  can be related to a vinyl-content in both polymers. However, GOLUB and STEPHENS observed, that after irradiation of a natural all-cis-polyisoprene sample with UV-light *in vacuo*, the content of 1,4-units was 47.2%, of which 80% are in the 1,4-cis configuration [19]. This suggests, that this natural sample contained cis- and trans-units. They report further, that 31.2% were transformed into trisubstituted cyclopropyl structures (cis or trans), 12.0% occurred as vinylidene double bonds, 3.3% as vinyl C=C double bonds and that 6.3% are unaccounted for, but may have been lost in various end- or cross-linked structures [19]. Contrarily, polyisoprene consisting of a high 3,4-vinylidene content and a low content of 1,4-polyisoprenic double bonds showed upon irradiation under these conditions pronounced decrease in the 1,4-unsaturation and

a moderate loss for 3,4-units. The 1,4-units are assumed to produce cyclopropyl groups, additional 3,4-units, and some instable vinyl units [20]. This shows, that C=C double bonds in polyisoprene may undergo various transformations upon irradiation and could explain why vibrational modes, due to different isomers, are present in a single sample.

**Raman spectra of cis and trans reference compounds** In the Raman spectra of the cis- and trans-polyisoprene references (Fig. 6.2) less bands than in the IR spectra are observed. The Raman spectra are dominated by very intense methyl and methylene stretching bands between 3000 and 3200  $\text{cm}^{-1}$  and by the C=C stretching mode, which showed only a weak band at 1664  $\text{cm}^{-1}$  in the IR spectra. The fingerprint region of the Raman spectra is dominated by few broad features at 1450-1050  $\text{cm}^{-1}$ , while numerous bands at this spectral range were observed in the IR. This also applies to the low-energy spectral region, where only few and weak deformational Raman modes between 1060 and 990  $\text{cm}^{-1}$  are present.

Overall, there are more peaks in the trans- than in the cis-spectrum. The position of the Raman modes matches the literature data for the trans-sample well, but for the cis-spectrum, a shift to higher frequencies of 3-7  $\text{cm}^{-1}$  as compared to literature data is noticed. Since the Raman data for cis-polyisoprene was recorded using a different type of spectrometer, the observed shift is most likely due to different calibration [47].

**Comparison of Raman spectra of cis and trans references** The most striking difference between the cis- and the trans-polymer is located in the high-energy range. For the cis-form, there is only one asymmetric maximum at 2913  $\text{cm}^{-1}$ , which is accompanied by shoulders at 2932 and 2860  $\text{cm}^{-1}$  and at 2964 and 2881  $\text{cm}^{-1}$  due to CH<sub>2</sub> and CH<sub>3</sub> stretching, respectively.

In the trans-spectrum, the two bands at 2909 and 2881  $\text{cm}^{-1}$  due to CH<sub>2</sub> and CH<sub>3</sub> stretching are most intense. Weaker peaks of CH<sub>2</sub> stretching at 2941 and 2680  $\text{cm}^{-1}$  and of CH<sub>3</sub> stretching at 2974 and 2829  $\text{cm}^{-1}$  flank the two intense Raman modes in the trans-spectrum. Additionally, between these two bands, a small peak at 2896  $\text{cm}^{-1}$  is observed, for which no assignment has been provided. In literature, an unassigned band at 2890  $\text{cm}^{-1}$  in the IR-spectrum of trans-polyisoprene has been reported, that might have the same origin.

Another noticeable difference between the two constitutional isomers is the peak shift of the C=C stretching mode from 1666  $\text{cm}^{-1}$  in cis- to 1671  $\text{cm}^{-1}$  in trans-polyisoprene. More-

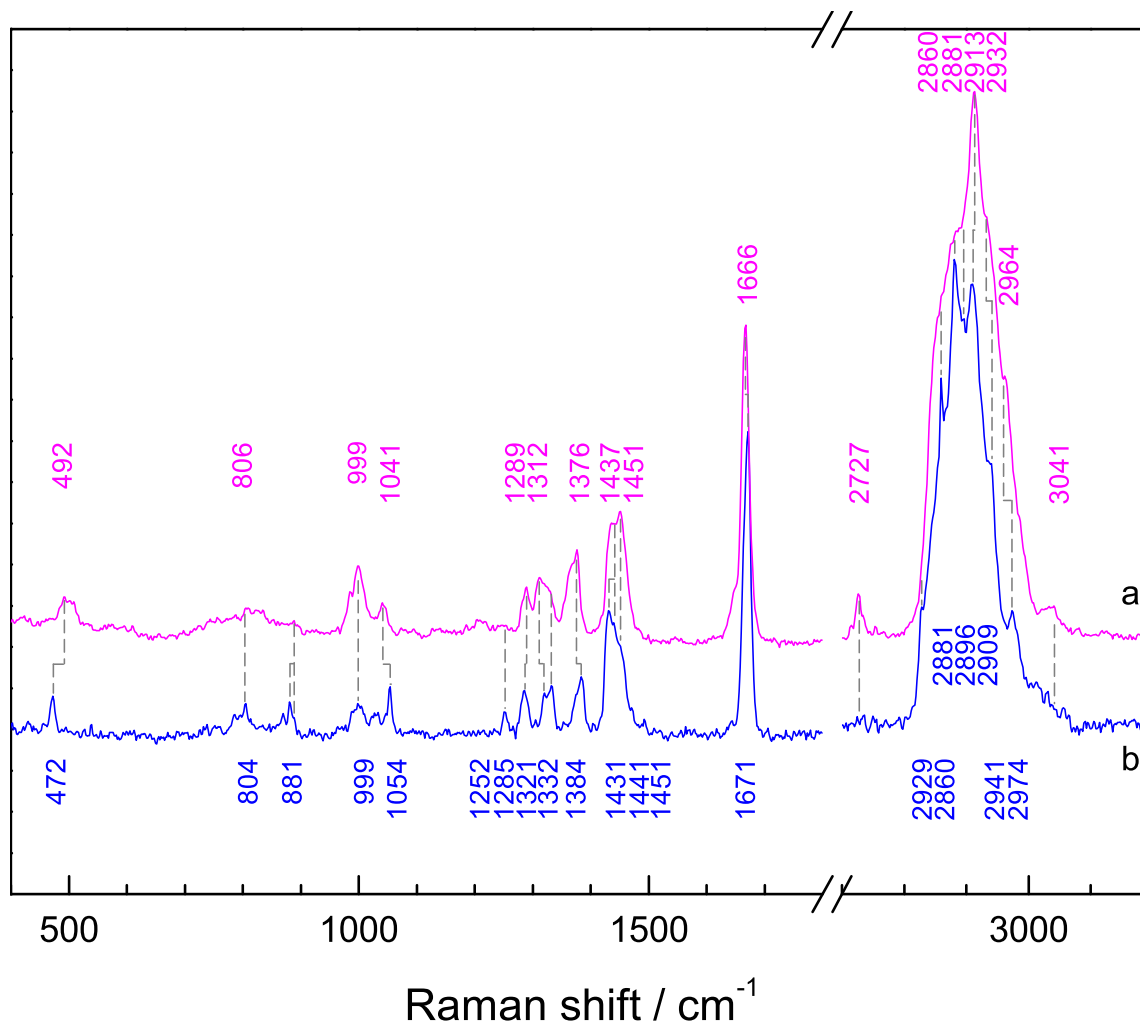


Figure 6.2: Comparison of Raman spectra of (a) 1,4-cis (red line) and of (b) 1,4-trans polyisoprene references (blue line) from SIGMA-ALDRICH. In order to improve comparability, spectrum (a) is multiplied by a factor of 0.6.

over, the weak shoulder at  $1645\text{ cm}^{-1}$ , that was noted in both IR spectra and possibly is related to vinyl stretching, is only found in the Raman spectrum of the cis-reference. In contrast to the IR-spectra, no bands related to degradation products are observed.

The cis-polymer displays bands of medium to weak intensity at  $1451$  and  $1437\text{ cm}^{-1}$ , while there are three partially overlapping bands at  $1451$ ,  $1441$  and  $1431\text{ cm}^{-1}$  in the trans-standard. The band at  $1441\text{ cm}^{-1}$  has been assigned to  $\text{CH}_3$  deformations of 1,2- or 3,4-vinyl units, whereas the other two are related to  $\text{CH}_2$  deformations. Thus, also the Raman mode at  $1441\text{ cm}^{-1}$  accounts for a small vinyl content in the trans-reference.

Three deformation vibrations in the cis-spectrum at  $1376$  ( $\text{CH}_3$ ),  $1312$  ( $\text{CH}_2$  or  $=\text{C-H}$  due to 3,4-vinyl units) and  $1289\text{ cm}^{-1}$  ( $=\text{C-H}$ ) oppose five bands at  $1384$  ( $\text{CH}_3$ ),  $1332$  ( $\text{CH}_2$ ),  $1321$  ( $=\text{C-H}$  deformations related to 1,2-vinyl-units),  $1285$  ( $\text{CH}_3$ ) and  $1252\text{ cm}^{-1}$  ( $\text{CH}_2$ ) in the trans-spectrum. However, the feature at  $1312\text{ cm}^{-1}$  in the cis-compound is broad ( $1340\text{-}1300\text{ cm}^{-1}$ ) and seems to contain three or four Raman modes. Raman bands located at this range are caused by  $\text{CH}_2$  wagging and 1,2- and 3,4-vinyl  $=\text{C-H}$  deformations.

The observations give rise to the assumption, that trans-polyisoprene indeed contains a small amount of 1,2-vinyl contributions, and that 1,2- and / or 3,4-units are also present in the reference sample of the cis-isomer.

The weak peaks at  $2725$  and  $3036\text{ cm}^{-1}$  next to the  $\text{CH}_2$  and  $\text{CH}_3$  stretching modes, which are found in the IR spectra also occur in the Raman spectrum of the cis reference compound at similar positions (ie, at  $3041$  and  $2727\text{ cm}^{-1}$ ). The former was assigned to  $=\text{C-H}$  stretching vibrations, while an assignment to the  $\text{CH}_3$  deformation overtone at  $1376\text{ cm}^{-1}$  seemed to be most likely. Since this Raman mode is weaker and also shifted to  $1384\text{ cm}^{-1}$  in the trans-spectrum, the band is probably swamped by the spectral noise. Although weak features seem to be present between  $3000$  and  $3080\text{ cm}^{-1}$  in the trans-spectrum, too, they are also overlaid by noise.

In the low-energy region of the cis-spectrum, there are small bands at  $1041$ ,  $1000$ ,  $975$  and  $492\text{ cm}^{-1}$  assigned to  $\text{CH}_3$  rocking,  $\text{C-CH}_3$  stretching ( $1000$  and  $975\text{ cm}^{-1}$ ), and  $\text{C-C}$  bending. In trans-polyisoprene, related bands are observed at  $1054$ ,  $1000$ ,  $881/889$ ,  $804$  and  $472\text{ cm}^{-1}$ , due to  $\text{CH}_3$  deformations ( $1054$ ,  $1000$  and  $472\text{ cm}^{-1}$ ) and to  $=\text{C-H}$  bending and wagging ( $881$  and  $804\text{ cm}^{-1}$ ).

The comparison of the spectra of cis- and trans-polyisoprene showed, that differences between the two forms can be observed throughout the IR and Raman spectra.

## 6.2 Spectra of Natural Rubber Samples

**IR spectra of artificially aged raw latex** The IR spectra of the light-aged latex specimens were recorded with the diamond ATR crystal and are plotted in Fig. 6.3. The spectra were recorded three months after irradiation and storage in dark. Spectra of the front and rear side of the naturally degraded sample are also displayed. The main features in the spectra are hydroxyl stretching modes located  $3640\text{-}3200\text{ cm}^{-1}$ , methyl and methylene stretching modes between  $3200\text{ and }3000\text{ cm}^{-1}$ , carbonyl stretching at  $1830\text{-}1600\text{ cm}^{-1}$ , and the deformation vibration region at  $1000\text{-}600\text{ cm}^{-1}$  [21].

The absorption bands between  $2970\text{-}2800\text{ cm}^{-1}$  characteristic for methyl and methylene groups disappeared upon increasing irradiation as well as the absorption band at  $835\text{ cm}^{-1}$ , which is most likely caused by a C-H twisting vibration belonging to a tri-substituted C=C double bond. Moreover, a peak shift from  $841\text{ cm}^{-1}$  in fresh to  $835\text{ cm}^{-1}$  in the most degraded sample was observed. The decrease of the weak features at  $3036\text{ cm}^{-1}$  related to =C-H stretching and the band at  $2725\text{ cm}^{-1}$ , which is assumed to be an overtone of a  $\text{CH}_3$  deformation shows the same tendency. Also the weak stretching band of the carbon-carbon double bond at  $1666\text{ cm}^{-1}$  decreases during oxidation, while carbonyl bands arise in the region of  $1830\text{-}1600\text{ cm}^{-1}$ . Broad band features show up in the range of  $1200\text{-}800\text{ cm}^{-1}$  with contributions of C=O, C-O and CCO stretching vibrations of degradation products such as peroxides, alcohols, aldehydes, carboxylic acids, ketones, and epoxides. A list of typical degradation products found in polyisoprene including band assignment is given in Tab. 6.2.

The weak absorption band at  $2725\text{ cm}^{-1}$  can be observed in all spectra of polyisoprenes and may be regarded as a characteristic spectral feature of polyisoprenes. It is found for fresh and partially degraded cis- and trans-polyisoprenes, but vanishes in completely oxidised samples (see Figs. 6.3 h and 6.5 g-i). In all spectra, the absorption band at  $2725\text{ cm}^{-1}$  seems to be related to the bands at  $3036$  and  $837\text{ cm}^{-1}$  (assigned to =C-H stretching and twisting), but also to  $\text{CH}_2$  and  $\text{CH}_3$  deformations at  $1446$  and  $1375\text{ cm}^{-1}$ , an observation, that was already made in the previous section.

In the course of the ongoing degradation, initially an increase of hydroxyl absorptions was observed ( $3640\text{-}3200\text{ cm}^{-1}$ ), followed by a subsequent decrease. The two spectra of the naturally degraded specimen fit well in the spectral progression of artificially degraded polyisoprene samples. In the low-energy spectral range there are two prominent features at  $565$  and  $498\text{ cm}^{-1}$ , which are described as a characteristic feature of the 1,4-cis form of

polyisoprene [47, 9], such as C-C skeletal vibrations.

**Raman spectra of artificially aged raw latex** In Fig. 6.4 the FT-Raman spectra of fresh and severely degraded latex specimens are displayed. As can be seen in Fig. B.2, colour changes of the sample occurred during degradation. Despite the different degrees of oxidation, all three spectra are very similar. Contrary to the IR spectra, the valence vibration of the carbon-carbon double bond at  $1666\text{ cm}^{-1}$  is very prominent here. A very weak band at  $1556\text{ cm}^{-1}$  is found in all three spectra, which is usually not observed in polyisoprene spectra. Is very likely due to an N-H deformation vibration of secondary amines [48]. The latex milk contains a small amount of ammonia pre-vulcaniser which is probably the nitrogen-source. In Tab. 6.1 IR and Raman bands for cis-polyisoprene including band assignment are given.

**Naturally degraded polyisoprene** The IR spectra of naturally degraded cis-polyisoprene samples and recently prepared solid and liquid material references are displayed in Fig. 6.5. Since the sample's interior is protected to a certain extent against oxidative degradation, spots of different colour and depth were probed to study various degrees of degradation. Spectra of the aged samples were recorded using the ATR objective of the microscope, while fresh samples were characterised with the diamond ATR crystal. An adequate arrangement of the respective spectra allowed a match with the course of the degradation process observed for the artificially aged samples (Fig. 6.3).

### 6.3 Artificially versus Naturally Degraded Rubber Samples

The observed increase and subsequent decrease of the hydroxyl absorption during ageing by artificial light is in accordance with the degradation process displayed in Fig. 3.1. In the present case, the artificial ageing process is in good agreement with the real photochemically induced oxidation processes of polyisoprene (see Figs. 6.3 and 6.5). Interestingly, the visual impression of a sample's condition did not always match the results derived from the vibrational spectra. This observation is in agreement with [5] and could be due to different penetration depth of the probing radiation, especially as some of the samples revealed an inhomogeneous composition. Since spectra of the old samples were recorded with the ATR-objective of the microscope, the seemingly inconsistent results might also

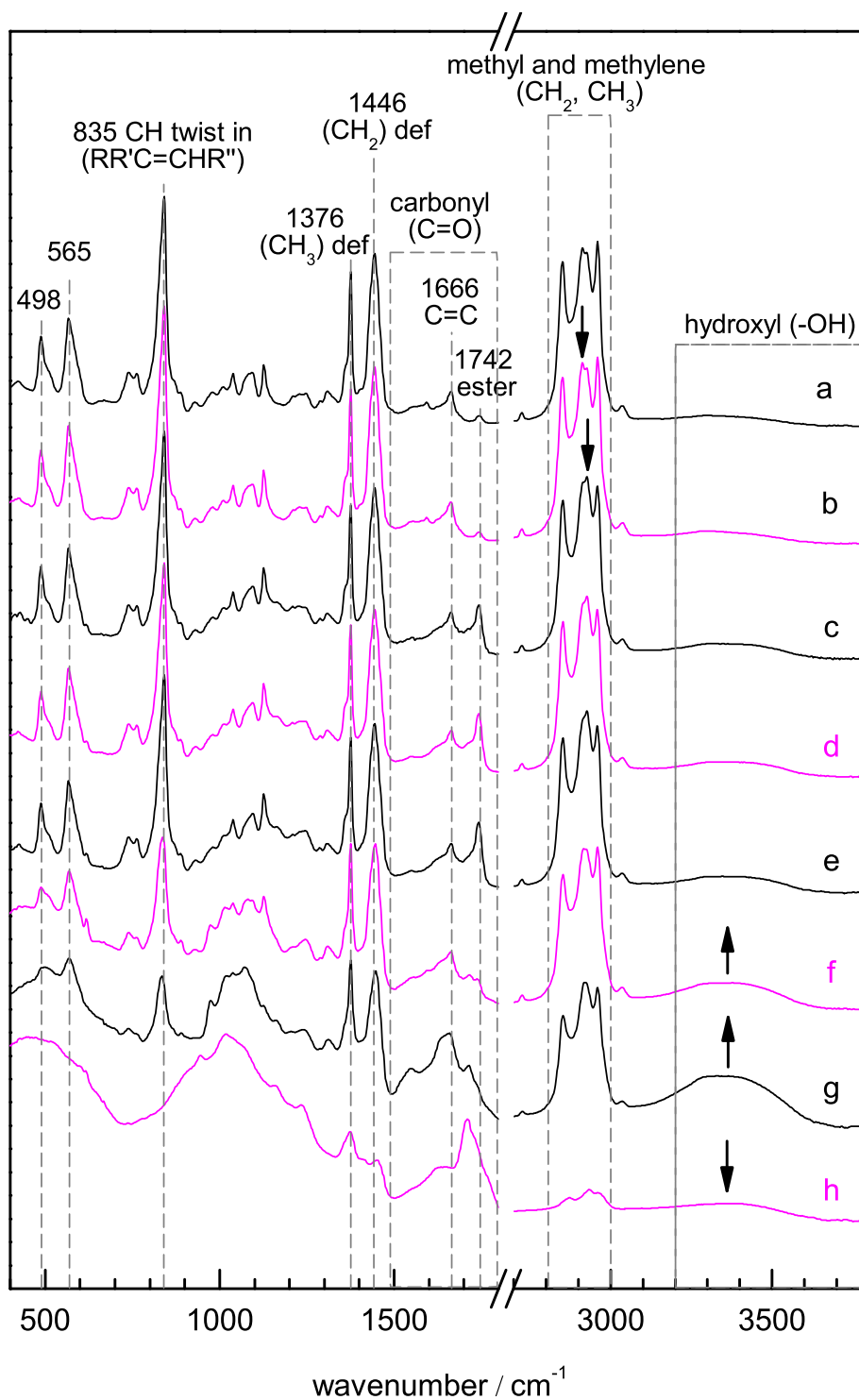


Figure 6.3: IR spectra of light-aged 1,4-cis polyisoprene and of samples, which have been irradiated for 4.5 months with daylight through window glass, recorded with a diamond ATR cell. (a) 0 h, (b) 1h, (c) 3 h, (d) 4h, (e) 5 h, (f) naturally degraded reverse side, (g) naturally degraded front, (h) 73 h irradiation.

Band $\text{cm}^{-1}$	Assignment	
3435	associat. alcohols	O-H
3325	associat. hydroperoxides photoinstable	
3070		O-H str
3005	epoxide	
2725*	aldehydes	C-H str
2715	aldehydes	C-H str.
1775	peroxyesters or monomeric carb. acid	C=O str.
1715	carb. acid	C=O str
1740	esters	C=O
1715 or 1766	sat. carb. acid	C=O str
1715 or 1722	sat. methylketones photoinstable	C=O str
1693	$\alpha, \beta$ unsat. methylketones very photoinstable not for 1,4-cis	C=O
1175	peroxides or monom. carb. acids more for thermo-oxidation	C=O
1165	sat. carb. acids	C-O str
1080*		CCO str <sub>asym</sub>
1022*	primary alcohols ch	CCO str <sub>sym</sub>
888	tert. hydroperoxides	O-O
874	epoxides	ring vibr.

Table 6.2: Absorption bands of degradation products of polyisoprene rubber [21]. Values marked by an asterisk are found in [15].

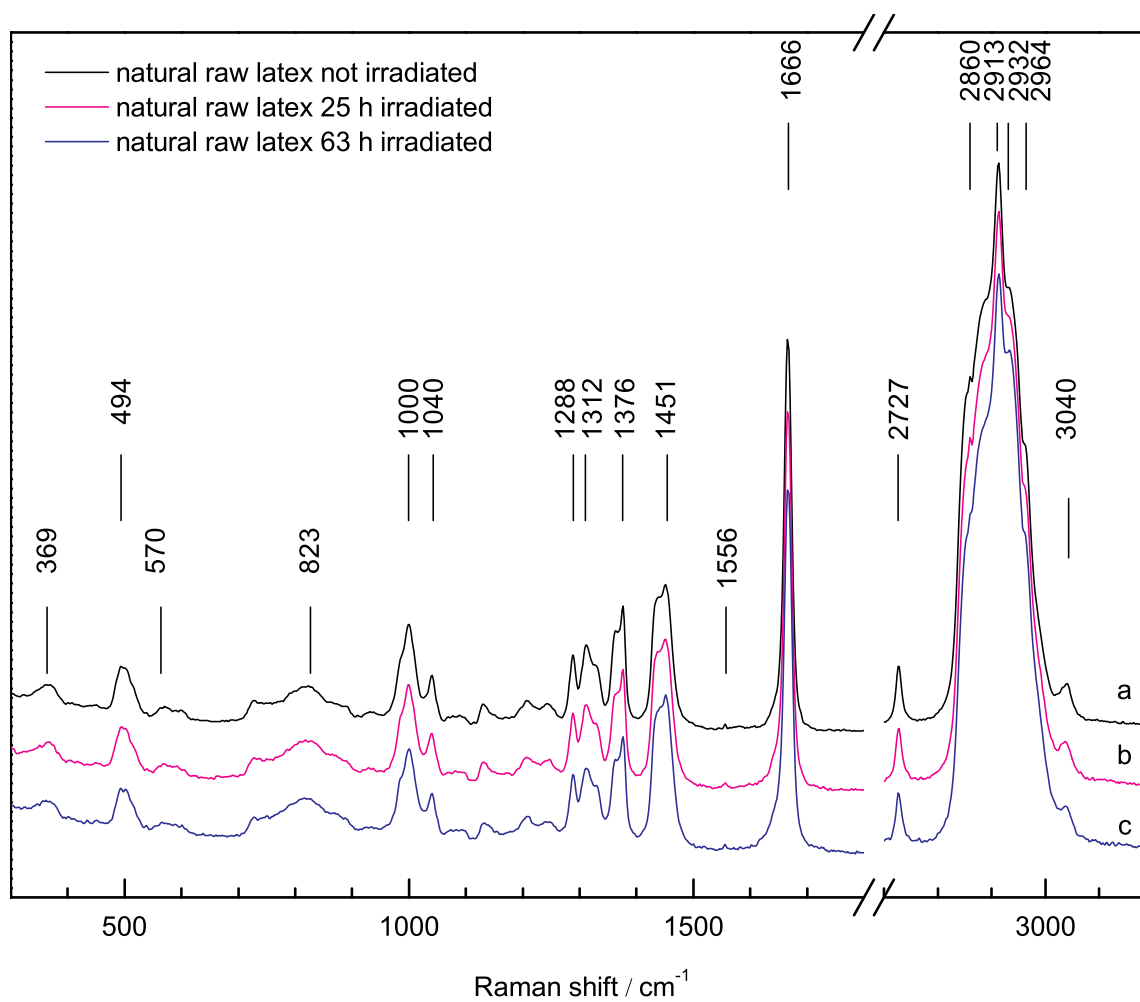


Figure 6.4: Raman-microscope spectra of light-aged 1,4-cis polyisoprene. (a) 0 h, (b) 25 h, (c) 63 h irradiated.

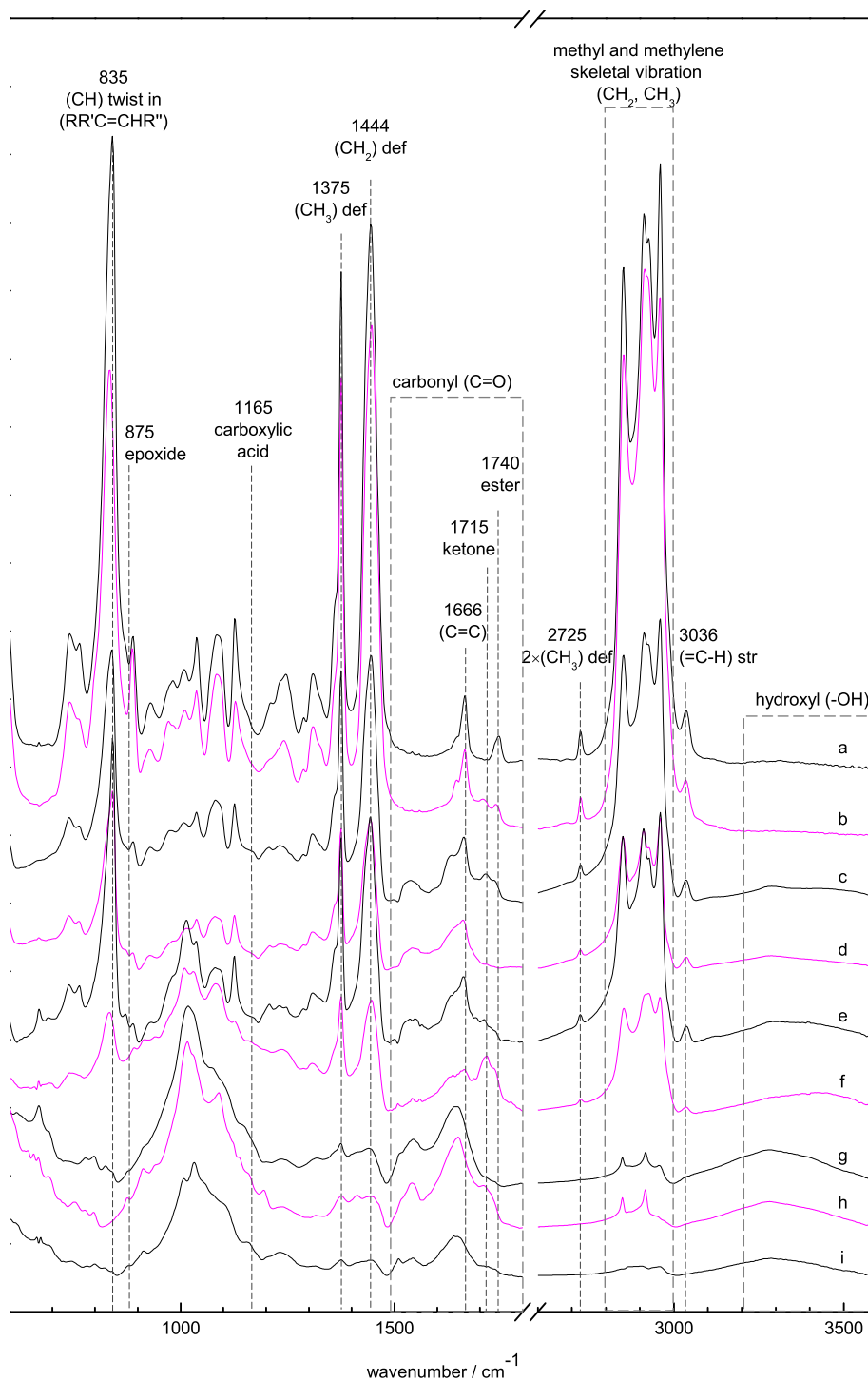


Figure 6.5: IR spectra of freshly cut surfaces of naturally degraded 1,4-cis polyisoprene and two reference samples. (a-b): recorded with a diamond ATR cell. (c-i): recorded in an ATR microscope. (a) solid synthetic (b) liquid natural, (c) Ceylon scraps freshly cut, (d) Lanadron freshly cut, (e) Parasoft Brazil freshly cut, (f) Lanadron old surface, (g) Ceylon scraps old cut, (h) Parasoft Brazil old surface, (i) Ceylon scraps old surface.

be due to pressure-induced relaxation processes of the high viscous samples during the measurements. In addition, previous research on polyethylene bags has shown, that the physical sample condition is not always in agreement with the spectroscopically determined degree of oxidation [49]. In future, this could be clarified by the use of differential scanning calorimetry, which is suitable to determine the degree of crystallinity and rheological measurements for molecular weight studies.

The corresponding Raman spectra recorded with the respective microscope showed, that this optical setup still delivers enough signal for the investigation of rubber. Due to the 1064 nm excitation source, no fluorescence or heat irradiation obscure the spectra. All bands characteristic for cis-polyisoprene were found in the Raman spectra after artificial ageing.

A comparison between the FT-IR and the Raman spectra of the specimen that was irradiated for 73 h (see Figs. 6.3 and 6.4) revealed, that the Raman spectrum contains valuable information which cannot be obtained from the FT-IR spectrum any more, since it is dominated by degradation products. The respective Raman spectra still allowed a structural identification of this sample. Moreover, the C=C stretching vibration at  $1666\text{ cm}^{-1}$  is very pronounced in the Raman spectrum. Its intensity seems to remain constant during the degradation process. However, this observation does not indicate that no double bonds were consumed during the artificial ageing, especially, since a clear decrease of the  $835\text{ cm}^{-1}$  absorption band was observed in the IR spectra, which arises most likely from a C-H twisting of a hydrogen attached to the C=C double bond. This observation may be related to higher Raman cross-sections of the C=C stretching modes for the educts (parent states) as compared to the degradation products. COLOMBINI and LÉAR [28] have published Raman spectra of naturally degraded latex in which this band had vanished. From this it can be concluded, that the duration of the artificial ageing was either not long enough, or that the laser focus mainly probed non-degraded material below the surface. While the Raman intensity of the C=C stretching vibration mode dominates the fingerprint region, other modes which are exclusively related to the degradation products like C=O stretching showed negligible contribution to the Raman spectrum. Since the mode intensity is proportional to the changes in polarisability ( $I \sim \alpha^2$ ), it will be very high for those vibrations involving electron-rich and non-polarised functional groups such as the C=C stretching. Yet, these modes, in which changes in the permanent dipole are involved, will present very little contribution to the Raman spectrum (see above). Hence,

the degradation products of oxidised C=C bonds do not contribute significantly to the Raman spectrum. The assumption of the different scattering cross-sections could possibly be proven by quantitative measurements of the Raman spectra, which were, however, not possible in the chosen setup.

## 6.4 Brown and White Balata

IR and Raman spectra of two different grades of natural 1,4-trans polyisoprenes, namely processed brown and purified white balata from Brazil, were recorded using the diamond ATR and the Raman microscope, respectively. Spectra with labelled peak positions are given in the appendix in Figs. A.3 (brown and white balata, IR), A.10 (brown balata, Raman) and A.11 (white balata, Raman). In Figs. 6.6 and 6.7 the differences in the IR and Raman spectra of the two grades of natural 1,4-trans polyisoprenes are displayed, respectively. Band assignments for spectra of 1,4-trans polyisoprene from literature are reproduced in Tab. 6.3. The table comprises IR data of fresh and degraded material [15] and Raman data of  $\alpha$ - and  $\beta$ -modifications [9]. Additionally, bands of calculated Raman spectra are cited [24].<sup>1</sup> According to the producer, the purification of the brown balata yields the white balata, which is used for the production of dental cones for root fillings.

**Discussion of the IR spectra of balata** The IR spectra of balata are in very good agreement with the data given for 1,4-trans polyisoprene in Tab. 6.3. Nearly all characteristic bands reported in literature are observed in the methyl and methylene C-H stretching region. Moreover, the C=C stretching mode at  $1665\text{ cm}^{-1}$  is present in the two samples as well as characteristic features of CH<sub>2</sub> and CH<sub>3</sub> deformation vibrations ( $1450\text{-}1200\text{ cm}^{-1}$ ), skeletal stretching modes of the C-C bonds ( $1300\text{-}900\text{ cm}^{-1}$ ) and deformation vibrations of a tri-substituted C=C double bond, such as the important C-H twisting mode at  $835\text{ cm}^{-1}$ . Only two CH<sub>3</sub> stretching modes at  $2975$  and  $2830\text{ cm}^{-1}$  and an unassigned mode at  $2890\text{ cm}^{-1}$  have been reported in literature, but are not identified in the brown or white balata. However, they may well be included in the broad feature in this spectral range. Especially in the range of  $1750\text{-}1500\text{ cm}^{-1}$ , some differences to literature standards are observed. They can be related to carbonyl and C=C stretching vibrations (found in the

---

<sup>1</sup>In the Raman analysis, a commercial >95% 1,4-trans polyisoprene from SIGMA-ALDRICH (182168) was used [9], which is most likely the same product as the 1,4-trans polyisoprene standard SIGMA-ALDRICH that was investigated by [15] and as was also studied in the present work. The material was determined as the  $\alpha$ -1,4-trans modification [9].

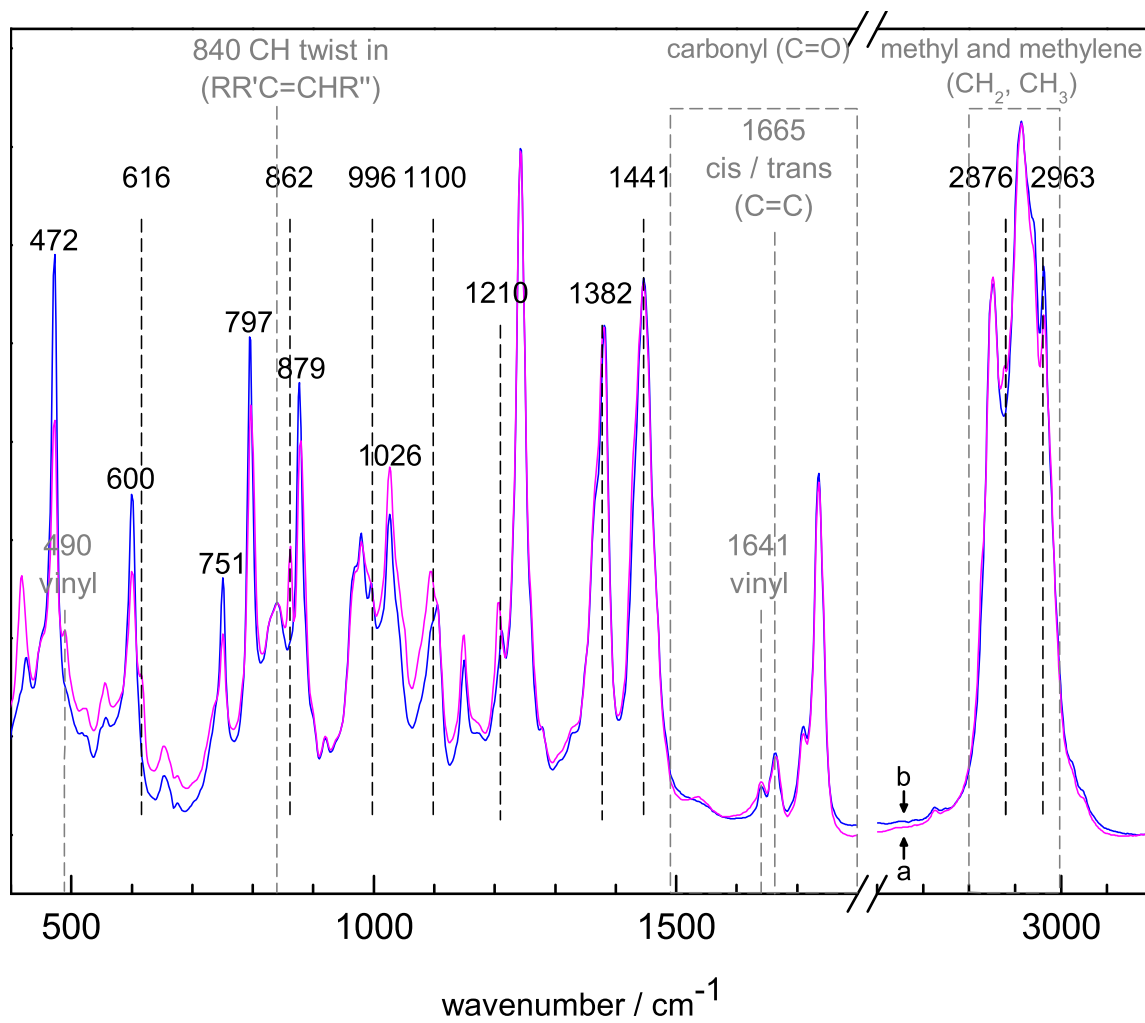


Figure 6.6: Differences in IR spectra of natural balata: (a) purified white (red line), (b) processed brown balata (blue line).

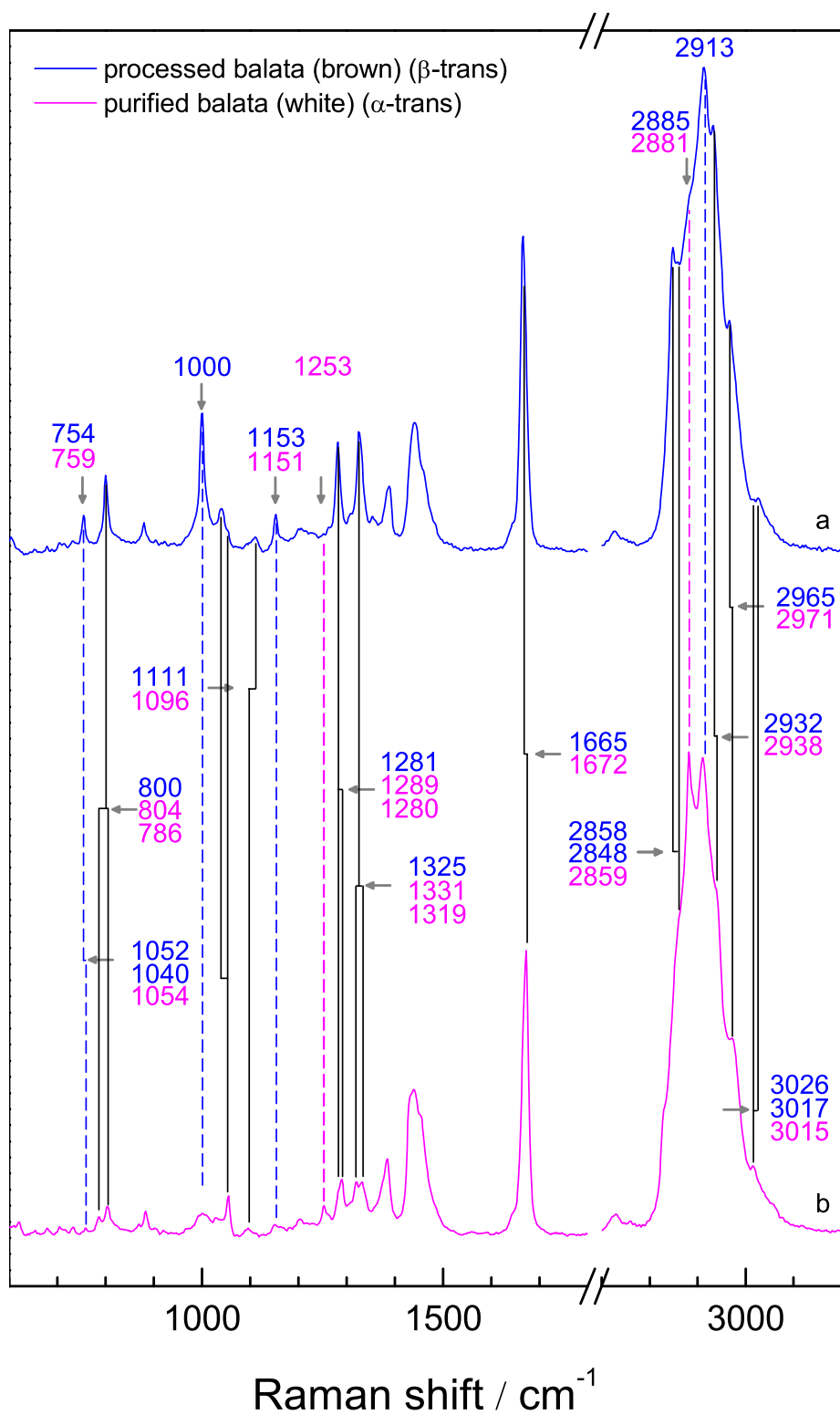


Figure 6.7: Raman spectra of two different types of 1,4-trans polyisoprenes. (a) processed brown balata, predominantly in the  $\beta$ -state, (b) purified white balata, predominantly in the  $\alpha$ -state, both from TANARIMAN Ltd. Brasil. Dashed lines indicate bands that are only observed in one of the spectra.

Raman meas.	Raman calc.	Raman $\alpha$ -trans	Raman $\beta$ -trans	IR $\alpha$ -trans fresh	IR $\alpha$ -trans degr.	Assignment
3050 w	3041	3052 w/sh <b>3019</b> m	3057 w/sh <b>3022</b> m	3053 vw 3015 w	3053 vvw	=C-H str =C-H str
2970 vs	2965	<b>2972</b> m	<b>2964</b> m	2975 vs	2970 vs	CH <sub>3</sub> str <sub>asym</sub>
2960 m	2951			2965 sh		CH <sub>3</sub> str <sub>asym</sub>
2935 m	2932	<b>2934</b> s/sh	<b>2931</b> s	2936 sh	2933 vs	CH <sub>2</sub> str <sub>asym</sub>
2912 vs	2906	2910 vs	2910 vs	2915 vs 2890 wsh		CH <sub>2</sub> str <sub>sym</sub>
2895 vs	2889	2881 vs	2882 vs	2880 wsh	2878 wsh	CH <sub>3</sub> str <sub>sym</sub>
2854 vs	2848	<b>2857</b> s/sh	<b>2850</b> s	2852 vs	2856 wsh	CH <sub>2</sub> str <sub>sym</sub>
2835 s	2830	2828 m/sh 2728 w/br <b>1670</b> s	2829 m/br 2728 vw/br	2830 sh	2830 sh	CH <sub>3</sub> str <sub>sym</sub>
1669 vs	1662	1666 s/sh 1643 w/sh	1666 s 1642 w/sh	1668 m	1671 vwsh	(1,4) C=C C=C str C=C vinyl
1465 m	1458	1452 m	1453 m	1447 s	1450 s	CH <sub>2</sub> def <sub>asym</sub>
1444 s	1434	1432 ms	1434 m	1433 sh	1430 s	CH <sub>2</sub> def <sub>sym</sub>
1384 s	1378	1384 m 1371 mw	1384 m	1382 s	1381 s	CH <sub>3</sub> def/C-C str CH <sub>3</sub> def
1365 s	1356	1361 vw		1358 sh	1358 sh	CH <sub>3</sub> def <sub>sym</sub> /CH <sub>2</sub> def
1335 m	1329					CH <sub>2</sub> wag
1330 m	1321	<b>1329</b> m <b>1319</b> vw	<b>1325</b> m	1330 vw		CH <sub>2</sub> wag/twist
1290 m	1284	1288 m <b>1279</b> m	1288 m	1280 vw		=C-H bend <sub>ip</sub> CH <sub>2</sub> wag/twist
1250 m	1239	<b>1252</b> mw		1254 vw	1244 wbr	CH <sub>2</sub> wag/twist
1215 w	1204			1207 m	1206 w	=C-H bend <sub>ip</sub>
1154 w	1142	1158 w/br	<b>1151</b> w	1150 m	1150 wsh	CH <sub>3</sub> wag
1098 m	1104	<b>1100</b> w/br		1096 m 1089 w		C-CH <sub>2</sub> str C-CH <sub>2</sub> str
1048 m	1041	1053 m	1053 m	1051 w	1052 sh	CH <sub>3</sub> rock
1035 m	1029	1035 m/br	1035 m/br	1030 w		CH <sub>3</sub> rock
1010 m	1001		1009 m/sh			C-C str
985 m	981	998 m	<b>997</b> m 972 w	990 w		C-C str/C-CH <sub>3</sub> str CH <sub>2</sub> / CH <sub>3</sub> rock
882 m	880	881 mw	877 mw	883 m 862 m 844 w	881 w 862 w	=C-H bend <sub>oop</sub> / CH <sub>3</sub> wag
		<b>802</b> m	<b>800</b> m	800 m	801 v	=C-H wag
780 w	774	<b>785</b> m				CH <sub>2</sub> rock
770 w	758	758 mw/br	<b>752</b> mw	751 w	750 vw	CH <sub>2</sub> rock

Table 6.3: Literature values for bands in the following spectra of 1,4-trans polyisoprene: measured and calculated Raman spectra [24]; measured Raman spectra of  $\alpha$ - and  $\beta$ -modifications [9]; IR spectra of fresh and degraded material [15]. Numbers in bold indicate the bands that are suitable for the discrimination from  $\alpha$ - and  $\beta$ -modification.

range of 1800-1500  $\text{cm}^{-1}$  [22]). The additional bands at 490  $\text{cm}^{-1}$  (predominantly in white balata) and 1640  $\text{cm}^{-1}$  (found in brown and white balata) are of particular interest, as they can be assigned to 1,4-cis and 3,4-vinyl deformations (490  $\text{cm}^{-1}$ ) and to 1,2- or 3,4-vinyl C=C stretching modes, respectively. BUNCE et al. [9] and CORNELL and KOENIG [47] have studied the differences in Raman spectra of the various constitutional isomers of polyisoprene (see Fig. 2.1). Vibrational modes of the different constitutional isomers of polyisoprene are given in Tab. 6.4. Bands at 1710 and 1736  $\text{cm}^{-1}$  can be assigned to degradation products such as saturated carboxylic acids, methylketones and / or esters (see Tab. 6.2).

1,4-cis	1,4-trans	1,2-vinyl	3,4-vinyl	Assignment
3033	3010	3074	3068	C=C str
		2987	2980	C=C sym str
1662 /1666*	1662/1666*	1639/1645*	1641/1645*	C=C
1445	1445	(1440)	1442	CH <sub>3</sub> asym def
1369	1380		1362	CH <sub>3</sub> sym def
1321	1323			=C-H def
1312**				
1308		1304	1304	=C-H def
1130	1148	(1131)	1162	C-CH <sub>3</sub> str
1070	1094		1083	
		910/906*		C-H def/CH <sub>2</sub> def
889	879		885*	C-H def
835*	835*			C-H def
	798**			
565			588	C-C skel. or =C-C-C bend.
572				
496**				
490**			490**	
	472**	472**	472**	

Table 6.4: Raman bands related to unsaturations in different polyisoprene conformers [47], with asterisk: IR-bands [21], double asterisk: Raman modes [9].

Since mixtures of the constitutional isomers are never found in nature [7], and vinyl functions have not been reported for natural polyisoprene [7, 15], the relatively high intensity of the band at 490  $\text{cm}^{-1}$  may on the one hand lead to the conclusion, that the white balata was mixed with another natural or synthetic polyisoprene. On the other hand, one

may conclude, that it has undergone some isomerisation during the purification process. Moreover, a broad vinyl feature has been reported in the range of 1400-1300  $\text{cm}^{-1}$ . Bands in 1,4-trans polyisoprene at 1382, 1358 and 1330  $\text{cm}^{-1}$  were assigned to  $\text{CH}_2$  and  $\text{CH}_3$  deformation modes [15], while [9] assigns a band at 1384  $\text{cm}^{-1}$  to a C-C stretch or to a  $\text{CH}_3$  deformation mode. In both samples a broad band with a maximum at 1382  $\text{cm}^{-1}$  was observed, which may well contain features of a vinyl content, too. Since the peak at 1640  $\text{cm}^{-1}$  is present in both samples, already the brown sample seems to have been either mixed or to have undergone some constitutional changes.

When comparing the IR-spectra of brown and white balata with each other, small differences are observed (see Fig. 6.6). For brown balata, the peak intensity at 2963  $\text{cm}^{-1}$  (asym.  $\text{CH}_3$  str) is higher and also bands at 879 and 797  $\text{cm}^{-1}$ , related to =C-H deformations, are more intense. Moreover, a band at 996  $\text{cm}^{-1}$  assigned to the C- $\text{CH}_3$  stretching, that is not found in the white sample, was also observed.

The white balata exhibits a band at 2876  $\text{cm}^{-1}$  (sym.  $\text{CH}_3$  str) instead of the asymmetric  $\text{CH}_3$  str at 2963  $\text{cm}^{-1}$  in the brown sample. Additionally, a peak at 862  $\text{cm}^{-1}$  (assigned to  $\text{CH}_3$  wagging) is found, which is not present in the brown sample. Moreover, the vinyl content seems to be slightly higher (1640 and 490  $\text{cm}^{-1}$ ) in white balata.

Peak shifts at 1212 and 1105  $\text{cm}^{-1}$  (brown) and 1207 and 1095  $\text{cm}^{-1}$  (white), respectively, are observed. They are related to =C-H bending (1212 / 1206  $\text{cm}^{-1}$ ) and to C- $\text{CH}_2$  stretching modes (1105 / 1095  $\text{cm}^{-1}$ ).

These differences, in particular at 879 and 797  $\text{cm}^{-1}$  are either due to differences in the nature of the C=C unsaturation or due to a slightly modified environment of the =C-H bond. The former case could be explained by a content of polyisoprene other than 1,4-trans, the latter by differences in the crystalline modification, as is discussed in the following.

**Discussion of the Raman spectra of balata** Although both samples consist of the same material, the small spectral differences found in the IR spectra become more obvious in Raman spectra. The most pronounced difference is found for the methyl and methylene stretch region (3000-2800  $\text{cm}^{-1}$ ). Moreover, a band shift of the C=C stretching modes from 1665 in brown to 1672  $\text{cm}^{-1}$  in white balata is visible. Numerous bands in the fingerprint region (1430-1000  $\text{cm}^{-1}$  [22]) are also shifted. A  $\text{CH}_2$  wagging mode at 1325  $\text{cm}^{-1}$  and a =C-H bending mode at 1281  $\text{cm}^{-1}$  in brown balata are split in two bands at 1331 and 1319  $\text{cm}^{-1}$  and at 1289 and 1280  $\text{cm}^{-1}$  in the white sample. In white, but not in brown balata a band at 1253  $\text{cm}^{-1}$  ( $\text{CH}_2$  deformations) is present. The Raman bands at 1153, 754 and in

particular at  $1000\text{ cm}^{-1}$  due to  $\text{CH}_3$  wagging,  $\text{CH}_2$  rocking and C- $\text{CH}_3$  stretching modes are more pronounced in the processed brown balata than in the white sample, while the  $\text{CH}_3$  rocking mode at  $1052\text{ cm}^{-1}$  is less intense in the brown sample.

The observations match very well the differences between the two crystalline modifications of  $\alpha$ - and  $\beta$ -1,4-trans polyisoprene presented by BUNCE et al. [9] (see. Fig. 2.2). A double peak in the methyl and methylene region at  $2881$  and  $2911\text{ cm}^{-1}$   $\text{CH}_2$  and  $\text{CH}_3$  stretching found in the white balata is characteristic for the  $\alpha$ -trans. The single peak at approx.  $2913\text{ cm}^{-1}$  found in the brown sample matches the  $\beta$ -modification, and also the peak shift from  $1665$  ( $\beta$ ) to  $1672\text{ cm}^{-1}$  ( $\alpha$ ) has been described. For the  $\beta$ -form, a reduced peak intensity at  $1053\text{ cm}^{-1}$  and an increased intensity for the band at  $997$ - $1000\text{ cm}^{-1}$  has been reported, as well as the band splitting from  $1325\text{ cm}^{-1}$  ( $\beta$ ) into two bands at  $1329$  and  $1319\text{ cm}^{-1}$  ( $\alpha$ ). Moreover, the band at  $1253\text{ cm}^{-1}$  ( $\text{CH}_2$  deformations) is present only in the  $\alpha$ -form. Peaks at  $1009$  and  $972\text{ cm}^{-1}$  are characteristic for the  $\beta$ -form, and a feature at  $998\text{ cm}^{-1}$  has been noted for both crystalline forms. A possible superposition of both bands could explain, why there is only a rather intense band in the brown sample at  $1000\text{ cm}^{-1}$ , while there is no pronounced feature in the white sample. A weak broad combined mode of  $\text{CH}_2$  and  $=\text{C-H}$  deformation vibrations at  $1158\text{ cm}^{-1}$  was reported for the  $\alpha$ -modification, whereas it is located at  $1151\text{ cm}^{-1}$  for  $\beta$ -1,4-trans polyisoprene. For the white sample, a weak and broad feature with its maximum at  $1151\text{ cm}^{-1}$  is observed, which is located at  $1153\text{ cm}^{-1}$  for the brown balata. This slight shift may be due to noise or due to contributions of  $\text{CH}_3$  modes of the  $\beta$ -form at  $1151\text{ cm}^{-1}$ .

A peak shift from  $758\text{ cm}^{-1}$  in  $\alpha$ -trans to  $752\text{ cm}^{-1}$  in the  $\beta$ -form is reported. The weak band at  $754\text{ cm}^{-1}$  in the brown sample thus seems to consist of the contributions of both crystalline forms. Additionally, the band at  $1281\text{ cm}^{-1}$ , which has been described as a feature of the  $\alpha$ -form, is also found in the brown sample.

The results show, that both balata samples contain both crystalline modifications of 1,4-trans polyisoprene. While the brown balata seems to consist predominantly of the  $\beta$ -form, the purified white balata shows more features that argue for the  $\alpha$ -form. As described by SAUNDERS and SMITH, the evaporation speed of the dissolved polymer and the speed of a melt cooling influence the crystallisation process. If the transformation from the liquid to the solid state occurs slowly, the  $\alpha$ -modification is preferred. The authors reported, that evaporation of a solution in benzene and slow cooling ( $0.5^\circ\text{C}$  per hour) nearly always yielded polymer films in the  $\alpha$ -modification. On the contrary, a polymer film in the  $\beta$ -state

was predominantly obtained by cooling the melt from temperatures  $>80^{\circ}\text{C}$  down to room temperature [7]. Further, mixtures of both crystalline forms are frequently obtained if the samples are not treated properly. From this, the conclusion can be drawn that the brown balata was most likely dissolved in the purification process, and that purified material was not molten after the purification process.

## 6.5 Analysing an Art Object

**IR spectra of “Mies” and a raw latex film** Spectra of an old and a new sample of the seating of the chaise longue “Mies” and a non degraded latex film were recorded in the diamond ATR cell. The spectra are shown in Fig. 6.8. IR spectra with marked peak positions for these three samples are given in the appendix, Figs. A.4 - A.6.

Most of the absorption bands that are characteristic of 1,4-cis polyisoprene are found in all three samples. These bands are in the methyl and methylene C-H stretching region at 2958, 2917 and 2851  $\text{cm}^{-1}$ . Moreover, the strong bands at 1446 and 1376  $\text{cm}^{-1}$  ( $\text{CH}_2$  and  $\text{CH}_3$  deformation vibrations) as well as the =C-H twisting at 835  $\text{cm}^{-1}$  and a medium intense band 566  $\text{cm}^{-1}$  are related to 1,4-cis structures. Also the C=C stretching mode at 1665  $\text{cm}^{-1}$  is present, albeit only with a weak intensity.

**Degradation products found in the “Mies” spectra** Despite the spectral similarities, some differences between the “Mies” samples and the raw latex are obvious: very strong and broad bands dominate the regions of 1200-1000 and of 480-420  $\text{cm}^{-1}$  in the two “Mies” samples. The absorption band at approx. 835  $\text{cm}^{-1}$  is much more pronounced for the reference sample than for both “Mies” samples, and the same peak shift from 841 to 835  $\text{cm}^{-1}$  that is observed during the degradation of artificially and naturally degraded rubber (see Figs. 6.3 and 6.5) has occurred. As can be seen in Fig. 6.3 (f, reverse side of a raw latex, exposed to daylight through window glass for 4.5 months), the bands at 2925 and 2913  $\text{cm}^{-1}$  merge upon ageing to a single broadened band at 2917  $\text{cm}^{-1}$ , as is observed for the “Mies” samples, too. All this indicates that the “Mies” samples are degraded. The band at around 1200-1000  $\text{cm}^{-1}$  is in the range of C-O stretching bands as can be found in degradation products. The peak at 1091  $\text{cm}^{-1}$  can be assigned to primary alcohols. It is already present in raw latex, but increases drastically for the new and even more for the old “Mies” sample. The feature at 480-420 could as well be due to primary unsaturated alcohols, namely C-O deformations with a peak at 465  $\text{cm}^{-1}$ . Possibly, it comprises also

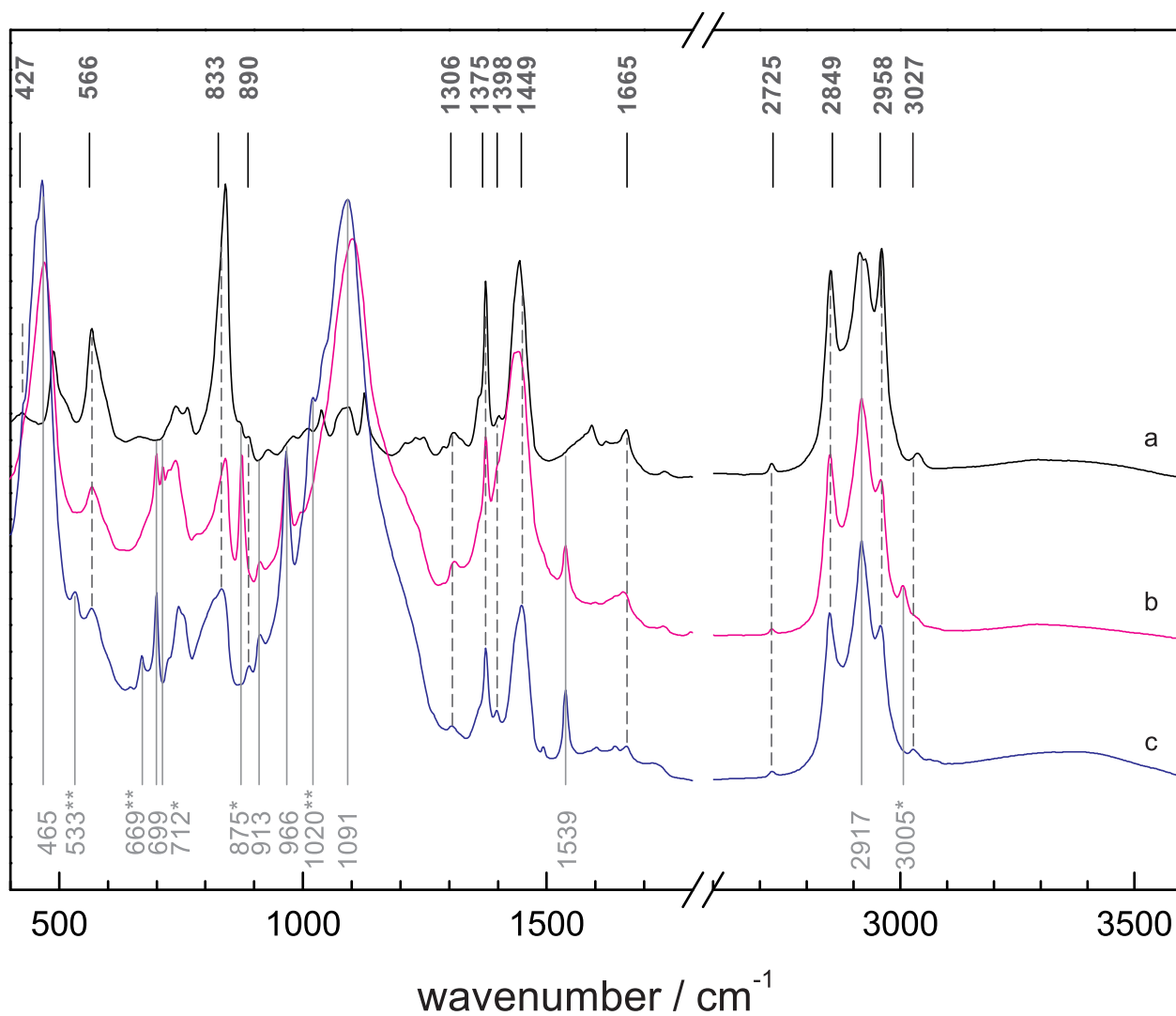


Figure 6.8: IR spectra of samples from the old and recently replaced seating of “Mies” by ARCHIZOOM and of a cast film of ammonia-prevulcanised latex milk: (a) raw latex not aged, (b) “Mies” new, (c) “Mies” old. Fat numbers (top): absorption bands found both in “Mies” samples and in raw latex. Grey numbers (bottom): absorption bands found in both “Mies” samples but not in raw latex. Asterisks refer to absorption bands only present in the new sample, double asterisks indicate bands only found in the old sample.

the cis-characteristic band at  $496\text{ cm}^{-1}$ .

As was shown before, also the reduced peak intensity of the  $835\text{ cm}^{-1}$  band proves degradation. If it is used as an indicator for the degree of degradation of polyisoprene rubber, the two samples of the seating are much more degraded than the latex reference. The new seating of “Mies” was mounted in fall 2011, but it may have been stored for a much longer period. On the contrary, the reference film was cast in May 2011 and has been stored in a zip-lock plastic bag in the dark since then. Therefore, little or no degradation was expected.

The absorption band at  $890\text{ cm}^{-1}$  is due to O-O stretching in tertiary hydroperoxides which are amongst the first degradation products to be formed [50] (see Fig. 3.1). However, they are photoinstable and are quickly consumed. Thus, it is not surprising, that this feature was found as a weak absorption band in the latex sample and also in the old “Mies”-sample. Instead of an absorption band at  $890\text{ cm}^{-1}$ , there is a sharp band of medium intensity at  $875\text{ cm}^{-1}$  and a weak band at  $3005\text{ cm}^{-1}$  in the spectrum of the new seating. They can be assigned to epoxides, where the  $875\text{ cm}^{-1}$  band represents the ring vibration [21]. The weak  $889\text{ cm}^{-1}$  feature might be included.

As can be seen in Fig. 3.1, epoxides occur in early stages of the degradation process of polyisoprene, but are consumed in the course of degradation. Consistently, both bands are not found in the spectrum of the roughly 40 year old seating. Since the absorption band at  $890\text{ cm}^{-1}$  is present in the old sample, it has to be assumed, that the prevailing reaction pathway changed. As stated in [21], chain scission processes dominate in early stages, while cross-linking dominates towards later stages. A shift and broadening of the weak band at  $1741\text{ cm}^{-1}$  in the new sample to  $1721\text{ cm}^{-1}$  in the old sample also accounts for two different pathways: the band at  $1740\text{ cm}^{-1}$  was assigned to the C=O stretch vibration of an ester [21], which is mainly formed, if the prevailing degradation process is the alcohol route (see Fig. 3.1). The band at  $1722\text{ cm}^{-1}$  was assigned to the C=O stretching of saturated methylketones or carboxylic acids, which are predominantly formed, if the  $\beta$ -scission is the main degradation route. Although this species is a photo-instable state, it may well be found in the old seating of “Mies”, that has been kept in dark in a museum’s storage.

In the old seating, a shoulder at  $1020\text{ cm}^{-1}$  is present, that could be assigned to the C-O stretching mode of unsaturated primary alcohols. Other bands found in the old seating that account for this species are located at  $669\text{ cm}^{-1}$  (O-H deformation) and at  $533\text{ cm}^{-1}$  due to C-O deformation [48]. Partially, these three bands are also found in the spectra of the other two samples and seem to belong to an early degradation product with a steadily

increasing intensity. Since unsaturated primary alcohols can be formed by several reaction pathways, they are a good candidate for the assignment.

Additional bands at, 699, 913, and 966  $\text{cm}^{-1}$  are found in the two “Mies”-samples, but not in the latex reference. Since they are not found in the raw latex, but appear in the new seating and increase for the old seating, they must belong to degradation products. A weak but sharp band at 712  $\text{cm}^{-1}$ , found in the new seating only, might also be related to the epoxide species. The exact assignment is not possible for all of these bands, since there are numerous degradation products, which may differ gradually, depending on factors such as chain length and environment of the functional groups as well as on associations such as hydrogen-bonding in alcohols.

For both “Mies” samples, there is a pronounced band at 1539  $\text{cm}^{-1}$ , that has an increasing intensity upon ageing. However, an assignment for this band is not unambiguous. As a possible explanation, this band may be ascribed to an N-H deformation bond of secondary amines. Since this bond is a strong absorber, small amounts of an ammonia pre-vulcaniser might be its source. However, one would expect this band also in latex reference, for which an ammonia-pre-vulcanisation is known, which is not the case. Another possibility are antioxidants or light stabilisers, that often contain nitrogen-functionalities. Since they are only additives, the concentration in the material should be very low. Thus it is questionable if an additive can cause the rather pronounced absorption band at 1539  $\text{cm}^{-1}$ .

**Raman spectra of “Mies”-samples** Raman spectra of both “Mies”-samples and of the cast film of ammonia-prevulcanised latex milk are shown in Fig. 6.9. The respective Raman spectra with marked peak positions are found in the appendix in Figs. A.9 - A.13. In Tab. 6.5, the Raman bands of the degraded “Mies” sample and the 1,4-cis polyisoprene reference are given. Moreover, the corresponding literature values of an IR spectrum of a cis polyisoprene standard sample [15] are displayed in this table.<sup>2</sup> Since there is no local symmetry in the repeat unit of polyisoprene, no selection rules due to symmetry should occur. Thus, the IR modes can be used for assignments in the Raman spectrum [47].

Again, the three Raman spectra match quite well and the features that are characteristic of 1,4-cis polyisoprene are visible (*vide supra*). For the new “Mies”-sample, however, there is a very sharp and intense peak at 2860  $\text{cm}^{-1}$  due to the  $\text{CH}_2$  stretching, which is

---

<sup>2</sup>The material used by [15] is described as a commercial 1,4-cis polyisoprene from SIGMA-ALDRICH, which is most likely the same product as is used as the 1,4-cis polyisoprene reference in this study: synthetic 1,4-cis polyisoprene (SIGMA-ALDRICH no. 182141, chunks,  $M_w > 600.000$ ).

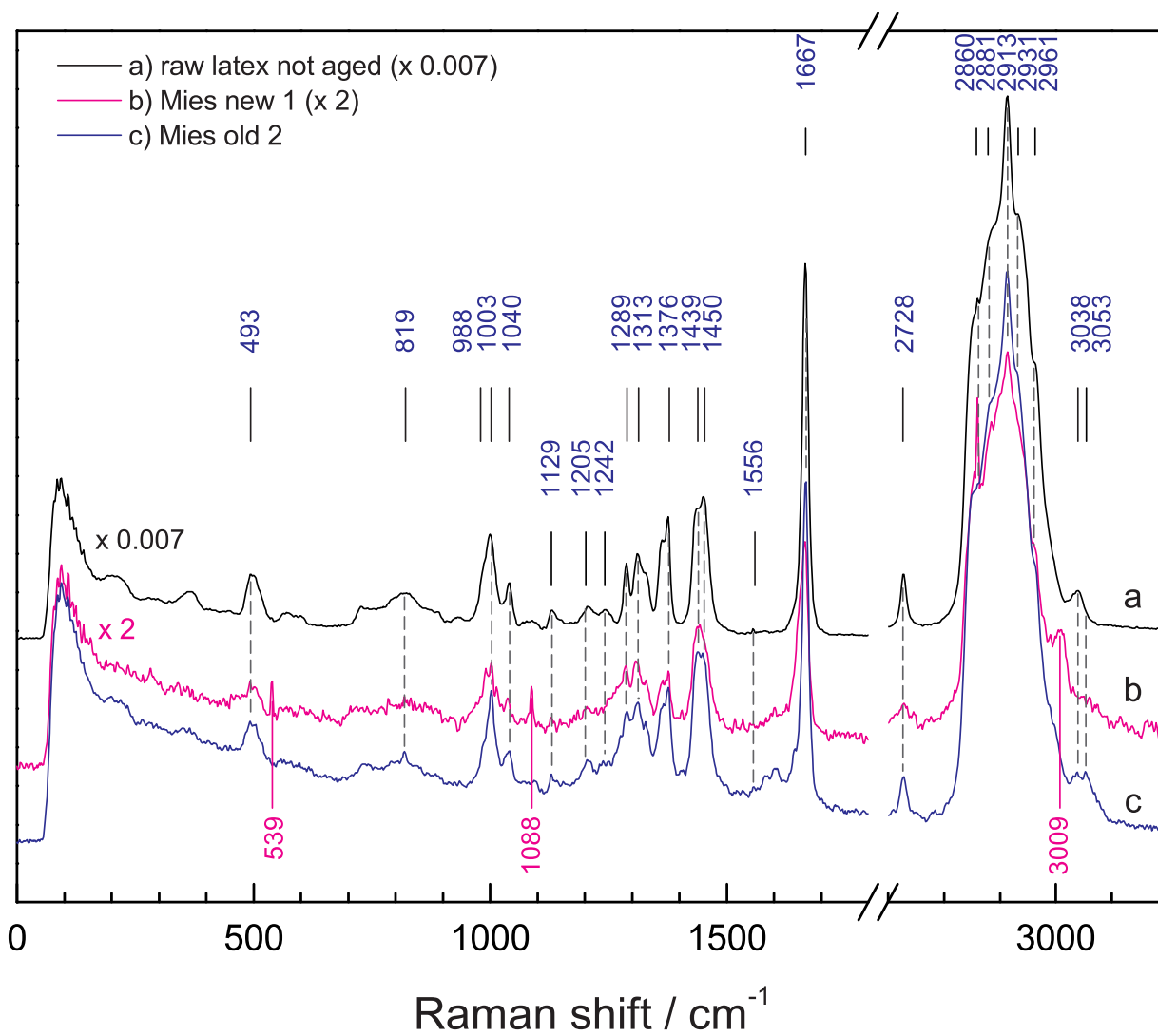


Figure 6.9: Raman spectra of samples from the old and recently replaced seating of “Mies” and of a cast film of ammonia-prevulcanised latex milk: (a) raw latex not aged, (b) “Mies” new, (c) “Mies” old. To improve comparability, spectrum (a) is multiplied by a factor of 0.007 and spectrum (b) is multiplied by a factor of 2.

Raman "Mies"	Raman cis reference	IR cis	Assignment
3053			=C-H str
3039	3036	3036 w	=C-H str
2964	2964	2962 vs	CH <sub>3</sub> asym str
2946	2932	2928 vs	CH <sub>2</sub> asym str
2913	2913	2915 sh	CH <sub>2</sub> sym str
2881	2890		CH <sub>3</sub> sym str
2860	2860	2855 vs	CH <sub>2</sub> sym str
2728	2728		
		1766 sh*	C=O str carb. acid
		1715 vs*	C=O str ketones
1667	1667	1665 w	C=C str
1642	1637	1645 w	C=C str vinyl
1582	1590		
1450	1453	1450 s	CH <sub>2</sub> def
1439	1436		CH <sub>2</sub> def
1376	1376	1377 s	CH <sub>3</sub> asym def
1361	1364	1359 sh	CH <sub>3</sub> sym def
1356	1329		
1313	1313	1311 w	CH <sub>2</sub> wag
1289	1288	1286 vw	=C-H ip bend/CH <sub>2</sub> twist
1239	1242	1242 w	CH <sub>2</sub> twist
1154	1157		CH <sub>3</sub> wag
		1166 m*	C-O str carb. acid
		1130 w	CH <sub>2</sub> wag
	1095	1100 w	C-CH <sub>2</sub> str
1088		1089 w	C-CH <sub>2</sub> str
	1080	1077 mbr*	CCO sym str
1040	1040	1038 w	CH <sub>3</sub> rock
1002	1000		C-C str
	928	975 w*	C-C str
	890	889 mw	CH <sub>3</sub> wag or
		888 wbr*	O-O str perox.
	830	837 m	=C-H wag
822	819		
		764 w	CH <sub>2</sub> rock
	726	740 w	CH <sub>2</sub> rock
	671		C-C ip bend
	648		C-C ip bend
	568	565**	cis C-C ip bend
539	538		
493	494	496**	cis C-C oop bend
441	442		C-C oop bend

Table 6.5: Bands found in the Raman spectra of "Mies"-samples, in a 1,4-cis polyisoprene reference and literature values of an IR spectrum of a commercial 1,4-cis polyisoprene [15]. Bands found in the spectrum of degraded cis polyisoprene are marked with an asterisk. Double asterisk: [9].

much more pronounced, than for the raw latex reference and the old seating. However, quantitative observations are very difficult due to the signal-to-noise ratios of the spectra. Although there is much noise in the new sample's spectrum, weak, but well-defined features at 539, 1088 and 3009  $\text{cm}^{-1}$  can be identified, which are not found in the other two spectra. There are several possibilities for a band assignment of these Raman modes. The feature at 3005  $\text{cm}^{-1}$  was assigned to an epoxide-mode in the previously discussed IR spectrum. This band appears at weak to medium intensities in the Raman spectrum. The band at 1088  $\text{cm}^{-1}$  was assigned to a C-CH<sub>2</sub> stretching or alternatively to an IR-active C-CO stretching mode in [21]. Thus, it might also be related to an epoxide ring vibration. The sharp band at 539  $\text{cm}^{-1}$  resembles the band at 1088  $\text{cm}^{-1}$ , since it is equally sharp and intense. GOLUB and STEPHENS have observed cyclopropyl groups for 1,4-cis and 1,4-trans polyisoprene that was irradiated with UV-light *in vacuo*. This species may have developed in the bulk of the sample below the surface and could alternatively explain the bands at 3005 and 539  $\text{cm}^{-1}$  [19, 20]. Furthermore, CORNELL and KOENIG have observed unassigned bands at 3010 and 3007  $\text{cm}^{-1}$  for synthetic 1,4-trans and 1,2-vinyl polyisoprene, respectively, and features at 1094 and 1083  $\text{cm}^{-1}$  in the 1,4-trans and in the 1,2-vinyl form, respectively. They assign the mode at 539  $\text{cm}^{-1}$  (which is only found in 1,2-vinyl) to =C-C<sub>2</sub> wagging or to a C-C-C deformation mode [47].

In the old seating's spectrum, broad features between 3020 and 3090  $\text{cm}^{-1}$  are present. By a comparison to modes described for 1,4-trans polyisoprene, their maxima at 3039 and 3053  $\text{cm}^{-1}$  can both be assigned to =C-H stretching modes.

As was discussed in the previous section, the Raman spectra are not swamped by degradation products, as it can be the case for IR spectra. However, epoxide features seem to appear also in the Raman spectrum of the new "Mies"-sample. In this example, an identification also by IR analysis was possible, since the samples were not too degraded. The fact, that even the new seating shows strong degradation supports the observation, that polyisoprene is highly sensitive to degradation. Conversely, one may conclude, that the "new" seating must have been stored for a certain amount of time before it was mounted to the art object.



## Chapter 7

# Conclusions

Five different setups were employed for the vibrational spectroscopic characterisation of approximately forty cis- and trans-polyisoprenes, including natural and synthetic samples, of which only a limited number could be discussed in the present study. However, not all approaches appeared equally suitable.

FT-IR spectra of the specimen surfaces could be successfully recorded in the ATR mode, employing either a germanium tip in a microscope objective or a diamond crystal. Although the features of the ATR microscope exhibit clear advantages such as the small tip and the possibility to probe the sample entirely non-invasive, handling was complicated as well as time consuming. Furthermore, the results were not as reproducible as desired, due to the consistency of the sample materials. The application of the diamond ATR crystal on the other hand was by far easier and the spectra were highly reproducible. However, selecting specific spots on the sample surface with high precision is not possible and larger amounts of samples are required.

Raman spectra of polyisoprene were recorded with good quality using a microscope setup with NIR (1064 nm) excitation. Under these conditions sample fluorescence was circumvented and the probability of photo-induced degradation was lowered. The risk of pyrolysis due to laser light absorption was further reduced by adjusting the laser power and by cooling the probed sample surface to room temperature using a stream of nitrogen. However, Raman spectra of samples containing carbon black could not be recorded, since they started to burn immediately upon laser exposure. For all techniques, no specific sample preparation was required which is a prerequisite for employing these techniques to analyse museum objects.

For such applications, an interesting alternative to the Raman-microscope with 1064 nm excitation is a compact Raman spectrometer (CCD detection) equipped with a mobile probe head connected via a glass fibre. Good results have already been obtained mainly for inorganic materials. However, these systems are restricted to excitation lines below 800 nm (e.g. 785 nm diode laser excitation) and thus may not be sufficiently red-shifted with respect to fluorescence of rubber materials.

However, with the setups used in this work, all the different conformations and crystalline forms of polyisoprene could be distinguished by vibrational spectroscopy. The comparison of *cis*- and *trans*-polyisoprene reference compounds showed, that both constitutional isomers exhibit characteristic features in the IR and Raman spectra. IR spectra of artificially light-aged raw latex samples, recorded after different irradiation times, revealed light-induced oxidation. By comparing these spectra with IR spectra of naturally aged raw rubber samples, it was possible to assess the extent of degradation of these materials, both with respect to the type and amount of the degradation products. The comparison of IR and Raman spectra of the artificially aged samples demonstrated that Raman spectroscopy is a valuable tool especially for the analysis of severely degraded rubber. In addition, it was possible to identify a spectra marker for ammonia (presumably due to an N-H deformation mode) used as pre-vulcaniser in the latex. For highly degraded polyisoprene, the use of IR spectroscopy was found to be less instructive, as the absorption bands of the polymeric chain were entirely swamped by the signals of degradation products. For less degraded samples, the band at  $835\text{ cm}^{-1}$  appeared to be a good indicator for monitoring the relative contribution of C=C double bonds, which can otherwise not be studied directly by IR spectroscopy.

Raman measurements of two fresh balata samples could be identified as  $\alpha$ - and  $\beta$ -modifications of 1,4-*trans* polyisoprene. Unlike to IR spectroscopy, a differentiation between both sample types could easily be achieved using Raman spectroscopy, which, on the basis of the respective vinyl stretching, revealed the presence of minor contributions of vinyl groups of *cis*- and *trans*-isomers in the spectra of balata.

In most of the spectra of pure 1,4-unsaturated polyisoprenes, small bands were present, which can be related to 1,2- and 3,4-vinyl units and often also to the respective 1,4-*cis* or 1,4-*trans* constitutional isomer. These observations were made for both natural and synthetic samples. Given, that rubber-furnishing plants only yield one constitutional isomer (1,4-*cis* or 1,4-*trans*), this finding suggests that isomerisation-processes take place, in which all four constitutional isomers may be formed and even cyclisation may occur, as has been

reported for samples irradiated with UV-light *in vacuo*. The alternative conclusion would be, that all natural polymers are mixed with synthetic polyisoprene, and that synthetic polyisoprene references of high purity contain traces of various constitutional isomers. Due to the occurrence of different constitutional isomers in the samples that are classified as 100% natural rubber, it is not possible to discern natural and synthetic 1,4-unsaturated polyisoprenes.

The insight into the behaviour and spectral features of degraded rubber was employed to characterise two samples of a design object from a museum's collection. The original seating of the chaise longue "Mies" from 1969 as well as the replacement seating, which was mounted in fall 2011 were identified by IR and Raman spectroscopy as a pure 1,4-*cis* polyisoprene. In the IR spectra of both samples large amounts of degradation products became detectable. Their presence also in the new seating may be, on the one hand, interpreted as a proof of the sensitivity of natural rubber to degradation and it can be assumed that no or only small amounts of anti-degradants were added. On the other hand, the presence of the degradation products suggests that the new seating has not been prepared "freshly" before delivery to the museum. By comparing the degradation products found in the "Mies"-samples with degradation mechanisms proposed in literature, it was possible to relate these findings to two different mechanisms.

Although no other material but polyisoprene was identified in both seatings, this does not necessarily mean that no additives are present, since the percentage of light stabilisers or anti-oxidants is usually very low and possibly not detectable by the present methods. For instance, it has to be assumed that some kind of pre-vulcaniser or cross-linker is present, as it was detected for the raw latex sample in the Raman spectra. Since no sulphur or nitrogen containing functional groups were identified in the "Mies"-samples, a dicumyl peroxide vulcaniser may have been used. It is possible, that the degradation products in the new seating are partially due to such kind of additive. The lack of sensitivity of vibrational spectroscopy might be a limitation of the methods; however, further studies are required to determine the detection limit in a quantitative manner.

The number of artworks made of plastics that are already severely degraded is enormous. Thus, a fast and non-destructive material analysis is essential to plan and perform conservation treatments and for developing save storage conditions.

The *in situ* analysis of rubber artifacts in a museum is of particular importance, since sulphur-vulcanised rubber may emit sulphur dioxide and hydrogen sulphide, leading to the

formation of  $\text{HSO}_3$ , which in turn enhances corrosion processes of many materials. As a consequence, sulphur-containing rubber objects require separate storage. On the other hand, very low temperatures may cause crystallization of polyisoprene. Thus, cold storage, which is already used in many museums to slow down degradation processes may induce further artifacts in rubber materials.

Raman-microscopy and ATR-IR spectroscopy can be adjusted to be such fast and non-destructive techniques that meet museum requirements. Whereas ATR-spectroscopy is amongst the most common analytical methods in museum laboratories, the *in situ* application of Raman spectroscopy is still at its infancy. However, with the development of commercial easy-to-use bench-top setups, this technique seems to become increasingly popular in museums nowadays. It was demonstrated here, that Raman spectroscopy provides important complementary information for material identification.

# Bibliography

- [1] S. Blank. An introduction to plastics and rubbers in collections. *Studies in Conservation*, 35(2):53–63, 1990.
- [2] T. Bechthold. Fantastisch plastisch? Tom Dixons S-Chair. *Restauro*, 116(1):38–47, 2010.
- [3] N. Dahlhaus. Die tote Klasse. Eine Installation des polnischen Künstlers und Theater-machers Tadeusz Kantor. Diploma Thesis, Technische Universität München, 2008.
- [4] M. Pfenninger. Retroactive stabilization for natural rubber artworks. *ZKK Zeitschrift für Kunststechnologie und Konservierung*, 2:368–377, 2006.
- [5] M. Langer. Die Latex-Skulpturen der deutsch-amerikanischen Künstlerin Eva Hesse (1936-1970). *ZKK Zeitschrift für Kunststechnologie und Konservierung*, 2:285–337, 2001.
- [6] T. Winther. Understanding ‘Flocked’ - a case study of a Keith Sonnier latex art work from the late 1960’s. Talk presented at the National Gallery of Denmark’s conference on Permanence in Contemporary Art - Checking Reality, 3/4 Nov 2008, Copenhagen. <http://www.smk.dk/en/explore-the-art/web-tv/research/seminar-om-samtidskunst/thea-winter/>, last checked 20.02.2012.
- [7] R. Saunders and D. Smith. Infrared spectra of hevea and gutta elastomers. *Journal of Applied Physics*, 20 (10):953–965, 1949.
- [8] Friederike Waentig. *Kunststoffe in der Kunst*. Michael Imhof Verlag, 2004.
- [9] S.J. Bunce, H.G.M. Edwards, A.F. Johnson, I.R. Lewis, and P.H. Turner. Synthetic polyisoprenes studied by fourier transform raman spectroscopy. *Spectrochimica Acta Part A: Molecular Spectroscopy*, 49(5-6):775 – 783, 1993.

- [10] J.A. Malmonge, E.C. Camillo, R.M.B. Moreno, L.H.C. Mattoso, and C.M. McMahan. Comparative study on the technological properties of latex and natural rubber from *hancornia speciosa gomes* and *hevea brasiliensis*. *Journal of Applied Polymer Science*, 111:2986–2991, 2009.
- [11] Encyclopædia Britannica. [www.britannica.com/EBchecked/topic/555844/South-America/41833/Principal-crops?anc](http://www.britannica.com/EBchecked/topic/555844/South-America/41833/Principal-crops?anc), last checked 09.12.2011.
- [12] J.S. Mills and R. White. *The organic chemistry of museum objects*. Butterworth-Heinemann, 1994.
- [13] Wayne's Word. <http://waynesword.palomar.edu/ecoph13.htm>, last checked 09.12.2011.
- [14] Webster's Revised Unabridged Dictionary, 1913. <http://dictionary.die.net/chicle>, last checked 20.02.2012.
- [15] K.A.M. dos Santos, P.A.Z. Suarez, and J.C. Rubim. Photo-degradation of synthetic and natural polyisoprenes at specific uv radiations. *Polymer Degradation and Stability*, 90(1):34 – 43, 2005.
- [16] C. Maniglia-Ferreira, J. Silva, and R. de Paula. Degradation of trans-polyisoprene over time following the analysis of root fillings removed during conventional treatment. *International Endodontic Journal*, 40 (1):25–30, 2007.
- [17] Transport-Informationen-Service, Fachinformationen der Deutschen Transportversicherer. [http://www.tis-gdv.de/tis\\_e/ware/kautschuk/naturkautschuk/naturkautschuk.htm](http://www.tis-gdv.de/tis_e/ware/kautschuk/naturkautschuk/naturkautschuk.htm), last checked 20.02.2012.
- [18] J. Morand. Photodegradation of rubber. *Rubber Chemistry & Technology*, 39 (3):537–753, 1966.
- [19] M.A. Golub and L.C. Stephens. Photoinduced microstructural changes in 1,4-polyisoprene. *Journal of Polymer Science: Part A-1*, 6(4):763–776, 1968.
- [20] M.A. Golub. Photocyclization of 1,2-polybutadiene and 3,4-polyisoprene. *Macromolecules*, 2(5):550–552, 1969.

- [21] C. Adam, J. Lacoste, and J. Lemaire. Photo-oxidation of polyisoprene. *Polymer Degradation and Stability*, 32:51 – 69, 1991.
- [22] H. Günzler and H.U. Gremlich. *IR-Spektroskopie. Eine Einführung*. Wiley-VCH Weinheim, 1998.
- [23] S. Yano. Photo-oxidation of an IR vulcanizate. *Rubber Chemistry & Technology*, 54(1):1–14, 1981.
- [24] V. Arjunan, S. Subramanian, and S. Mohan. Fourier transform infrared and Raman spectral analysis of trans-1,4-polyisoprene. *Spectrochimica Acta Part A: Molecular and Biomolecular Spectroscopy*, 57(13):2547 – 2554, 2001.
- [25] K.D.O. Jackson, M.J.R. Loadman, C.H. Jones, and G. Ellis. Fourier transform raman spectroscopy of elastomers: An overview. *Spectrochimica Acta Part A: Molecular Spectroscopy*, 46(2):217 – 226, 1990.
- [26] P.J. Hendra and K.D.O. Jackson. Applications of raman spectroscopy to the analysis of natural rubber. *Spectrochimica Acta Part A: Molecular Spectroscopy*, 50(11):1987 – 1997, 1994.
- [27] P. Vandenaabeele. Raman spectroscopy in art and archaeology. *Journal of Raman Spectroscopy*, 35:607–609, 2004.
- [28] A. Colombini and V. Léal Romero. Limitations of Raman spectroscopy in the degradation assessment of polyurethane artworks. Poster presented at the Lacona VII conference in Madrid in 2007. <http://www.cicrp.fr/limites-raman-spectroscopie.html>, last checked 23.02.2011.
- [29] PerkinElmer Inc. <http://shop.perkinelmer.com>, last checked 03.02.2012.
- [30] F. Mirabella. *Handbook of Vibrational Spectroscopy*, volume 1, chapter Principles, Theory and Practice of Internal Reflection Spectroscopy. John Wiley & Sons Ltd., 2002.
- [31] F. Siebert and P. Hildebrandt. *Vibrational Spectroscopy in Life Science*. Wiley VCH, 2008.

- [32] J. Grochol. *Raman Spectroelectrochemical Investigations of Immobilized Redox Proteins*. PhD thesis, Technische Universität Berlin, 2007.
- [33] B. Schrader. Die Möglichkeiten der Raman-Spektroskopie im Nah-Infrarot-Bereich, Teil 1. *Chemie in unserer Zeit*, 31(5):229–234, 1997.
- [34] B. Schrader, A. Hoffmann, A. Simon, R. Podschadlowski, and M. Tischer. NIR-FT-Raman-spectroscopy, state of the art. *Journal of Molecular Structure*, 217:207–220, 1990.
- [35] F.J. Bergin. A microscope for Fourier Transform Raman spectroscopy. *Spectrochimica Acta Part A: Molecular Spectroscopy*, 46(2):153–159, 1990.
- [36] N.H. Tennent, J. Caen, P. Courtney, and E. Lozano Diz. In situ Raman spectroscopic characterization of polymers used in past conservation treatments. *e-Preservation Science*, 6:107–111, 2009. <http://www.morana-rtd.com/e-preservation-science/2009/Tennent-01-07-2008.pdf>, last checked 23.02.2012.
- [37] ISO 4892-1 Plastics – Methods of exposure to laboratory light sources. Part 1: General guidance, 1999.
- [38] ISO 4892-2 Plastics – Methods of exposure to laboratory light sources. Part 2: Xenon arc lamps, 2006.
- [39] DIN EN ISO 11341 Beschichtungstoffe – Künstliches Bewittern und künstliches Bestrahlen – Beanspruchung durch gefilterte Xenonbogenstrahlung; Deutsche Fassung EN ISO 11341:2004.
- [40] R. Feller. *Research in Conservation 4*, chapter Accelerated aging: photochemical and thermal aspects. The J. Paul Getty Trust, Los Angeles, 1994.
- [41] ATLAS Material Testing Technology B.V. *Betriebsanleitung SUNTEST CPS / CPS+*. ATLAS Material Testing Technology B.V., 63589 Linsengericht/ Altenhaßlau.
- [42] A.S. Tweedie, M.T. Mitton, and P.Z. Sturgeon. How reliable are artificial light sources for predicting degradation of textiles by daylight? *Journal American Association Textile Chemists and Colorists*, 3(2):22–35, 1971.

- [43] Pike Technologies. *GladiATR™ Vision Single Reflection ATR Accessory. Installation and user guide*. Pike Technologies, Madison WI, 2011.
- [44] B. Schrader, G. Baranovic, S. Keller, and J. Sawatzki. Micro and two-dimensional NIR FT-Raman spectroscopy. *Fresenius' Journal of Analytical Chemistry*, 349:4–10, 1994.
- [45] B. Schrader and A. Simon. Routine FT-Raman spectroscopy with modified standard FT-IR instrument. *Microchimica Acta*, 95:227–230, 1988.
- [46] Bruker Optik. *RFS/100 User Manual*. Bruker Optik GmbH, Ettlingen. 2004.
- [47] S.W. Cornell and J.L. Koenig. Raman spectra of polyisoprene rubbers. *Macromolecules*, 2(5):546–549, 1969.
- [48] N.P.G. Roeges. *A guide to the complete interpretation of infrared spectra of organic structures*. John Wiley & Sons Ltd., 1994.
- [49] K. Haider and T. van Oosten. Plastic bags – research into polyethylene bags of the series ‘Bicycles’ by Andreas Slominski. In T. Bechthold, editor, *Future Talks 009. The Conservation of Modern Materials in Applied Arts and Design, 22/23 Oct 2009, Die Neue Sammlung. The International Design Museum Munich*, pages 41–48, Munich, 2011.
- [50] A.V. Tobolsky, D.J. Metz, and R.B. Mesrobian. Low temperature autooxidation of hydrocarbons: the phenomenon of maximum rates. *Journal of the American Chemical Society*, 72:1942–1952, 1950.
- [51] O.D. Hummel and F. Scholl. *Atlas of Polymer and Plastics Analysis*, volume 2, Plastics, Fibres, Rubbers, Resins; Starting and Auxiliary Materials, Degradation Products, Part B/I Text. Carl Hanser Verlag/VCH, 1988.
- [52] I. Zebger, Barriola Goikoetxea A., Jensen S., and Ogilby P.R. Degradation of vinyl polymer films upon exposure to chlorinated water: the pronounced effect of a sample’s thermal history. *Polymer Degradation and Stability*, 80(2):293 – 304, 2003.
- [53] I. Zebger, A. Lopez Elorza, J. Salado, A. Garcia Alcalá, E. Silva Gonçalves, and P.R. Ogilby. Degradation of poly(1,4-phenylene sulfide) on exposure to chlorinated water. *Polymer Degradation and Stability*, 90(1):67 – 77, 2005.



# List of Figures

1.1	Images of design classics made of rubber and found in museum's collections. Image "Mies": © <a href="http://www.decoratum.com">http://www.decoratum.com</a> ; images "S-Chair": © Die Neue Sammlung. The International Design Museum Munich. . . . .	10
2.1	Scheme of different polyisoprene constitutional isomers. The formation of the polymeric chain is assumed to start with homolytic cleavage of the monomer units. . . . .	12
2.2	Proposed $\alpha$ - and $\beta$ -structure of 1,4-trans polyisoprene [9]. . . . .	12
3.1	Scheme of photo-induced oxidation processes of 1,4-cis polyisoprene in air at wavelengths $>300$ nm, according to the mechanism suggested by [21]. . .	17
4.1	Scheme of the ATR setup. Image taken from [29]. . . . .	22
4.2	Attenuated total reflection (ATR) at an internal reflection element (IRE). Image taken from [30], modified. . . . .	23
4.3	Possible consequences of a photon-molecule interaction [32]. . . . .	24
4.4	Setup of a Raman microscope. . . . .	26
5.1	Sample case with naturally degraded, uncompounded and unvulcanised rubber materials. . . . .	29
5.2	Original and replacement seating of the chaise longue "Mies" by ARCHIZOOM. © Susanne Graner. . . . .	30
5.3	Tip attachments for the pressure clamp [43]. . . . .	32
6.1	Comparison of IR spectra of 1,4-cis and 1,4-trans polyisoprene references from SIGMA-ALDRICH. . . . .	36

6.2	Comparison of Raman spectra of 1,4-cis and 1,4-trans polyisoprene references from SIGMA-ALDRICH. . . . .	41
6.3	IR spectra of light-aged 1,4-cis polyisoprene recorded with a diamond ATR cell. . . . .	45
6.4	Raman-microscope spectra of light-aged 1,4-cis polyisoprene. . . . .	47
6.5	IR spectra of freshly cut surfaces of naturally degraded 1,4-cis polyisoprene and two reference samples. . . . .	48
6.6	Differences in IR spectra of natural processed brown and purified white balata. . . . .	51
6.7	Raman spectra of two different types of 1,4-trans polyisoprenes: processed brown and purified white balata. . . . .	52
6.8	IR spectra of "Mies" samples and of a cast latex film. . . . .	58
6.9	Raman spectra of "Mies" sample and of a cast latex film. . . . .	61
A.1	IR spectrum of a 1,4-cis polyisoprene reference from SIGMA-ALDRICH. . . . .	80
A.2	IR spectrum of a 1,4-trans polyisoprene reference from SIGMA-ALDRICH. . . . .	81
A.3	IR spectra of natural processed brown and purified white balata. . . . .	82
A.4	IR spectrum of a non-aged film of cast raw latex, pre-vulcanised with ammonia. . . . .	83
A.5	IR spectrum of the new seating of "Mies". . . . .	84
A.6	IR spectrum of the old seating of "Mies". . . . .	85
A.7	Raman spectrum of a 1,4-cis polyisoprene reference from SIGMA-ALDRICH. . . . .	86
A.8	Raman spectrum of a 1,4-trans polyisoprene reference from SIGMA-ALDRICH. . . . .	87
A.9	Raman spectrum of a non-aged film of cast raw latex, pre-vulcanised with ammonia. . . . .	88
A.10	Raman spectrum of natural processed brown balata. . . . .	89
A.11	Raman spectrum of natural purified white balata. . . . .	90
A.12	Raman spectrum of the new seating of the chaise longue "Mies". . . . .	91
A.13	Raman spectrum of the old seating of the chaise longue "Mies". . . . .	92
B.1	New reference samples of natural and synthetic cis- and trans-polyisoprene ( $\alpha$ - and $\beta$ -form). . . . .	93
B.2	Cast films of natural latex milk, new and artificially aged for 4 and 73 hours. . . . .	94
B.3	Ceylon Scraps, plantation rubber. . . . .	94
B.4	Ceylon Scraps, plantation rubber, lateral cut. . . . .	95
B.5	Parasoft Brazil. . . . .	95

B.6	Parasoft Brazil, side view. . . . .	96
B.7	Parasoft Brazil, detail. . . . .	96
B.8	Lanadrone block: plantation rubber, Ceylon. . . . .	97
B.9	Lanadrone block: plantation rubber, Ceylon, reverse side. . . . .	97
B.10	Lanadrone block, plantation rubber, Ceylon, side view. . . . .	98
B.11	Lanadrone block: plantation rubber, Ceylon, detail. . . . .	98
C.1	Sketch of the sample chamber in a Suntest CPS (ATLAS) device for artificial light-ageing [41]. . . . .	100



## Appendix A

# IR and Raman Spectra

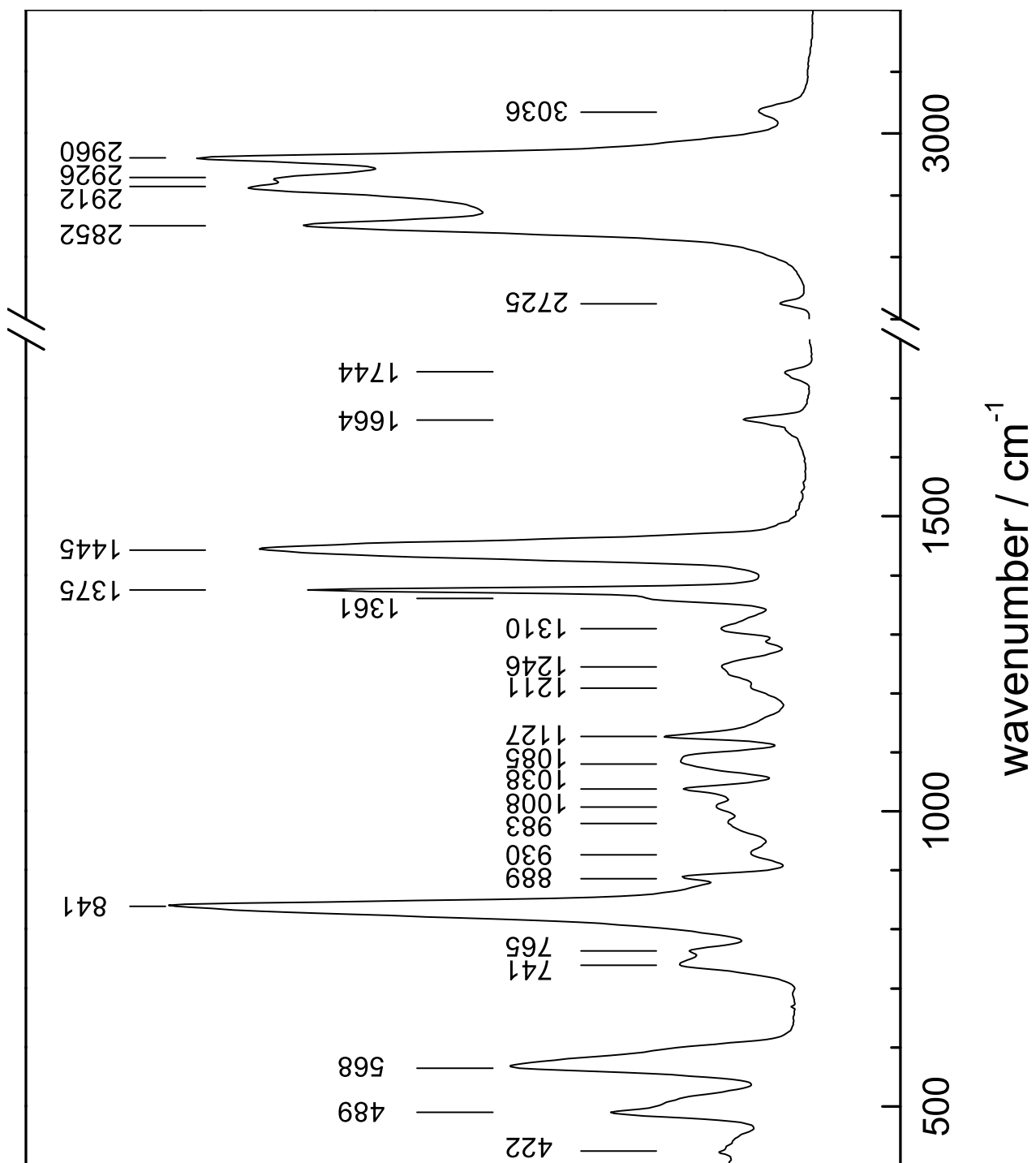


Figure A.1: IR spectrum of a 1,4-cis polyisoprene reference from SIGMA-ALDRICH.

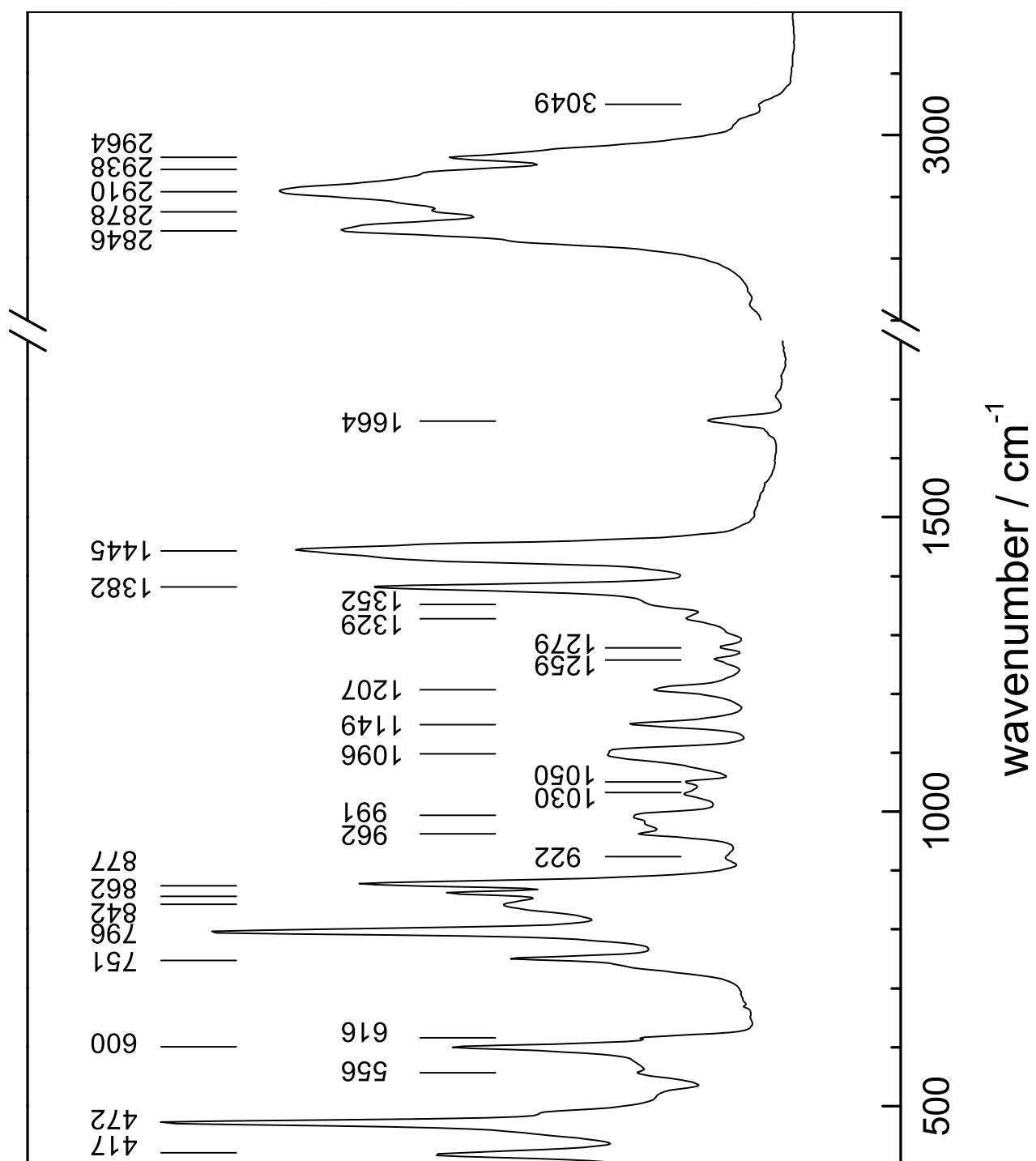


Figure A.2: IR spectrum of a 1,4-trans polyisoprene reference from SIGMA-ALDRICH.

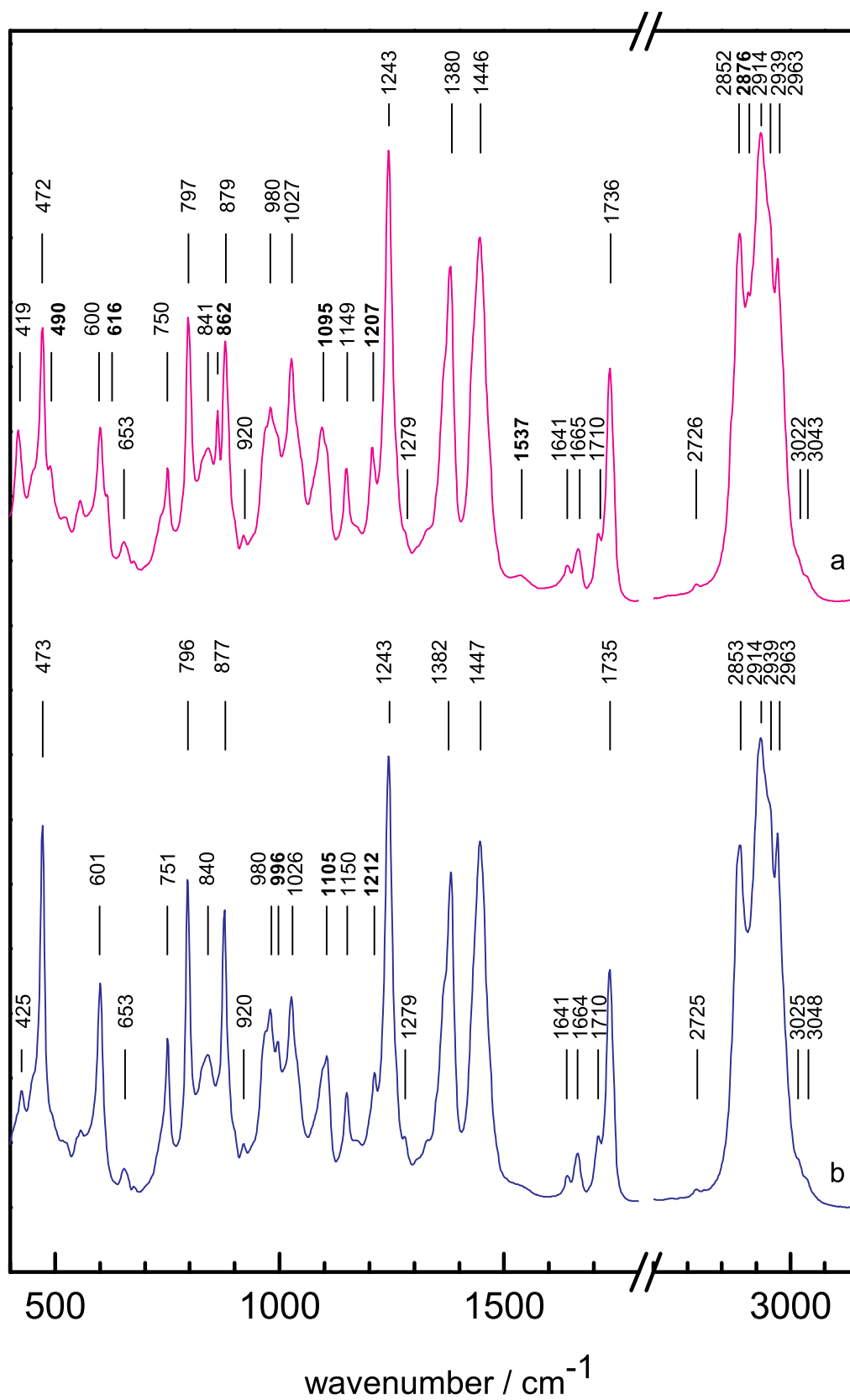


Figure A.3: IR spectra of natural balata: (a) purified white, (b) processed brown balata.

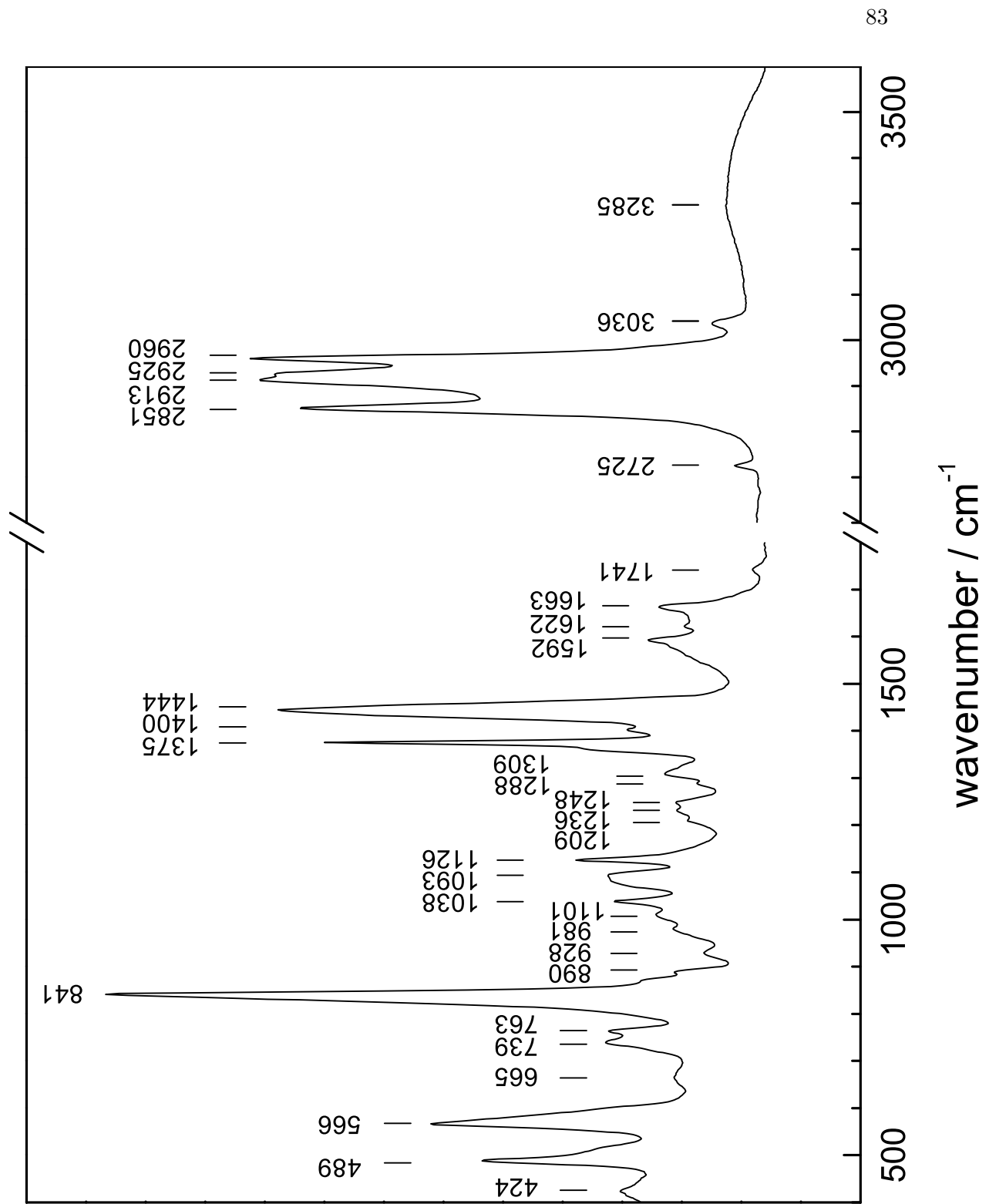


Figure A.4: IR spectrum of a non-aged film of cast raw latex, pre-vulcanised with ammonia.

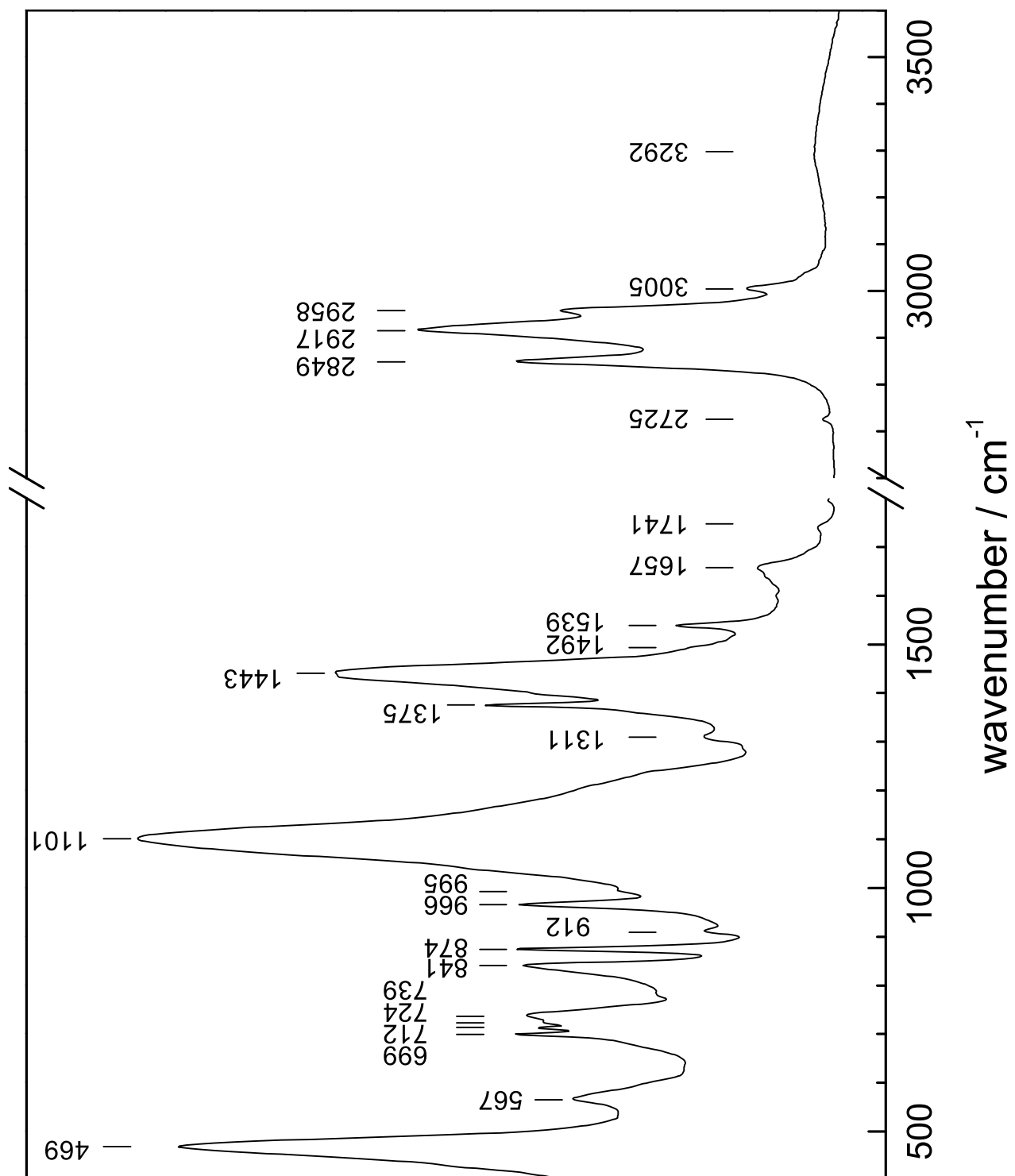


Figure A.5: IR spectrum of the new seating of “Mies”.

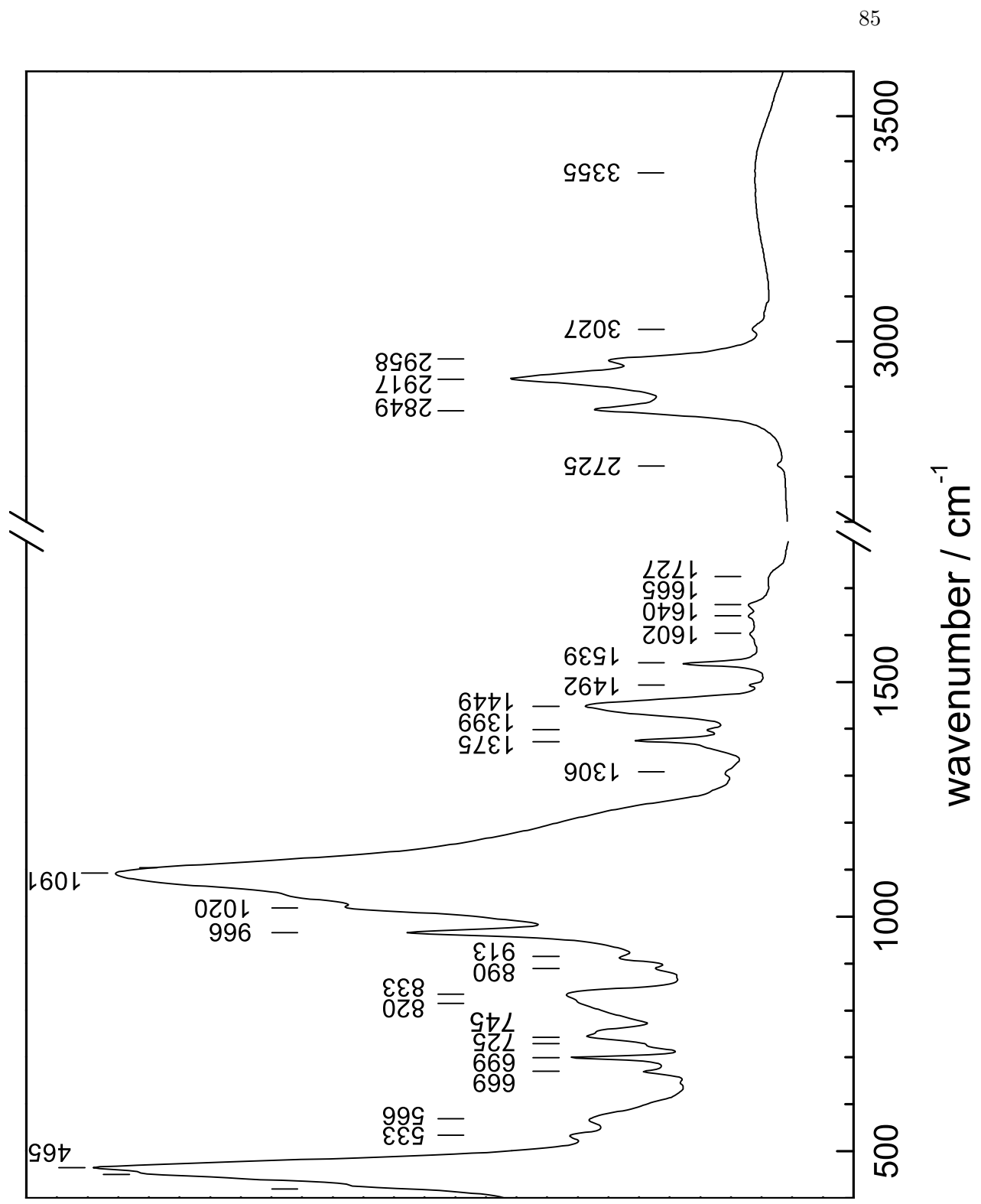


Figure A.6: IR spectrum of the old seating of "Mies".

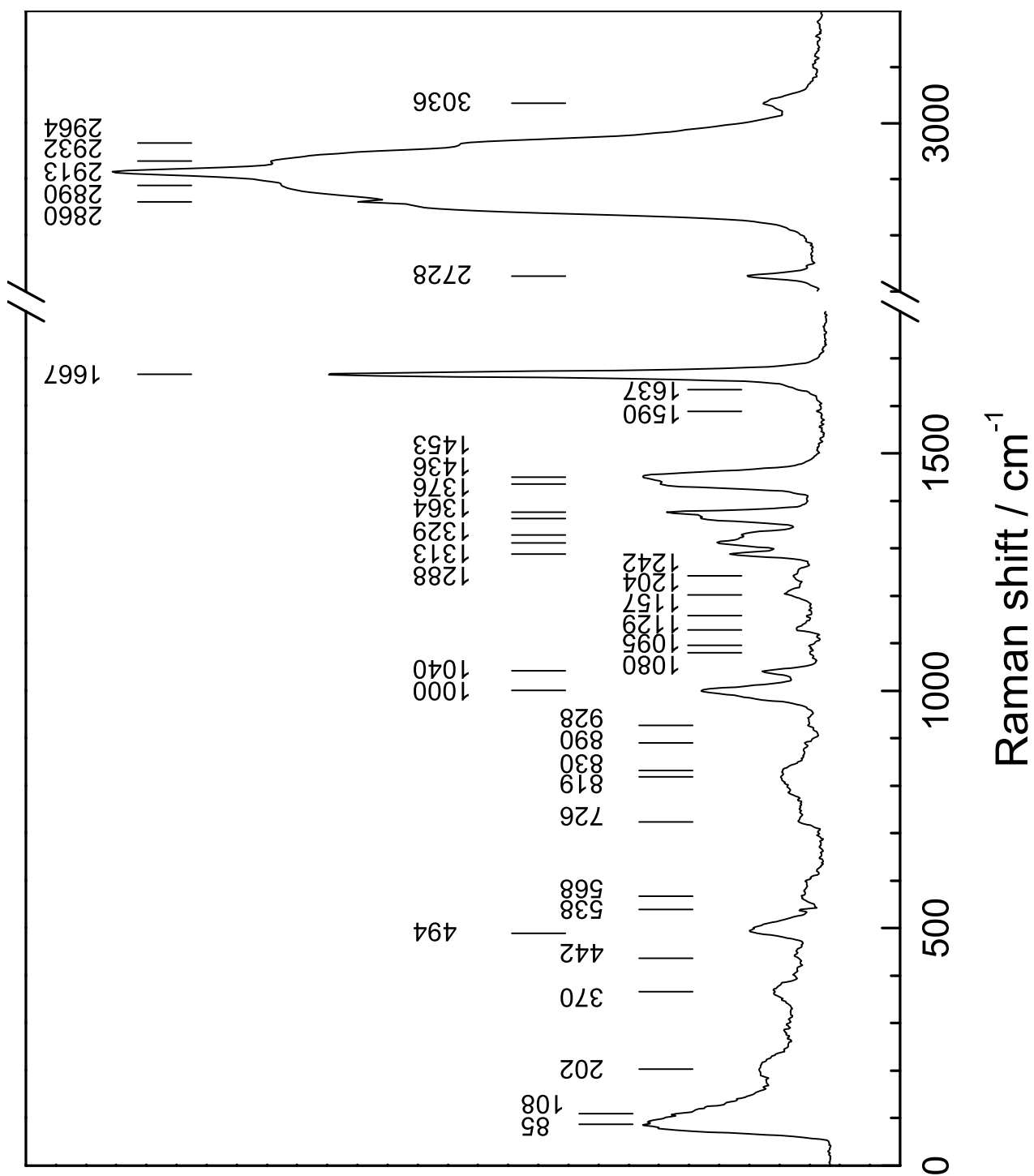


Figure A.7: Raman spectrum of a 1,4-cis polyisoprene reference from SIGMA-ALDRICH.

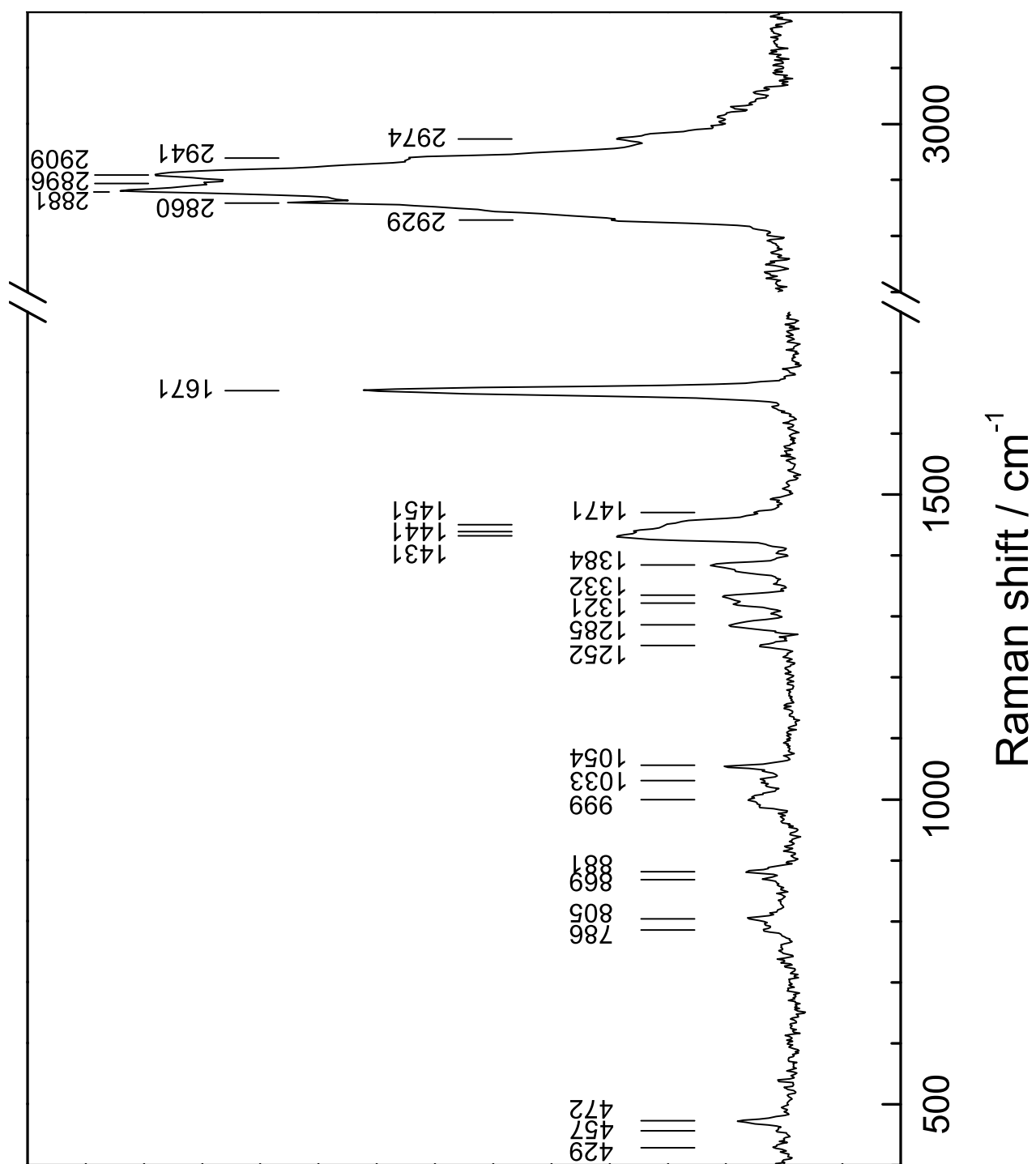


Figure A.8: Raman spectrum of a 1,4-trans polyisoprene reference from SIGMA-ALDRICH.

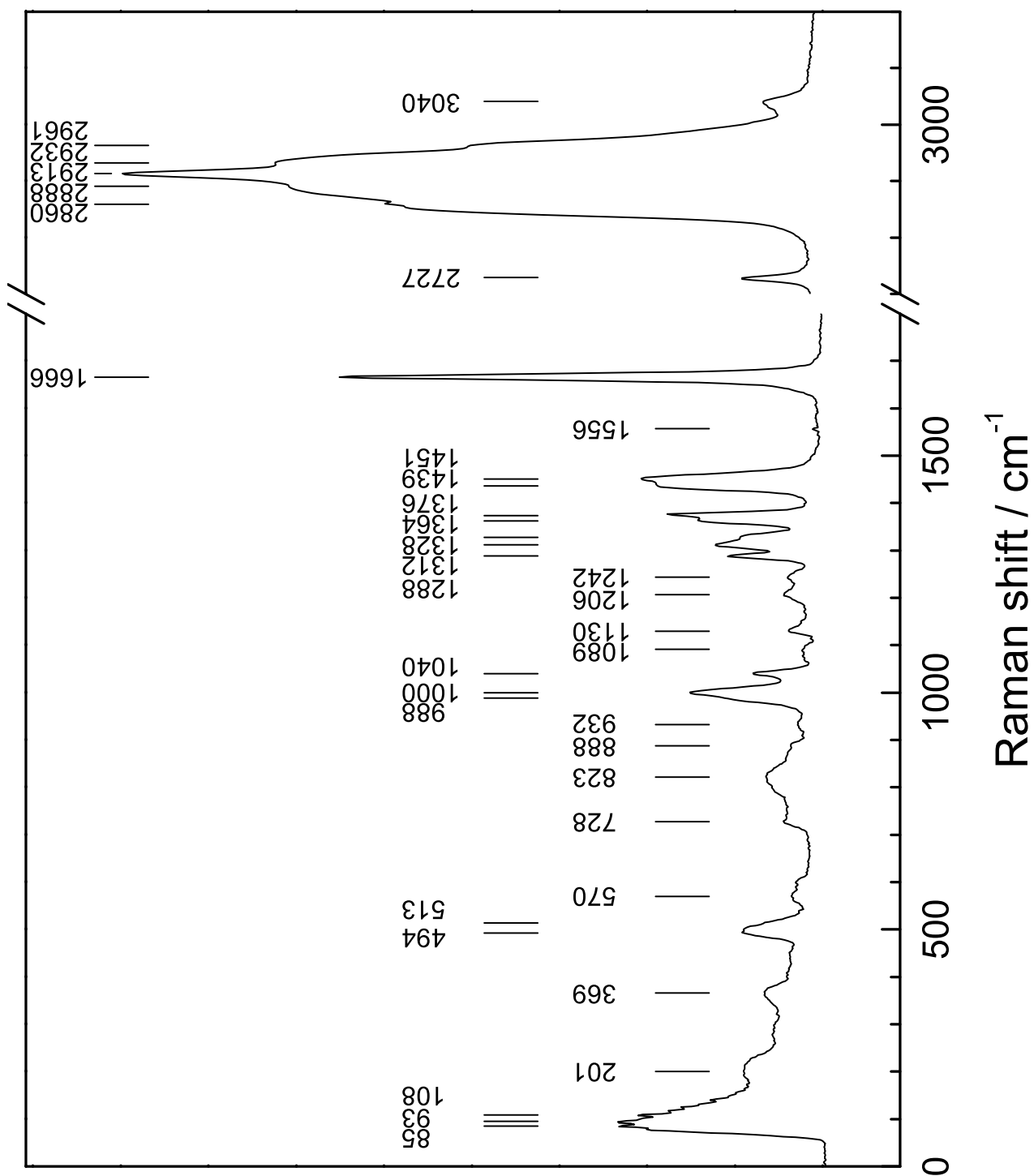


Figure A.9: Raman spectrum of a non-aged film of cast raw latex, pre-vulcanised with ammonia.

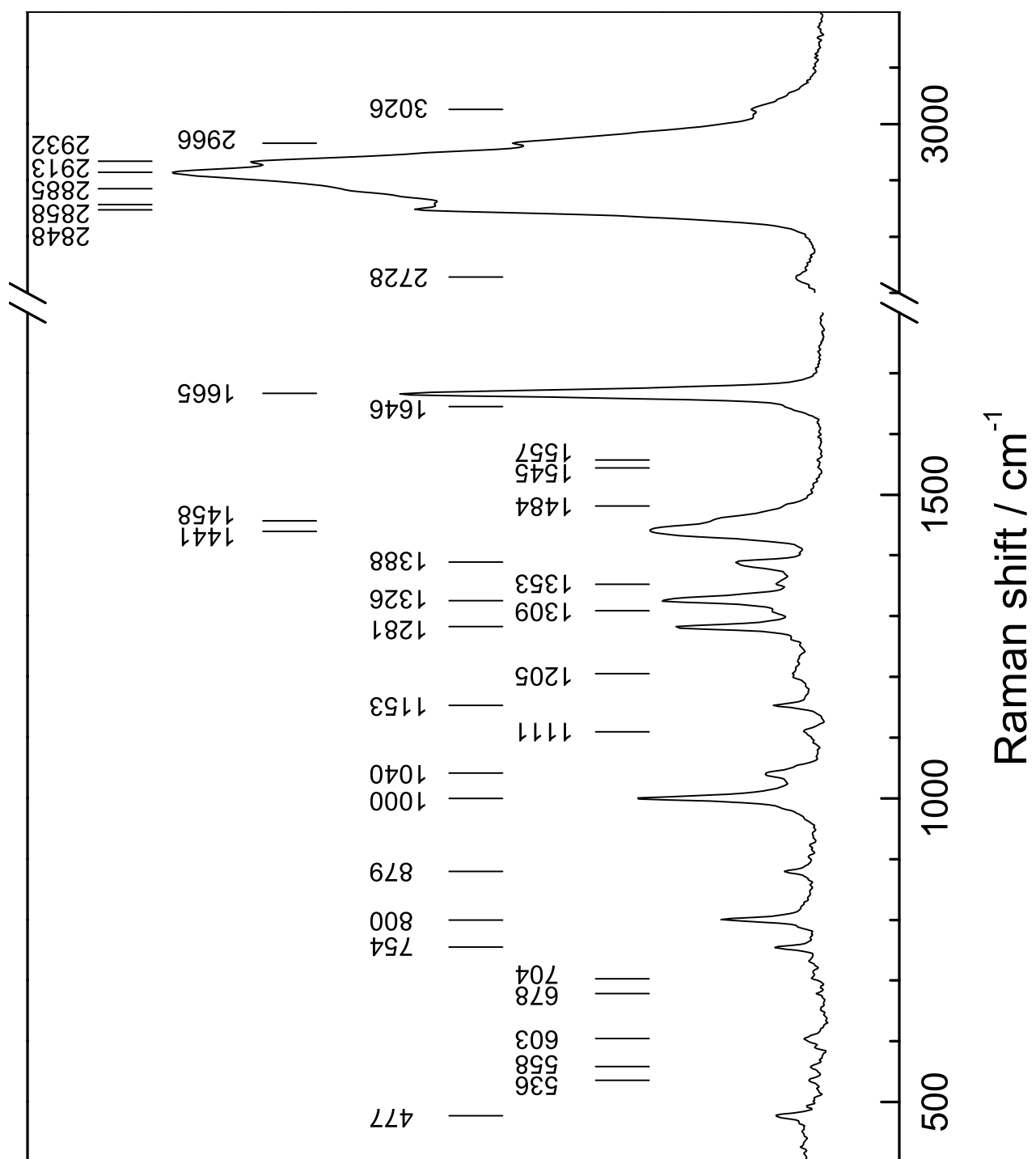


Figure A.10: Raman spectrum of natural processed brown balata from TANARIMAN Ltd., Brasil.

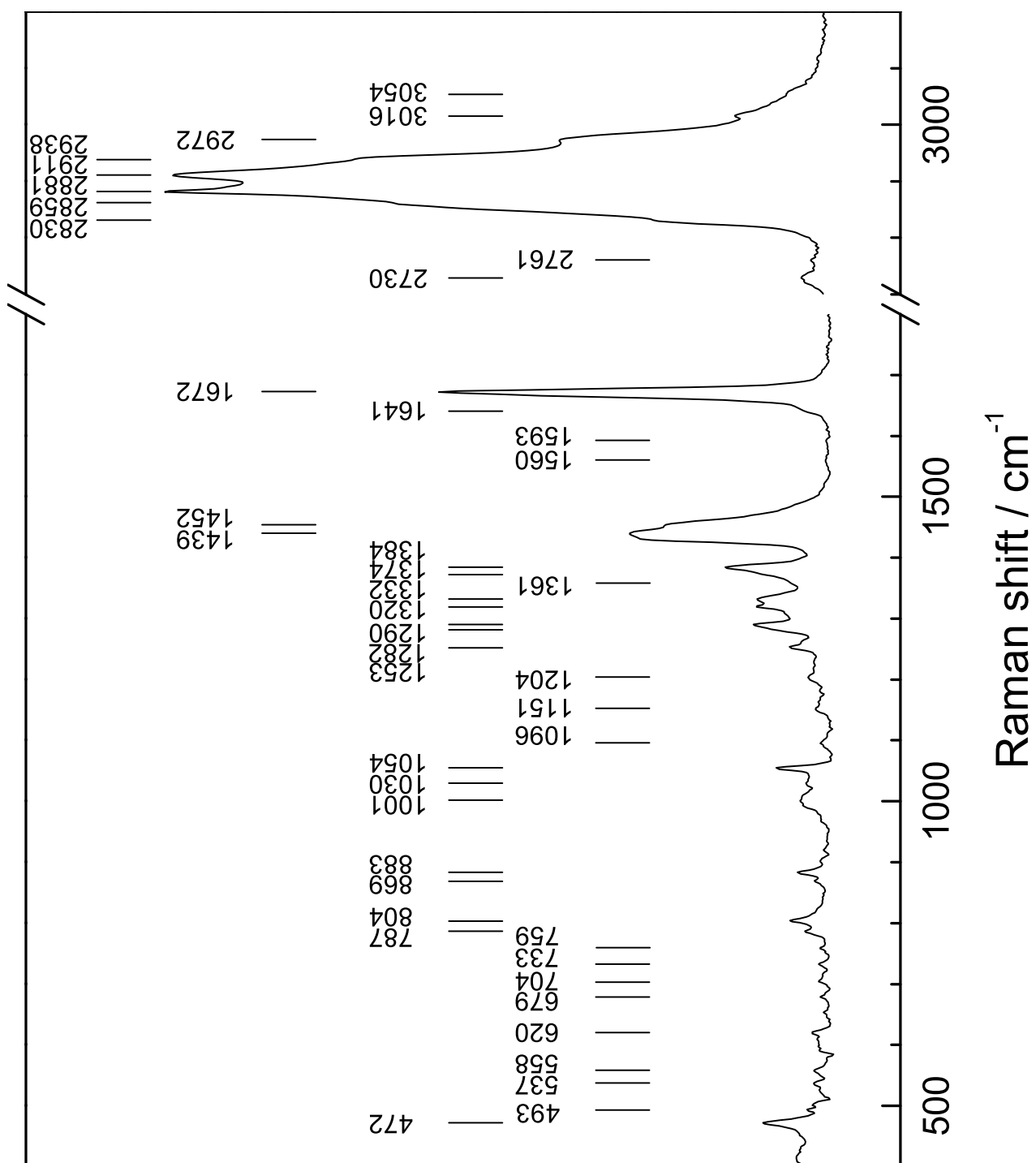


Figure A.11: Raman spectrum of natural purified white balata from TANARIMAN Ltd., Brasil.

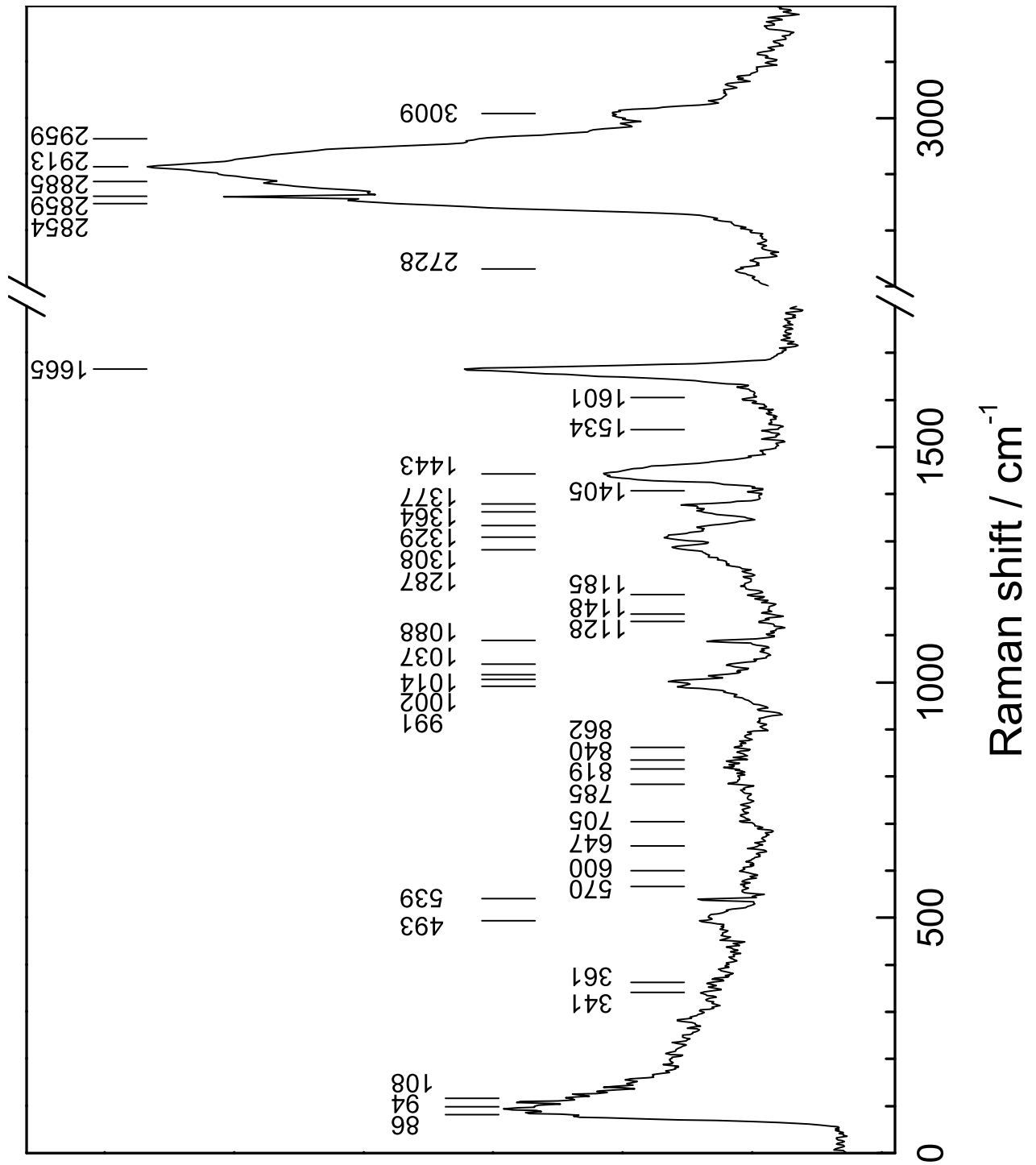


Figure A.12: Raman spectrum of the new seating of the chaise longue “Mies”.

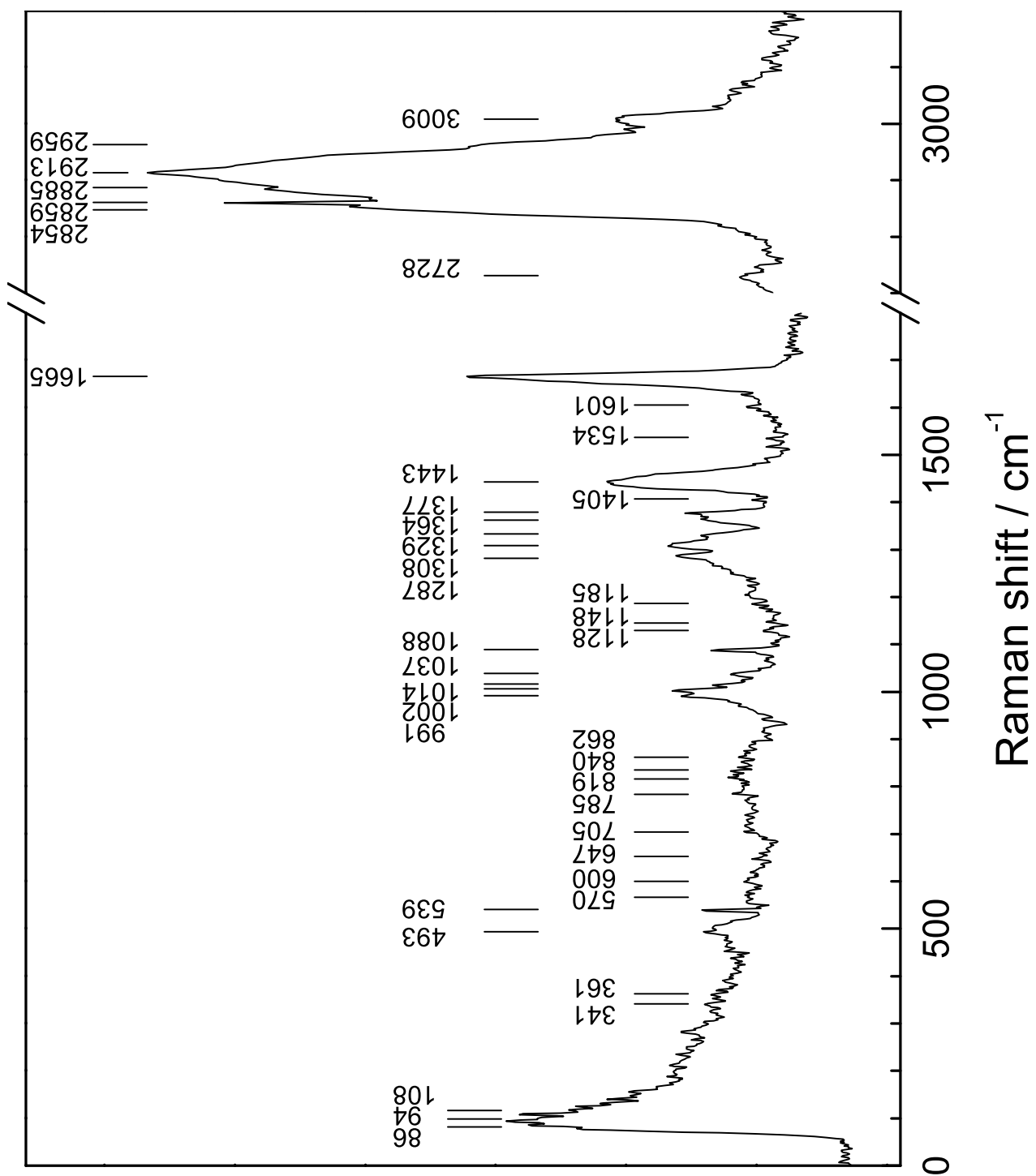


Figure A.13: Raman spectrum of the old seating of the chaise longue “Mies”.

## Appendix B

### Images of Rubber Samples

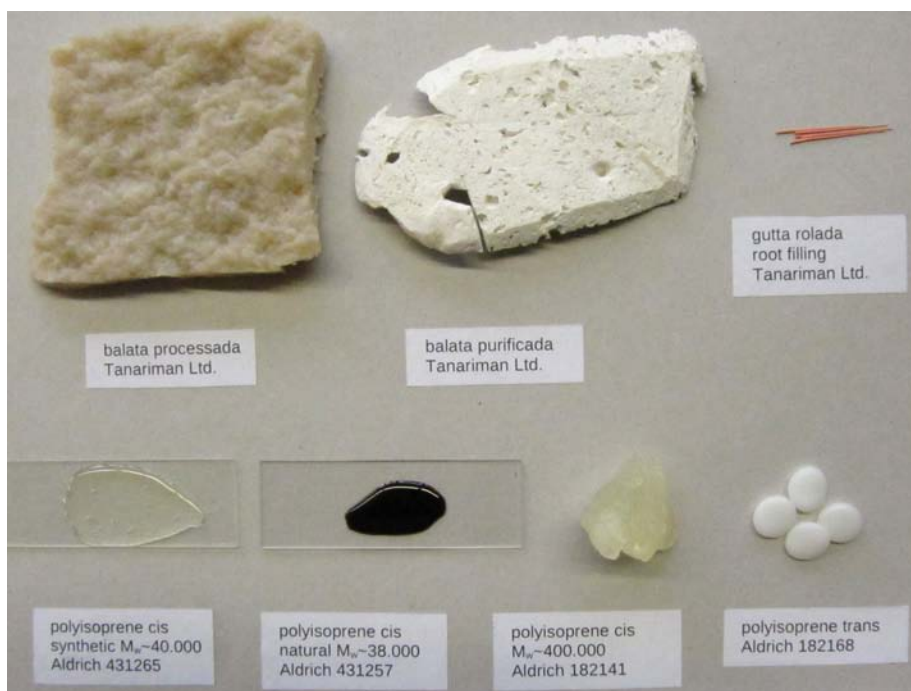


Figure B.1: New reference samples of natural and synthetic cis- and trans-polyisoprene ( $\alpha$ - and  $\beta$ -form).



Figure B.2: Cast films of natural latex milk, new and artificially aged for 4 and 73 hours.



Figure B.3: Ceylon Scraps, plantation rubber.



Figure B.4: Ceylon Scraps, plantation rubber, lateral cut.



Figure B.5: Parasoftware Brazil.



Figure B.6: Parasoft Brazil, side view.



Figure B.7: Parasoft Brazil, detail.



Figure B.8: Lanadrone block: plantation rubber, Ceylon.



Figure B.9: Lanadrone block: plantation rubber, Ceylon, reverse side.



Figure B.10: Lanadrone block, plantation rubber, Ceylon, side view.

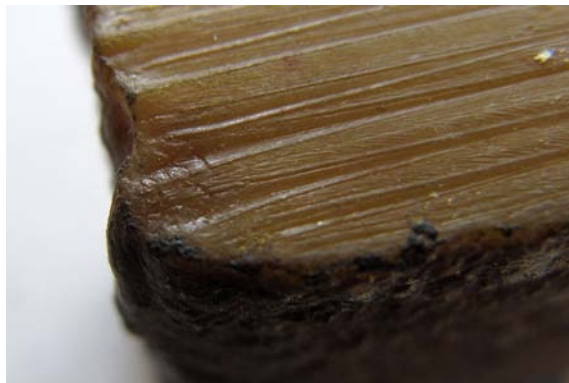


Figure B.11: Lanadrone block: plantation rubber, Ceylon, detail.



## Appendix C

# Light Ageing Apparatus

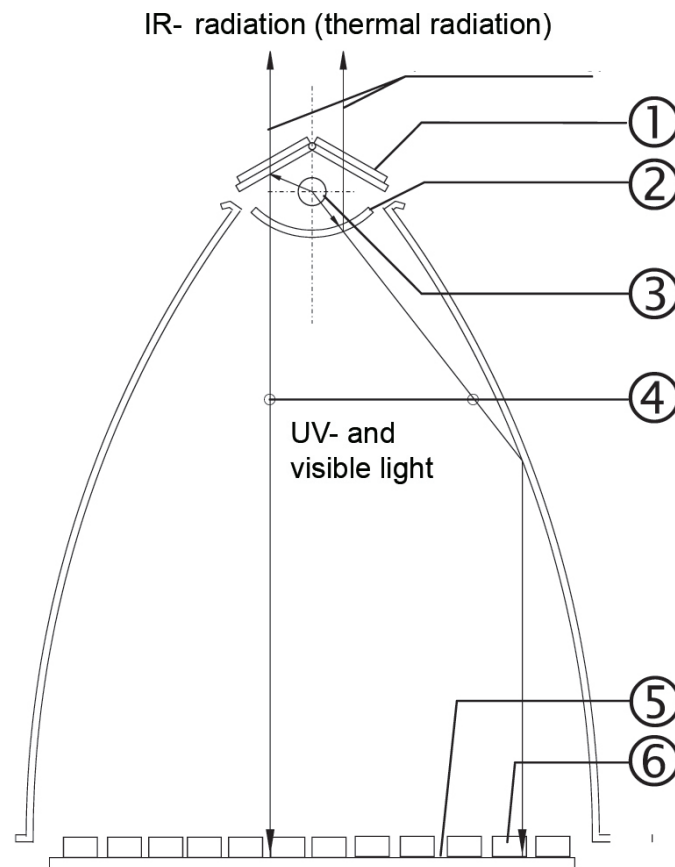


Figure C.1: Sketch of the sample chamber in a Suntest CPS (ATLAS) device for artificial light-ageing [41]. (1) mirror for UV and VIS light; (2) optical filter (coated quartz); (3) xenon arc lamp; (4) radiation; (5) sampling table; (6) test specimens.

## Appendix D

# Suppliers List

Latex milk: CREARTEC trend-design GmbH, Lauenbühlstrasse 59, D-88161 Lindenberg/Allgäu,  
[www.creattec.de](http://www.creattec.de)

Natural balata: TANARIMAN Industrial Ltda., 112 Av. Eduardo Ribiero, BR-69400000  
Manacapuru/Amazonas, [www.tanari.com.br](http://www.tanari.com.br)

Polyisoprene (182141, 182168, 431257, 431265): SIGMA-ALDRICH Laborchemikalien GmbH,  
Wunstorferstr. 40, D-30926 Seelze, [www.sigmaaldrich.com](http://www.sigmaaldrich.com)



## Appendix E

# Acknowledgements

The author wishes to thank Peter HILDEBRANDT for housing and supporting this research project, for his valuable advice and fruitful discussions. My sincere thanks go also to my supervisors Francisco VELAZQUEZ ESCOBAR and Ingo ZEBGER for their excellent assistance. I would like to thank Franz-Josef SCHMITT for determining the content of UV-light in the Suntest apparatus, Erwin EMMERLING, Dietmar LINKE, CREARTEC and TANARIMAN for material support, Christian WYRWICH for assisting with the artificial ageing, Manfred FEUSTEL from RESULTEC for providing the GladiATR™ unit and Thea VAN OOSTEN for sharing her experience. Special thanks to Marius HORCH, Johannes SALEWSKI, Anke KEIDEL and TILLMANN UTESCH for answering patiently hundreds of questions and to my fellow students Marieke FÜLLBRANDT and Martin UHLIG for cheerful lunch breaks and exam revision.



### **Statutory Declaration**

Hereby I confirm that I have completed the present thesis independently making use only of the specified literature and aids. Sentences or parts of sentences quoted literally are marked as quotations; identification of other references with regard to the statement and scope of the work is quoted. The thesis in this form or in any other form has not been submitted to an examination body and has not been published.

Berlin, 20<sup>th</sup> March 2012      Katharina Haider